CONTRACTOR: Serata Geomechanics, Inc.

CONTRACT SERIAL NO. 69021-01-SQ

TITLE: "APPLICATION OF STRESS - PROPERTY-DEFORMATION RELATION (SPDR) INTEGRATED METHOD IN DETERMINING SURFACE MINE STABILITY"

FINAL REPORT

BY

Serata Geomechanics, Inc.
4124 Lakeside Drive
Richmond, CA 94806

Work on this project was conducted under the auspices of the Department of Energy, Mines and Resources (Canada). This work was supported in part by the Federal Panel on Energy R&D (PERD).

DSS FILE NUMBER: 04SQ-23440-6-9021

DSS CONTRACT NUMBER: 23440-6-9021/01-SQ

EMR SCIENTIFIC AUTHORITY: Dr. B. Manas Das

116 pp

MICROMEDIA

June 8, 1987

TABLE OF CONTENTS

EXECUTIVE SUMMARY ES-1
RESUME DIRECTEUR RD-1

1.0 INTRODUCTION 1

2.0 OBJECTIVES AND BENEFITS
2.1 Overall Objectives 1
2.2 Specific Objectives 2

3.0 METHOD OF MODEL APPLICATION
3.1 Focus and Scope of Study 3
TABLE 1. Designation of Simulation Runs 3A
FIG. 1. Schematic Illustration of Pit Geometry Parameters and Variants Employed in Simulations 3B

3.2 Parametric Study
1) Parametric variations in material properties 4
TABLES 2-4. Strong, Norm and Weak Material Property Sets 4A-4C
2) Parametric variations in slope angles 4
TABLE 5. Three Sets of Pit Design Variants 4D

3) Parametric variations in excavation sequence 5
TABLE 6. Sequence of Activities Simulated for the Excavation Sequence Variants 4D

4) Parametric variations in excavation timing 5
5) Parametric variations in initial stress state 5

4.0 PRESENTATION OF RESULTS
4.1 Format of Presentation 6
4.2 Data Plots 6

5.0 DATA ANALYSIS
5.1 Specific Analysis 6

5.2 Rationale for Parameter Selection 7
TABLE 7. Critical Results from Simulation of Parametric Variations 7A

5.3 Basis for Comparison of Results 8

6.0 DISCUSSION OF RESULTS
6.1 Effect of Material Properties 9

6.2 Effect of Slope Angles 10
FIG. 2. Tensile Stress Distribution in Normal Slope Geometry for Various Property Sets 10A
FIG. 3. Tensile Stress Distribution in Steepest Variant of Slope Geometry 10B

6.3 Effect of Excavation Timing 11
6.4 Effect of Excavation Sequence 11
6.5 Effect of Initial Stress State 12

7.0 CONCLUSIONS 13

8.0 RECOMMENDATIONS
8.1 Site-Specific Design for Pit 3 14
8.2 Future Model Development 14

REFERENCES 15

APPENDIX A. Results from Model Application

EXECUTIVE SUMMARY

This project is the first application of the integrated Stress-Property-Deformation Relation (SPDR Method) to the design and analysis of slopes in open pit mines. The SPDR method is the first quantitative attempt to analyze geomechanical behavior of the ground by directly relating the stresses acting on a ground mass and its properties to the deformation of the ground. This method is therefore expected to provide a truly quantitative tool for the design of slopes, achieving, therefore, improvements in safety and productivity of the mining operations. Important accomplishments of the work to date are briefly summarized below.

FIELD WORK

Two test sites were chosen in Pit 3 of the Highvale mine near Edmonton, Alberta, for this project. One site was within the inference zone of the pit, while the other was in virgin ground at a distance from the slope face. Cores were recovered from both sites to a depth of 54 m penetrating all the coal layers that are being mined. An additional test hole was drilled at each site for geophysical logging as well as for measurements with the Stressmeter (S-100) and Propertymeter (P-100). These instruments were used to determine in situ stress states and properties of the overburden and coal formations. The Propertymeter also yielded information on the location and characteristics of weak zones and other anomalies.

LABORATORY TESTING

Laboratory testing of the core samples extracted from the two test sites enabled determination of the material properties of most of the competent constituents of the Highvale geology. Properties obtained for these recoverable materials in the laboratory were correlated with field testing results from the same strata. This correlation was extended to the results from field testing in the weak and non-recoverable materials. This enabled determination of the complete set of properties for all the constituents of the Highvale mine. The importance of this method of characterizing the ground is the fact that in situ testing allow sampling of the weak zones that predominantly affect geomechanical behavior.

COMPUTER MODEL DEVELOPMENT

Information on the geology of the test site, data from piezometers, slope geometry employed at the site, and excavation sequence followed, were obtained from studies previously conducted at Pit 3. These results were combined with the material property information to construct a finite element model of the ground. For purposes of initial testing, stresses in the ground were assumed to be hydrostatic. Water table drawdown effects were modelled by assigning two sets of properties to those materials affected by this phenomenon, one set representing a fully saturated condition and the other set a partially saturated condition. For purposes of analysis, the cumulative effect of four consecutive excavation cycles (representing one to two years of mining) on the test slope was simulated. All excavation prior to these four cycles was simulated by the instantaneous removal of the pertinent material. This method was found to yield realistic and reasonably accurate results. Furthermore, the model assumed the simultaneous removal of the overburden and the coal layers to represent a worst-case scenario.

ESTABLISHING BASIC (NORM) MODEL BEHAVIOR

A trial simulation was conducted assuming operating conditions normally encountered at the test site in Pit 3. A chopcut angle of 45^{o}, bankcut angle of 57^{o}, and spoil pile angle of 30^{o} were assumed, along with 3-month excavation interval, simultaneous coal and overburden removal, and a hydrostatic stress state. Results from the simulation were presented in the form of octahedral shear stress and strain distributions, principal stress and strain distributions, and deformation of critical nodes on the slope face. Tensile stress distributions were also examined. The trial simulation yielded results that indicated extensive strain damage in the bentonitic mudstone layer at the toe of the slope, and the presence of large tensile stresses in the operating bench. These tensile stresses peaked at about 200 KPa at about 15 m from the chopcut, indicating a strong possibility of tensile failure in the weak sandstone at the surface of the bench. Tensile stresses were also noticed behind the chopcut. These findings, as well as the simulated deformations, matched well with observations made previously in Pit 3. The model was thus calibrated and rendered site-specific.

MODEL CAPABILITY

The flexibility built into the model enabled the user to vary parameters such as the material properties, initial stress state, excavation interval, coal removal delay, and slope geometry. The model was applied to a variety of cases with different combinations of input parameters in order to determine its sensitivity to these parameters and also to arrive at a site-specific design for the slope at the test site. Material properties of the different strata were weakened and strengthened by up to 20% with respect to the base properties determined by field and laboratory testing. This yielded three sets of material property classification -- "weak," "norm," and "strong." Three-month and 6-month intervals between successive excavations were considered, as was a 20-day delay between overburden removal and coal excavation. In addition, two additional slope geometries with increased angles were modelled. The effect of a 20% excess lateral stress was also examined. Three important parameters were extracted from the results of model application for purposes of comparison. These were maximum octahedral shear strain, maximum principal strain, and maximum displacement encountered on the slope face. These three results were used to evaluate slope stability in one case relative to another.

SENSITIVITY OF DESIGN PARAMETERS

Results of model application to a selected combination of operating conditions were studied to evaluate its sensitivity to the various input parameters. It was determined that the model exhibited large sensitivity to material properties. Weakening of the overburden formations resulted in an increase in slope instability. The peak tensile stress in the slope increased when the material properties were weakened. In a pseudo-continuum approach such as this, weakening of material properties is indicative not only of a decrease in the strength of the competent material itself, but also the presence of inhomogeneities, pre-existing fractures, and intense jointing. The model applied to this particular site did not show appreciable sensitivity to increased slope angles, though it did show marginal decrease in stability as measured by the shear strains in the toe of the slope. Excavation interval was shown to affect slope stability significantly, with longer intervals corresponding to increased probability of failure. Simultaneous overburden and coal removal was found to represent a worst-case assumption when compared to the case where there was a 20-day delay between overburden and coal excavation. Excess lateral stresses were also shown to adversely affect stability.

RECOMMENDATIONS

The model developed in this study was calibrated with the help of data acquired previously in Pit 3. The deformation monitoring previously done was not systematic, and hence it is recommended that a demonstration or test slope be excavated with a known geometry and that this slope be instrumented extensively with deformation measuring devices. A systematic measurement procedure would enable further improvements to the model and would make it more accurate. Further work on the model would also enable it to become a user-friendly tool for application to other sites in the Highvale mine.

RÉSUMÉ DIRECTEUR

Ce projet constitue la première application intégrée de la Relation Contrainte-Propriété-Déformation (Méthode RCPD) sur l'étude et l'analyse des pentes dans les exploitations à ciel ouvert. La méthode RCPD représente la première tentative d'analyse quantitative du comportement géomécanique du sol en mettant les contraintes agissant sur une masse de fond en relation directe avec ses propriétés sur la déformation du sol. Cette méthode promet donc de fournir un outil quantitatif réel destiné à l'étude des pentes, permettant ainsi des améliorations tant du point de vue de la sécurité que de celui de la productivité des exploitations minières. Les étapes importantes accomplies à ce jour dans ce domaine sont brièvement résumées ci-dessous.

TRAVAUX ACCOMPLIS SUR LE TERRAIN

Deux sites d'essai furent sélectionnés pour ce projet dans la fosse No. 3 de la mine Highvale située près de Edmonton dans la province d'Alberta. L'un des sites se trouvait à l'intérieur de la zone d'inférence de la mine, alors que l'autre se trouvait en terrain vierge à une certaine distance de la pente. Des carottes furent extraites à une profondeur de 54 m en pénétrant tous les dépôts de houille minés dans les deux sites. Un trou d'essai supplémentaire fut aussi foré dans les deux sites à des fins de diagraphie géophysique et de mesures effectuées avec le Stressmeter (S-100) et le Propertymeter (P-100). L'usage de ces instruments visait à déterminer sur le terrain les états et les propriétés de contrainte de la couverture et des formations houillères. Le Propertymeter permet également d'obtenir des renseignements sur l'emplacement et les caractéristiques des zones faibles et d'autres anomalies.

ESSAIS DE LABORATOIRE

Des essais de laboratoire effectués sur les carottes extraites des deux sites à l'étude permirent de déterminer les propriétés des matériaux pour la plus grande partie des composants compétents dans la géologie du Highvale. Les propriétés obtenues en laboratoire pour ces matériaux récupérables furent mises en corrélation avec des résultats obtenus sur le terrain pour les mêmes couches. Cette corrélation fut étendue aux résultats obtenus lors d'essais sur le terrain effectués avec les matériaux faibles et non-récupérables. La détermination qui en a résulté englobait l'ensemble de toutes les propriétés des composants de la mine Highvale. L'importance de cette méthode de caractérisation du sol est le fait que les essais sur le terrain permettent un échantillonnage des zones faibles affectant surtout les comportements géomécaniques.

MISE AU POINT D'UN MODÈLE ORDINATEUR

L'information géologique fournie par le site d'essai, les données obtenues des piézomètres, de la géométrie de pente employée sur le terrain et de la séquence d'excavation qui a suivi, résultent toutes d'études conduites au préalable dans la fosse No. 3. Ces résultats furent combinés avec les renseignements sur les propriétés des matériaux afin de construire un modèle d'éléments finis du sol. Pour les besoins des essais préliminaires, les contraintes du sol furent supposées hydrostatiques. Les effets dûs à la baisse de la nappe souterraine furent étudiés par affectation de deux groupes de propriétés aux matériaux affectés par ce phénomène, un groupe représentant une condition complètement saturée et l'autre une condition partiellement saturée. Pour les besoins de l'analyse, l'effet cumulatif de quatre cycles consécutifs d'excavation (représentant un ou deux ans d'exploitation minière) fut simulé sur la pente faisant l'objet de l'essai. Toute excavation préalable à ces quatre cycles fut simulée par extraction immédiate des matériaux pertinents. Cette méthode s'est avérée fournir des résultats réalistes et raisonnablement justes. De plus, le modèle supposait que l'extraction simultanée de la couverture et des dépôts de houille représentait un scénario du pire des cas.

ÉTABLISSEMENT D'UN COMPORTEMENT MODÈLE DE BASE (NORME)

Une simulation d'essai fut mise au point à partir des conditions normales d'exploitation du site d'essai dans la fosse No. 3. On supposa un angle de fente de 45°, un angle de talus de 57°et un angle d'excavation de 30°, ainsi que des intervalles d'excavation de 3 mois, une extraction simultanée de la couverture et de la houille, et un état de contrainte hydrostatique. Les résultats de cette simulation furent obtenus des distributions de contrainte tangentielle et d'extrusion isométriques, des distributions de contrainte et d'extrusion principales et des déformations des noeuds critiques sur la pente. On examina également les distributions de la contrainte de traction. La simulation d'essai fournit des résultats indiquant des dégâts extensifs d'extrusion dans la couche de pélite bentonite au pied de la pente, et la présence de contraintes importantes de traction dans le front de taille. Le sommet de ces contraintes de traction, mesurant près de 200 KPa à 15 m environ de la fente, indiquait une forte possibilité de défaillance de traction dans le grès plus faible à la surface du front de taille. On remarqua également des contraintes de traction derrière la fente. Ces résultats, ajoutés aux déformations simulées, concordaient avec les observations effectuées plus tôt dans la fosse No. 3. Le modèle fut alors étalonné et déclaré spécifique du site.

FIABILITÉ DU MODÈLE

La flexibilité intrinsèque du modèle permit à l'utilisateur de faire varier des paramètres tels que les propriétés des matériaux, l'état de contrainte initial, les intervalles d'excavation, les délais d'extraction de la houille et la géométrie de la pente. On appliqua ce modèle à une gamme de situations en utilisant différentes combinaisons de paramètres primaires afin de déterminer sa sensibilité à ces paramètres et d'obtenir une conception spécifique du site pour la pente du site d'essai. Les propriétés des matériaux des différentes couches furent tour à tour affaiblies et renforcées d'un taux allant jusqu'à 20 % par rapport aux propriétés de base déterminées lors des essais sur le terrain et en laboratoire. Cette opération permit d'obtenir trois classes de propriétés des matériaux -- "faible", "normale" et "forte". On considéra des intervalles de 3 mois et de 6 mois entre les excavations successives, ainsi qu'un délai de 20 jours avant extraction de la couverture et excavation de la houille. On étudia également deux géométries de pente supplémentaires avec des angles plus importants. On examina en outre l'effet d'une contrainte latérale excédentaire de 20 %. Trois paramètres importants furent extraits des résultats de l'application du modèle à des fins comparatives. Ces paramètres étaient constitués de l'extrusion tangentielle isométrique maximale, de l'extrusion principale maximale et du déplacement maximum enregistré sur la pente. On utilisa ces trois résultats dans l'évaluation de la stabilité de la pente entre les différents cas.

SENSIBILITÉ DES PARAMÈTRES DE L'ÉTUDE

On étudia les résultats du modèle appliqué par rapport à une combinaison définie de conditions d'exploitation afin d'évaluer sa sensibilité aux différents paramètres primaires. Il fut déterminé que le modèle faisait preuve d'une sensibilité élevée aux propriétés des matériaux. Un affaiblissement des formations de couverture produit une augmentation de l'instabilité de la pente. Le pic de la contrainte de traction dans la pente se montra inversement proportionnel aux propriétés des matériaux. Lors d'une telle approche de pseudo-continuum, un affaiblissement des propriétés des matériaux est non seulement significatif d'une diminution de force du matériau compétent, mais aussi de la présence de non-homogénéités, de cassures pré-existantes et d'un effet de joint intense. Le modèle appliqué à ce site particulier n'a pas fait preuve d'une sensibilité appréciable aux angles de pente plus forts, bien qu'il ait démontré une diminution marginale de la stabilité mesurée par l'extrusion tangentielle au pied de la pente. Les intervalles d'excavation se sont avérés affecter la stabilité de la pente de manière significative, les intervalles plus longs correspondant à une probabilité plus forte de défaillance. On déduit que l'extraction simultanée de la couverture et de la houille représentait une hypothèse du pire des cas par rapport à l'exemple selon lequel un délai de 20 jours fut observé entre l'extraction de la couverture et de la houille. Il apparut également que des contraintes latérales excessives jouaient un rôle néfaste sur la stabilité.

RECOMMANDATIONS

Le modèle mis au point dans cette étude fut étalonné grâce à des données préalables obtenues dans la fosse No. 3. L'enregistrement des déformations déjà effectué n'ayant pas été systématique, on recommande l'excavation d'une pente d'essai ou de démonstration à partir d'une géométrie connue, ainsi que des évaluations extensives de cette pente à l'aide de dispositifs de mesure des déformations. Une procédure de mesure systématique permettrait d'améliorer et d'affiner encore l'exactitude du modèle. Des travaux plus poussés sur ce modèle en ferait également un outil d'emploi plus facile quant à des applications dans d'autres sites de la mine Highvale.

1.0 INTRODUCTION

This report is being submitted in accordance with Subtask 4.4a of DSS Contract #23440-6-9021/01-SQ. This document constitutes a final report on the project dealing with activities undertaken in Subtask 3.3 of the above contract. The project involves a study undertaken by Serata Geomechanics, Inc. (referred to hereafter as SGI) on behalf of the Department of Energy, Mines and Resources, Government of Canada (referred to hereafter as CANMET). This study is being conducted at the Highvale mine owned and operated by TransAlta Utilities of Alberta, Canada, and involves an investigation of the application of the stress-property-deformation relation (SPDR method) in determining surface mine stability.

This project is being conducted under the supervision of Dr. Manas Das of CANMET, based in the Coal Research Laboratories, at Devon, Alberta. Mr. Dennis Nikols of TransAlta Utilities, based in Calgary, Alberta, provided liaison on behalf of the mine operators.

The work covered by this report was performed at SGI under the guidance of Dr. Shosei Serata, Principal, by Dr. S-J Chern, Sr. Math Analyst, Mr. Chetan Damania and Mr. Zheng-Yu Zhu, Geotechnical Engineers, and by Mr. K. Shrinivasan, Project Manager.

The work conducted in the phase covered by this report consisted of applying the results and conclusions of the model development report. More specifically, the finite element model of the ground that was developed as part of the previous phase [1] was applied to various slope geometries, excavation timing, and sequences, as well as classifications of material properties. This was done with a view to establishing sensitivity of the model to differing inputs and to identify a site-specific optimum design.

2.0 OBJECTIVES AND BENEFITS

2.1 Overall Objectives

The overall objective of this project is to develop a method for quantitatively assessing the stability of slopes in an open pit mine. This is to be accomplished by developing a site-specific finite element model of the ground in Pit 3 of the Highvale mine. This project seeks to accomplish this objective by employing the stress-property-deformation relation (SPDR method) as a tool to quantify the geomechanical behavior of the mine ground. By developing such a procedure, it is expected that design of slopes for increased productivity and safety would become truly quantitative.

The activities that comprise this project include a site-specific evaluation of material properties of the ground in Pit 3 at Highvale by conducting field and laboratory core sample testing [2]. Information from this testing regime is to be used as input to the SGI program REM (Rheological Element Method) which integrates the three constituent components of geomechanical behavior of the ground, namely stress, properties, and deformation. Behavior of the ground as predicted by REM in terms of deformation and stress/strain patterns will be compared to observations made by TransAlta in the Highvale mine. By minimizing the difference between predicted and observed behavior, a well-adjusted site-specific model is to be derived. A variety of different slope geometries, excavation sequences, and timings, and other parameters, will be tested with the improved model, first to quantify the sensitivity and second to arrive at a site-specific optimum design for Pit 3.

2.2 Specific Objectives

The specific objective of the particular phase of the project covered by this document is to apply the model developed in the previous phase [1]. Accuracy of the predictions made by the model applied to excavation parameters actually employed in Pit 3 is to be ascertained by referring to geotechnical studies made in the mine [3,4,5,6]. By adjusting the model to minimize any differences between the predicted and actual ground behavior, it is to be rendered accurate and site-specific.

This site-specific model will then be applied to a variety of different designs to ascertain:

1) Sensitivity of the model to variations in input reflecting different excavation parameters;
2) An optimum design for Pit 3 that maximizes safety and productivity.

These objectives will be addressed by testing the model by changing the following important parameters:

1) Material properties of the ground;
2) Slope angles;
3) Excavation sequence;
4) Excavation timing;
5) Initial stress state.

The results obtained from such a parametric analysis will be evaluated to determine slope stability in each case and to compare the degree of stability of different pit designs.

3.0 METHOD OF MODEL APPLICATION

3.1 Focus and Scope of Study

This study focussed essentially on the application of the model developed in the previous phase to a number of different design variants. Results were analyzed to evaluate slope stability in each instance and to compare designs with regard to their safety and productivity. Table 1 presents a compendium of the different parametric variants which were applied to the Highvale model. Essentially, five important parameters were studied in relation to one another. They are:

1) Material properties of the ground;
2) Pit slope angles;
3) Excavation sequence;
4) Excavation timing;
5) Initial stress state.

Only a few combinations of parameters were studied, as shown in Table 1. This was because the model exhibited a systematic difference in behavior when any one parameter was changed, enabling estimation of the slope stability for all combinations by applying the model selectively. For example, when it was established that increasing the time period between excavations caused greater instability in the cases of normal and strong material properties, weak properties and steeper slope angles were not tested with a 6-month interval. In all, only 19 out of a possible 72 combinations, as shown in Table 1, were applied, reflecting nonetheless enough redundance to double-check the behavior trends.

TABLE 1. Designation of Simulation Runs

MATERIAL TYPE	EXCAVATION ANGLES: $\alpha = 45^o$, $\beta = 57^o$ — EXCAVATION DETAILS*				EXCAVATION ANGLES: $\alpha = 50^o$, $\beta = 65^o$ — EXCAVATION DETAILS*				EXCAVATION ANGLES: $\alpha = 55^o$, $\beta = 72^o$ — EXCAVATION DETAILS*			
	3M,6	3M,10	6M,6	3M,σ_L	3M,6	3M,10	6M,6	3M,σ_L	3M,6	3M,10	6M,6	3M,σ_L
WEAK	CN1D06 CN1S06	TESD05 TESS05			CN1DG7 CN1SG7				CN1DG9 CN1SG9			
NORM	CN1D05 CN1S05	TESD02 TESS02			CN1DG6 CN1SG6				CN1DG8 CN1SG8	TESD03 TESS03	CN1DT3 CN1ST3	TESD11 TESS11
STRONG	CN1D08 CN1S08	TESD04 TESS04			CN1DG3 CN1SG3				CN1DG5 CN1SG5		CN1DT4 CN1ST4	

* Key to symbols denoting excavation details:

3M,6 -> 3 mo excav cycle with simultaneous coal/overburden removal
3M,10 -> 3 mo excav cycle with delayed coal removal
6M,6 -> 6 mo excav cycle with simultaneous coal/overburden removal
3M,σ_L -> 3 mo excav cycle with excess lateral stress and simultaneous coal/overburden removal

DESCRIPTION	SYMBOL	#1	#2	#3
Chop Cut Angle	α	45°	50°	55°
Bank Cut Angle	β	57°	65°	72°
Coal Excavation Angle	γ	80°	80°	80°
Spoil Pile Angle	δ	30°	30°	30°

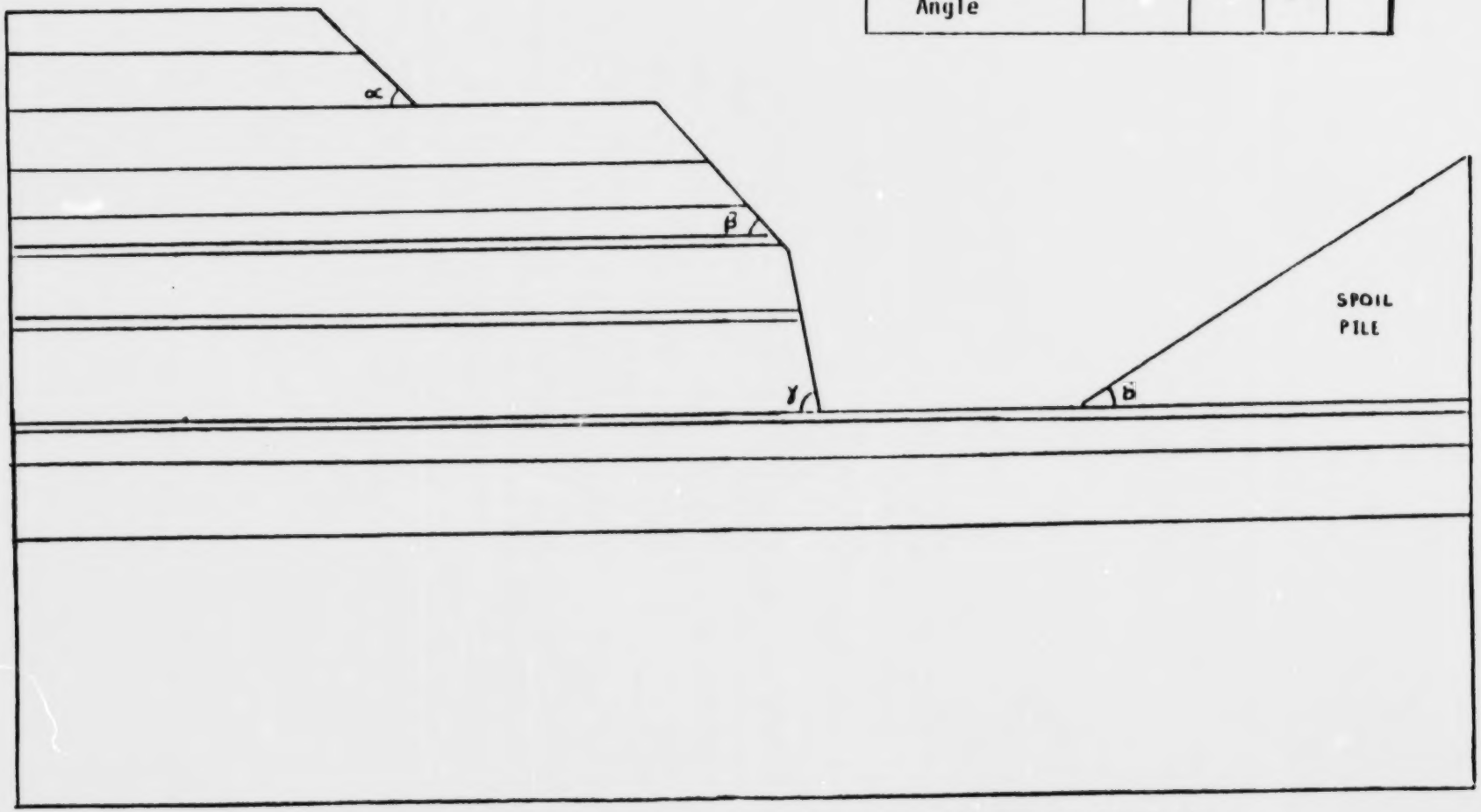

FIG. 1. Schematic Illustration of Pit Geometry Parameters and Variants Employed in Simulations.

3.2 Parametric Study

1) Parametric variations in material properties: Three sets of material properties were chosen for application in the site-specific model of Pit 3. The "norm" property set represents the results of the field and laboratory testing performed at the test site (refer to Field/Laboratory Testing Interim Technical Report [2]) in August 1986. There was, however, a certain amount of uncertainty linked to these results because of the following factors:

(1) The testing was done in the field in August and the cores were extracted during the same period. Seasonal variations in material properties were not therefore accounted for in one set of properties.

(2) Damage to the core samples could have taken place either due to mechanical shock or loss of moisture during shipment.

(3) The size effect had to be considered. This effect is discussed in the Field/Laboratory Interim Report [2] and concerns the phenomenon whereby properties attained by testing methods do not represent real properties of the ground on the global scale that whole mine pit simulations assume or imply.

(4) Lastly, it was important that the model be adaptable to local variations in the material properties encountered in Pit 3.

Accordingly, simulations of the slope behavior were calibrated to a range of properties that varied from strong to weak. Three sets of material properties were chosen for all materials. The "weak" and "strong" property sets represent the extremities of this range and were arrived at by using the "norm" material property set and making adjustments to it with the help of SGI's material property data base. Physically the "strong" property set represents conditions under which slope failure is highly improbable given current pit design and excavation patterns in Pit 3. The "weak" property sets represent a high probability of slope failure under the same conditions, whereas "norm" properties imply a marginal condition. Material property values for the different constituents of the Highvale geology are presented in Tables 2 ("strong"), 3 ("norm"), and 4 ("weak").

2) Parametric variations in slope angles: Three sets of slope angles were considered for a parametric analysis. The pit geometry currently in use at Pit 3 was ascertained from geotechnical reports of studies performed in the mine [5,6]. This geometry involved a chopcut angle (denoted by α) of 45^{o} and a bank cut angle (denoted by β) of 57^{o}, while the angle subtended by the slope with the pit floor subsequent to coal removal, the coal excavation angle (denoted by γ) was 80^{o}. These angles are explained in Fig. 1. At the request of TransAlta Utilities, steeper variants of this slope geometry were tested. These variants involved increasing the chopcut angle (α) and the bankcut angle (β), while the coal excavation angle, γ, and the spoil pile angle, δ, were not changed. The three pit design variants used in this study are summarized in Table 5.

TABLE 2. "Strong" REM Material Property Set

REM MATERIAL PROPERTY PARAMETERS			TILL	WEAK SANDST.	NORM SANDST. (fully satur.)	BENTON. MUDSTN. (fully satur.)	COAL	SHALEY SILTST.	NORM SANDST. (part. satur.)	BENTON. MUDSTN. (part. satur.)
DESCRIPTION	SYMBOL	UNIT								
Shear modulus	G	MPa	4.83	8.97	100.05	4.49	8.97	8.97	103.5	5.38
Retarded shear modulus ($\tau_o<K_o$)	G_2	MPa	8.97	8.97	179.4	17.94	22.08	26.91	179.4	31.4
Retarded shear modulus ($\tau_o>K_o$)	G_3	MPa	8.97	8.97	179.4	19.67	22.08	26.91	179.4	26.91
Elastoviscosity ($\tau_o<K_o$)	V_2	MPa da	17.94	17.94	89.7	17.94	17.94	31.05	89.7	26.91
Elastoviscosity ($\tau_o>K_o$)	V_3	MPa da	17.94	17.94	89.7	35.88	17.94	31.05	89.7	35.88
Plastoviscosity	V_4	MPa da	35.88	35.88	538.2	69	72.45	72.45	627.9	82.8
Ultimate bulk modulus	K_1^B	MPa	45.85	72.45	158.7	44.85	66.93	89.7	179.4	53.82
Retarded bulk modulus	K_2	MPa	89.7	89.7	224.25	75.9	72.45	89.7	269.1	89.7
Hydrostatic elastoviscosity	D_2	MPa da	269.1	269.1	448.5	151.8	200.1	269.1	448.5	151.8
Unconfined octah. shear strength	K_o^A	MPa	0.359	0.449	3.588	0.53	1.794	1.794	4.49	0.538
Ultimate octah. shear strength	K_o^B	MPa	3.59	4.49	21.39	2.76	4.49	4.49	22.43	4.14
Minimum octahedral shear strength	K_o^{min}	MPa	0.104	0.104	2.07	0.06	0.69	0.69	3.45	0.069
Yield surface coefficient	α	1/MPa	0.580	0.725	1.159	0.58	0.725	0.725	1.159	0.725
Critical strain of failure	γ_o^c	10^{-2}	3	3	1	4	2	2	0.8	3
Shear deterioration coefficient	C	--	5	5	9	4	6	7	10	4
Unconfined bulk modulus	K_1^A	MPa	2.76	4.14	8.28	2.76	4.49	5.52	10.35	2.76
Minimum bulk modulus	K_1^{min}	MPa	1.38	2.76	6.9	2.07	2.07	2.76	6.9	2.07
Density in X-direction	ρ_x	MPa/m	0	0	0	0	0	0	0	0
Density in Y-direction	ρ_y	MPa/m	0.020	0.022	0.026	0.01	0.014	0.020	0.026	0.017
Power coeff. of plastoviscosity	n	--	2.6	2.6	2.6	2.6	2.6	2.6	2.6	2.6
Thermal expansion coefficient	α_T	$1/^oC$	0	0	0	0	0	0	0	0

TABLE 3. "Norm" REM Material Property Set

REM MATERIAL PROPERTY PARAMETERS			TILL	WEAK SANDST.	NORM SANDST. (fully satur.	BENTON. MUDSTN. (fully satur.)	COAL	SHALEY SILTST.	NORM SANDST. (part. satur.)	BENTON. MUDSTN. (part. satur.)
DESCRIPTION	SYMBOL	UNIT								
Shear modulus	G	MPa	3.8	6.9	75.9	3.45	6.9	6.9	82.8	4.14
Retarded shear modulus ($\tau_o<K_o$)	G_2	MPa	6.9	6.9	138	13.8	17.25	20.7	138	24.15
Retarded shear modulus ($\tau_o>K_o$)	G_3	MPa	6.9	6.9	138	15.18	17.25	20.7	138	20.7
Elastoviscosity ($\tau_o<K_o$)	V_2	MPa da	13.8	13.8	69	13.8	13.8	24.15	69	20.7
Elastoviscosity ($\tau_o>K_o$)	V_3	MPa da	13.8	13.8	69	27.6	13.8	24.15	69	27.6
Plastoviscosity	V_4	MPa da	27.6	27.6	414	26.22	55.2	55.2	483	27.6
Ultimate bulk modulus	K_1^B	MPa	34.5	55.2	124.2	34.5	51.75	69	138	41.4
Retarded bulk modulus	K_2	MPa	69	69	172.5	58.65	55.2	69	207	69
Hydrostatic elastoviscosity	D_2	MPa da	207	207	345	117.3	151.8	207	345	117.3
Unconfined octah. shear strength	K_o^A	MPa	0.276	0.345	2.76	0.414	1.38	1.38	3.45	0.414
Ultimate octah. shear strength	K_o^B	MPa	2.76	3.45	16.56	2.07	3.45	3.45	17.25	3.45
Minimum octahedral shear strength	K_o^{min}	MPa	0.104	0.104	2.07	0.069	0.690	0.690	3.45	0.069
Yield surface coefficient	α	1/MPa	0.725	1.014	1.449	0.725	0.870	1.014	1.449	1.014
Critical strain of failure	γ_o^c	10^{-2}	3	3	1	4	2	2	0.8	3
Shear deterioration coefficient	C	--	5	5	9	4	6	7	10	4
Unconfined bulk modulus	K_1^A	MPa	2.76	4.14	8.28	2.76	4.49	5.52	10.35	2.76
Minimum bulk modulus	K_1^{min}	MPa	1.38	2.76	6.9	2.07	2.07	2.76	6.9	2.07
Density in X-direction	ρ_x	MPa/m	0	0	0	0	0	0	0	0
Density in Y-direction	ρ_y	MPa/m	0.020	0.022	0.026	0.018	0.014	0.014	0.026	0.017
Power coeff. of plastoviscosity	n	--	2.6	2.6	2.6	2.6	2.6	2.6	2.6	2.6
Thermal expansion coefficient	α_T	$1/^oC$	0	0	0	0	0	0	0	0

TABLE 4. "Weak" REM Material Property Set

REM MATERIAL PROPERTY PARAMETERS			TILL	WEAK SANDST.	NORM SANDST. (fully satur.)	BENTON. MUDSTN. (fully satur.)	COAL	SHALEY SILTST.	NORM SANDST. (part. satur.)	BENTON. MUDSTN. (part. satur.)
DESCRIPTION	SYMBOL	UNIT								
Shear modulus	G	MPa	3.8	6.9	69	2.76	6.9	6.9	75.9	3.45
Retarded shear modulus ($\tau_o < K_o$)	G_2	MPa	6.9	6.9	138	8.28	17.25	20.7	138	13.8
Retarded shear modulus ($\tau_o > K_o$)	G_3	MPa	6.9	6.9	138	11.04	17.25	20.7	138	15.18
Elastoviscosity ($\tau_o < K_o$)	V_2	MPa da	13.8	13.8	69	8.97	13.8	24.15	69	13.8
Elastoviscosity ($\tau_o > K_o$)	V_3	MPa da	13.8	13.8	69	27.6	13.8	24.15	69	27.6
Plastoviscosity	V_4	MPa da	27.6	27.6	345	24.84	55.2	55.2	414	26.22
Ultimate bulk modulus	K_1^B	MPa	34.5	55.2	110.4	27.6	51.75	69	124.2	34.5
Retarded bulk modulus	K_2	MPa	69	69	138	50.37	55.2	69	172.5	58.65
Hydrostatic elastoviscosity	D_2	MPa da	207	207	345	117.3	151.8	207	345	117.3
Unconfined octah. shear strength	K_o^A	MPa	0.276	0.345	2.07	0.414	1.38	1.38	2.76	0.414
Ultimate octah. shear strength	K_o^B	MPa	2.76	3.45	15.87	1.242	3.45	3.45	16.56	2.07
Minimum octahedral shear strength	K_o^{min}	MPa	0.104	0.104	1.38	0.069	0.690	0.690	2.07	0.069
Yield surface coefficient	α	1/MPa	0.725	1.014	1.449	0.725	0.870	1.014	1.449	1.014
Critical strain of failure	γ_o^c	10^{-2}	3	3	1	4	2	2	0.8	3
Shear deterioration coefficient	C	--	5	5	8	4	6	7	10	4
Unconfined bulk modulus	K_1^A	MPa	2.76	4.14	6.9	2.76	4.49	5.52	10.35	2.76
Minimum bulk modulus	K_1^{min}	MPa	1.38	2.76	6.9	2.07	2.07	2.76	6.9	2.07
Density in X-direction	ρ_x	MPa/m	0	0	0	0	0	0	0	0
Density in Y-direction	ρ_y	MPa/m	0.020	0.022	0.026	0.018	0.014	0.020	0.026	0.017
Power coeff. of plastoviscosity	n	--	2.6	2.6	2.6	2.6	2.6	2.6	2.6	2.6
Thermal expansion coefficient	α_T	$1/^oC$	0	0	0	0	0	0	0	0

TABLE 5. Three Sets of Pit Design Variants

DESCRIPTION	SYMBOL	DEGREES		
		#1	#2	#3
Chopcut angle	α	45	50	55
Bankcut angle	β	57	65	72
Coal excavation angle	γ	80	80	80
Spoil pile angle	δ	30	30	30

TABLE 6. Sequence of Activities Simulated for the Excavation Sequence Variants

VARIANT	TIME		
	t = 0	t=20 da	t = 3 mos
Simultaneous coal/ overburden simulation	Chopcut and bankcut made, coal removed		New chopcut and bankcut made, coal removed
Delayed coal removal	Chopcut and bankcut made	Coal removed	New chopcut and bankcut made

3) Parametric variations in excavation sequence: The excavation sequence refers to the sequence in which the extraction of coal takes place at any cut subsequent to the removal of the overburden. Since the REM model coducted a plane strain analysis, all excavation and addition to the spoil pile was assumed to take place in a time frame that was small when compared to the time frame of the simulation. Hence, in the REM model, all excavation at any cut was simulated as if it were performed instantaneously and the whole model simulation comprised of 6 excavation/loading stages.

In the operation of the Highvale mine, the coal is usually removed two to three weeks after the chopcut and bankcut are made to excavate the overburden. The numerical simulation of this process would have required two excavation stages at any cut, and the whole simulation would have to consist of 10 excavation/loading stages. This sequence was analyzed with respect to the slope stability problem, and it was determined that a worst case scenario would involve removal of coal simultaneously with the excavation of the overburden. This had the advantage of reducing the number of excavation stages for the whole simulation to six.

Six-stage and 10-stage excavation simulations were conducted, with all other parameters remaining constant. The former was found to represent a worst-case assumption in addition to effecting savings of up to 50% in computational time. Moreover, the difference between the two was found to be systematic and easily quantifiable. Hence, simulations used to compare the effect of other parameters were conducted with a 6-stage simulation representing simultaneous removal of coal and the overburden. Table 6 depicts the difference between the two approaches.

4) Parametric variations in excavation timing: Excavation timing is the parameter that defines the time interval between successive cuts in the advance of a pit. This operational parameter is constrained in the field by the demand for coal and other complicated logistical considerations. At Highvale, the time interval between successive cuts varies from 3 to 6 months. The model was therefore tested first assuming a 3-month interval and then a 6-month interval to check its sensitivity to variations in this parameter.

5) Parametric variations in initial stress state: Unfortunately, due to the limited stress testing that was possible at Highvale, no firm conclusions could be drawn about the in situ stress state of the ground at Highvale. However, bearing in mind the shallowness of the coal, and testing results that indicated no significant stress relief effects near the pit [2], properties of the weak zones rather than stresses, were considered critical for slope stability. In order to check this assumption, previous stress measurements were consulted and it was found that the vertical stress is the intermediate principal stress in the area around Edmonton. It was also determined that the maximum principal stress was oriented in the northeast-southwest direction, and was approximately 120% of the vertical stress [7,8,9]. This indicates that certain sections of Pit 3, specifically areas west of 4300W, would be subjected to an excess lateral stress in a direction perpendicular to the slope face.

To account for this, a few runs were performed to check the effect of a 20% excess lateral stress. The majority of other combinations assumed a hydrostatic stress state.

4.0 PRESENTATION OF RESULTS

4.1 Format of Presentation

Results from the application of the model to the different parametric combinations are presented in six plots as follows:

1) Octahedral shear stress contour plot:
2) Octahedral shear strain contour plot:
3) Principal stress vector diagram:
4) Principal strain vector diagram:
5) Mesh displacement:
6) Displacement of critical nodes as a function of time.

The REM model simulated four successive cuts. The main attention of the study was focussed on the slope of the last cut. The six plots that are presented as results pertain to this particular slope and its behavior. The first five plots concentrate on an area just behind the exposed face of the slope, while the sixth plot presents the displacement of critical points on the open face of the coal measures just above the pit floor.

4.2 Data Plots

Results from all the individual runs are plotted and presented in Appendix A. These results have been grouped together by run. The run designation is given in Table 1, and cross-reference with the figures in Appendix A will enable matching of the results with the parametric combinations.

5.0 DATA ANALYSIS

5.1 Specific Analysis

Results from all the different runs were analyzed based on the guidelines and principles enunciated in the model development report. The rationale for data analysis was to correlate the results of simulation, expressed as stress and strain distribution patterns, to slope instability. Slope instability is manifested in slope failure that can occur in a number of modes [1]. Analysis of simulation results seeks to establish whether circumstances exist that might cause failure of the slope. The parameters that were considered to be important in making such a determination are:

1) Octahedral shear stress and strain;
2) Principal stress and strain;
3) Deformation.

Consequently the distributions of the above parameters were examined with regard to the slope after the last cut. This analysis was performed within the context of two distinct failure criteria -- a maximum or failure shear strain and maximum tensile stress. These criteria enabled determination of the extent of failed regions behind the slope, which in turn enabled qualitative estimates of slope stability. For a comprehensive analysis incorporating comparisons between different simulations, three important parameters were extracted from the plots of results referred to in Section 4.0. These three parameters are:

1) Maximum displacement, δ_{max};
2) Maximum octahedral shear strain, γ_{max} and
3) Maximum principal strain, ε_{max}.

These three parameters are compared for the different simulations in Table 7. In addition to these parameters, the maximum tensile stress in the bench was determined for a few simulation runs. Comparisons of these parameters for these runs are presented in Figs. 2 and 3.

5.2 Rationale for Parameter Selection

As mentioned in Section 3.1, only 19 out of a possible 72 parametric combinations were selected. This selection involved a logical progression of choice based on analysis of the results. This is very apparent from an examination of the critical parameter comparisons in Table 7. Analysis of all results, however, must be placed within the context of this choice of runs, and the rationale behind such a procedure.

As mentioned in the model development report, the trial simulation was conducted employing input parameters reflecting normal operating conditions at the test site in Pit 3. The slope geometry corresponds exactly to the pit design employed in that section of the mine for operational purposes. The material properties reflected normal conditions during the summer months. Excavations were spaced by about three months, which is normal for Pit 3. At first it was assumed that the coal was removed 20 days after the overburden was excavated, resulting in the incorporation of 10 excavation/loading stages in the simulation. Another simulation was conducted assuming the coal was excavated along with the overburden, enabling completion of this simulation with only six excavation/loading stages. Comparison of results from the two runs, the only difference being the sequence of coal removal with regard to overburden excavation, confirmed the expectation that the latter was a worst case scenario. Comparison of the critical parameters for these two runs in Table 7 illustrates this.

TABLE 7. Critical Results from Simulation of Parametric Variations

MATERIAL TYPE		EXCAVATION ANGLES: $\alpha = 45^o$, $\beta = 57^o$				$\alpha = 50^o$, $\beta = 65^o$				$\alpha = 55^o$, $\beta = 72^o$			
		EXCAVATION DETAILS: 3M,6	3M,10	6M,6	3M,σ_L	3M,6	3M,10	6M,6	3M,σ_L	3M,6	3M,10	6M,6	3M,σ_L
WEAK	DESIG	CN1D06 / CN1S06	TESD05 / TESS05			CN1DG7 / CN1SG7				CN1DG9 / CN1SG9			
	δ_{max} (m)	0.5	0.5			0.52				0.52			
	γ_{max} (%)	20	20			20				20			
	ε_{max} (%)	26	24			26				26			
NORM	DESIG	CN1D05 / CN1S05	TESD02 / TESS02	CN1DT1 / CN1ST1	TESD10 / TESS10	CN1DG6 / CN1SG6				CN1DG8 / CN1SG8	TESD03 / TESS03	CN1DT3 / CN1ST3	TESD11 / TESS11
	δ_{max} (m)	0.48	0.48	0.5	0.65	0.48				0.48	0.50	0.52	0.65
	γ_{max} (%)	12	12	18	20	14				14	12	18	20
	ε_{max} (%)	20	19	25	24	19				19	19	25	24
STRONG	DESIG	CN1D08 / CN1S08	TESD04 / TESS04	CN1DT2 / CN1ST1		CN1DG3 / CN1SG3				CN1DG5 / CN1SG5		CN1DT4 / CN1ST4	
	δ_{max} (m)	0.38	0.37	0.38		0.38				0.38		0.38	
	γ_{max} (%)	9	8	10		9				9		10	
	ε_{max} (%)	12	9.5	15		11				12		15.5	

This exercise was repeated for the same pit design but with "weak" and "strong" material properties with the same result. A further check was made with a steeper slope design and "norm" properties, yielding similar findings. Hence, the 6-stage excavation sequence was preferred for all other simulations for reasons of economy. These were treated as worst case scenarios.

The next parameter to be studied was the material properties. A 6-stage simulation of the pit slope with normal operating parameters was compared with two other simulations, incorporating changes only in material properties. Simulations employing "weak" properties displayed the greatest amount of accumulated strain damage, while "strong" properties corresponded to the least damage. This comparison was conducted for both the steeper slope variants and found to yield consistent results.

Excavation interval or timing was considered next, and comparisons were made between results for a 3-month interval and a 6-month interval for "norm" and "strong" properties for the normal pit slope and the steepest design variant. It was felt that the "weak" property set represented unstable conditions for a 3-month interval, and would be more unstable given a 6-month cycle of excavation. No simulations were performed for intermediate pit slope steepness, since results from the two other slope steepness variants exhibited systematic patterns.

The effect of steeper slopes was studied with "strong," "norm," and "weak" material property sets for 3-month excavation cycles. Comparisons between steeper slope designs for 6-month cycles were performed for "strong" and "norm" properties only as reported before.

In all the above simulations, the in situ stress state had been assumed to be hydrostatic. That is, the vertical and horizontal initial stress components were assumed to be equal and a function of depth below ground surface. Excess lateral stress of up to 20% was simulated in only two cases -- for the normal and steepest slope designs employing "norm" properties. The results revealed greater instability caused by the excess lateral stress, and further comparisons were not considered essential.

5.3 Basis for Comparison of Results

Results from different simulations were compared, and the analysis of these results used to set up comparative estimates of slope stability. The extent of strain damage at the toe of the slope, coupled with the magnitude of tensile stress in the bench, was considered indicative of slope failure probability. Based on the significance of the input parameters and the physical conditions they imply, conclusions could be drawn as to the best combination of operational parameters for a given situation. Recommendations on pit slope geometry, for example, could vary greatly, depending on the presence of joints in an area or the weakening of overburden materials due to excessive pore water pressures. This issue is dealt with in detail in the next section.

6.0 DISCUSSION OF RESULTS

6.1 Effect of Material Properties

The model exhibits significant sensitivity to the variations in material properties. The "weak" properties reflect only a 20% weakening of strength and stiffness parameters of the "norm" sandstone and bentonitic mudstone when compared to the "norm" set, and yet the results as represented by the parameters γ_{max} and ε_{max} (see Table 7) indicate significantly increased deterioration.

The extent of strain-damaged zones is also shown to increase quite dramatically. For example, in Run CN1D05/CN1S05, representing "norm" properties, a strain-damaged zone extends about 20 m under the bench horizontally, and into the coal layers immediately adjacent to the bentonitic mudstone near the toe of the slope (see Figs. A1.1 and A1.3). On the other hand, in Run CN1D06/CN1S06, representing "weak" properties, the strain-damaged zone evaluated based on similar failure criteria extends nearly 35 m under the bench horizontally. Further strain damage is inflicted on the coal measures above the bentonitic mudstone and even penetrating into the bankcut (see Figs. A2.1 and A2.3). Comparison of "norm" properties with "strong" properties shows a similar increase in stability in the latter case. This pattern is similar even in cases of steeper slope angles, as well as for simulations of 6-month excavation intervals.

Analysis of the tensile stresses in the bench reveals another source of instability. The peak tensile stress in the case of "weak" properties (CN1D06/CN1S06) is larger than the peak tensile stress in the case of "norm" or "strong" properties (runs CN1D05/CN1D06 and CN1D08/CN1S08, respectively). Such a trend contributes to increased probability of failure in two ways:

1) Increased tensile stress: and
2) Decreased tensile strengths associated with weaker properties in the "weak" set vis-a-vis the "norm" set.

Therefore, these two phenomena coincide to contribute to a higher risk of failure.

Practical consequences of "weak" properties may be realized due to seasonal effects and the presence of joints and discontinuities. Given stability estimations based on "norm" properties, any weakening of material properties could cause slope failure. Such weakening may occur due to:

1) Precipitation during the rainy season, causing an increase in the water table level:
2) Presence of a joint suitably aligned with the peak tensile stress direction: or
3) Pinching of strong sandstone layers that constitute the toe of the chopcut.

The current design of Pit 3 exhibits reasonable operational safety when "norm" properties are encountered. Intervention of any of the above 3 scenarios, resulting in weakening the properties, could result in slope failure.

6.2 Effect of Slope Angles

The model shows only slight sensitivity to changes in the slope angles. Generally, critical parameters like δ_{max}, γ_{max}, and ε_{max} were seen to increase very slightly with increasing slope steepness as exemplified by comparing normal slope angles (α=45°, β=57°) with a steeper variant (α=55°, β=72°) for a "norm" property run with a 3-month excavation cycle. This sensitivity was, however, not as pronounced as expected, given the observations made in Pit 3. Steeper slopes, however, displayed the same sensitivity vis-a-vis material properties (see Table 7) as the normal slope geometry simulations did. This suggests the predominance of material properties in determining stability.

One interesting observation can be made regarding peak tensile stress in the operating bench. This value is higher for steeper slopes as is evident from a comparison of the distributions in Figs. 2 and 3 for "norm" properties. This increased tensile stress (10% in the case under examination) could become a destabilizing factor if mining proceeds into weaker ground.

A good way of ensuring stability in weaker ground would be to decrease slope angles. This would allow reducing tensile stresses in the bench to within limits imposed by the reduced tensile strengths of weaker materials. The model thus indicates that material properties and slope angles would have to be treated in a simultaneous fashion and that their effects are not mutually exclusive. For example, mining in Pit 3 is now taking place in an area without a band of hard sandstone in the operating bench. However, test holes in virgin ground, approximately 200 m from the bench, reveal a band of such competent sandstone at the base of the proposed chopcut [2]. Conceivably, mining in this area could be performed with steeper slopes, barring the presence of discontinuities like joints or other factors mitigating strength.

Seasonal effects on ground properties should also be kept in mine, especially considering the fact that increased pore water pressure results in decreased material strength and greater susceptibility to slope failure. In addition, areas showing joints warrant careful slope redesign with smaller angles to prevent aggravation of instabilities caused by the tensile stresses in the bench.

Any effort to fine-tune the sensitivity of the model to slope changes must involve two subtasks:

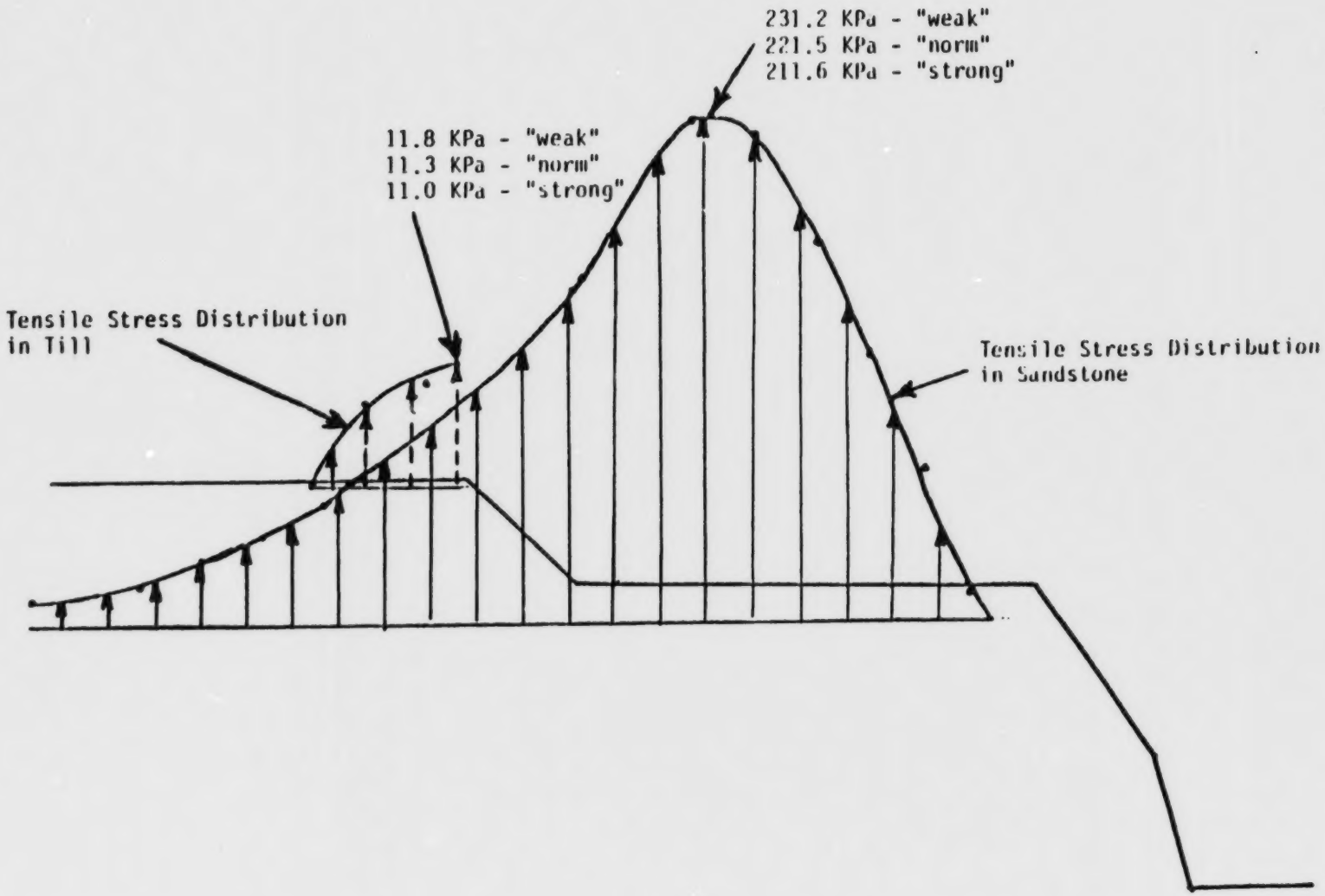
231.2 KPa - "weak"
221.5 KPa - "norm"
211.6 KPa - "strong"
11.8 KPa - "weak"
11.3 KPa - "norm"
11.0 KPa - "strong"
Tensile Stress Distribution in Till
Tensile Stress Distribution in Sandstone

FIG. 2. Tensile Stress Distribution in Normal Slope Geometry for Various Property Sets.

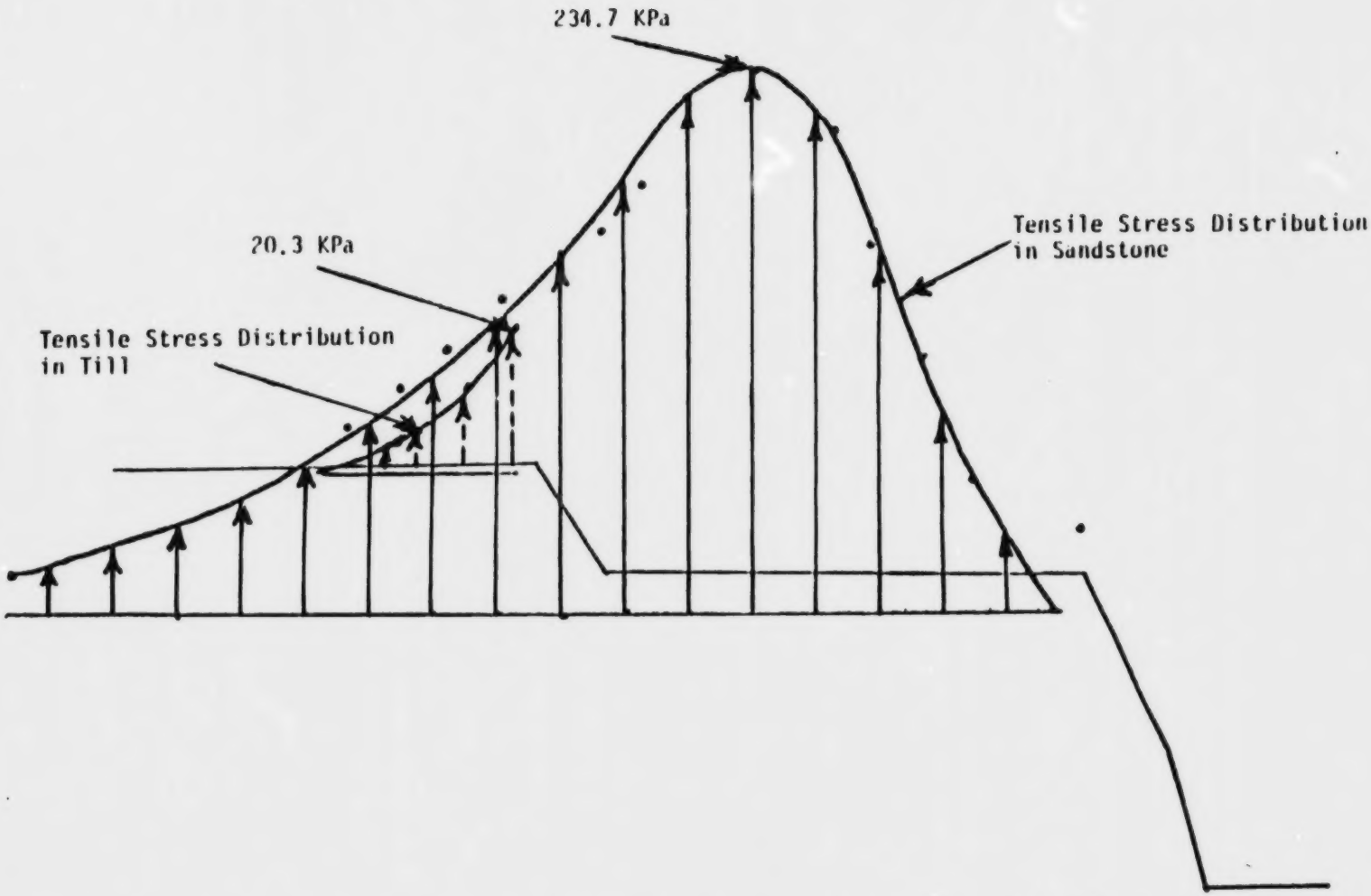

FIG. 3. Tensile Stress Distribution in Steepest Variant of Slope Geometry ($\alpha = 55°$, $\beta = 72°$) for "norm" Properties.

1) Simulating one excavation with a much smaller mesh, resulting in economy of effort, will allow quick determination of the input parameters that control sensitivity to slope changes.

2) By conducting intensive field deformation measurements at a chosen test/demonstration site, the model can be calibrated and made more site-specific. With information from this and the exercise described in Step 1, a suitable combination of input parameter modifications can be devised to improve stability to slope steepness.

6.3 Effect of Excavation Timing

Excavation timing refers to the time interval between consecutive excavations and is dictated by the demand for coal and other operational logistics. The results of simulations show very clearly that the larger the time interval between cuts, the greater the instability. this is true for all types of material property sets and angles. A comparison between a 3-month cycle simulation for normal operating conditions (Run CN1D05/CN1S05) and a 6-month cycle simulation with all other parameters remaining constant (Run CN1DT1/CN1ST1) reveals up to 50% increase in the accumulated strains, γ_{max} and ε_{max} (see Table 7).

Comparisons of the strain-damaged zones in both cases (refer to Figs. A1.1,A1.3 for CN1D05/CN1S05 and Figs. A.10.1,A10.3 for CN1DT1/CN1ST1) shows that in the 6-month cycle simulation, strain damage extends about 10 m further into the slope than in the 3-month cycle simulation. The vertical extent of the damage is also increased in the 6-month simulation, but not as dramatically. This pattern was repeated for simulations employing both steeper slopes (CN1DT3/CN1ST3) and strong properties (CN1DT2/CN1ST2).

Practical consequences of this finding are that when low demand for coal requires longer intervals between consecutive cuts, shallower slopes should be considered in areas where existing slopes may be vulnerable or marginal in design.

6.4 Effect of Excavation Sequence

The excavation sequence refers to the removal of coal after the excavation of the overburden. Two scenarios were studied, one involving a 20-day interval between the two events, and the other in which both occurred simultaneously. The latter was found to represent a worst case scenario with respect to slope stability, as is evident from a comparison of Runs CN1D05/CN1S05 and TESD02/TESS02. The latter shows smaller amounts of accumulated strain, γ_{max} and ε_{max} (see Table 7). It is observed that by leaving the coal in for 20 days after the overburden is mined, accumulation of strains is slightly retarded. However, if the coal is left unexcavated for too long a period, the probability of a bankcut failure due to the weak bentonitic mudstone layer just above the coal measures increases.

6.5 Effect of Initial Stress State

The model exhibits a large amount of sensitivity to a change in the initial or in situ stress state. Run CN1D05/CN1S05 employed an initial hydrostatic stress state, while TESD10/TESS10 represented a 20% excess lateral stress, all other parameters being the same. Table 7 shows the increased amount of instability caused by the 20% excess horizontal stress. Comparison of octahedral shear strain plots for the two simulations reveals significant lateral and vertical extension of the strain-damaged zones in the bench. Significant damage is revealed to extend about 25 m under the bench in the case with excess lateral stress, and also to the sandstones in the bench above the coal measures (Fig. A18.1). Similar comparisons are also found to hold true for steeper slopes.

The practical consequences of this finding will be manifested in areas of Pit 3 west of 4300W where the excess lateral stress (maximum principal stress in the ground) acts in a direction perpendicular to the slope face. This follows from previous studies of earth stresses which have determined that the maximum principal stress acts in the southwest/northeast direction.

7.0 CONCLUSIONS

The following conclusions were drawn from the parametric investigation of the Pit 3 slope.

1) The stability of the pit slope is heavily dependent on the properties of the ground. Even a marginal weakening of some of the constituents of the mine geology was shown to result in an appreciable increase in instability. The effect of environmental conditions, joints, weakness zones, and other factors should be studied closely with respect to material properties and slope stability.

2) The model did not show much sensitivity to slope angles, but revealed a 10% increase in peak tensile stresses in the bench for a design variant that was steeper than normal. This could contribute to greater instability, especially in weaker areas. The two parameters, slope steepness and material properties, were shown to be interdependent.

3) The excavation timing or interval was shown to have a significant effect on the stability of a slope. Greater strains and deformations were accumulated for simulations allowing greater intervals between successive excavations.

4) Removal of coal simultaneously with mining of the overburden was found to represent a worst case scenario and to cause greater strain damage at the toe of the slope. On the other hand, removal of coal 20 days after overburden excavation mitigated such strain damage near the toe at the expense of the bankcut stability.

5) The model shows significant sensitivity to lateral stresses that are in excess of the vertical stress. Excessive lateral stresses resulted in higher strains and deformation, and consequently in greater chances for slope failure.

8.0 RECOMMENDATIONS

8.1 Site-Specific Design for Pit 3

The "norm" property set and normal slope angle simulations showed marginal stability with a 3-month cutting cycle. In Pit 3, mining advance looks likely to move into an area with stronger sandstones that were sampled in Holes HV-86-901 and -902 [2]. Pit slopes could, if necessary, be made steeper to take advantage of the increased strength afforded by this sandstone. Weaker areas must be mined with shallower angles to avoid the mutually reinforcing effects of lower tensile strengths and higher tensile stresses. Areas with joints and discontinuities must be treated likewise to prevent aggravation of instability.

Longer intervals between excavations, if foreseen, should be accommodated by reducing slope angles. Likewise, retention of the coal for a few weeks after the chopcut and bankcut excavations, as is being practiced, improved stability.

8.2 Future Model Development

The site-specific model for Pit 3 needs a few improvements. A program of activities leading to such an enhancement could be summarized as follows:

1) Employing a 1-stage excavation reduced scale model. A few economical simulations could yield insight into the reason for the relative insensitivity to slope geometry. Based on the results, input parameters could be adjusted to increase such sensitivity.

2) A field test/demonstration site should be set up and instrumented with deformation measuring devices immediately after excavation. Such deformation measurements should be compared with results of application of the model to simulate the test slope. By minimizing the difference between measured and predicted behaviors, the model can be improved and made more accurate.

3) Once these two steps have been carried out, the model should be reapplied to determine a more accurate site-specific Pit 3 design.

The improved model, with some modifications, will then be ready for application to other sites in the Highvale mine.

REFERENCES

1. Serata Geomechanics, Inc., April, 1987, "Model Development Report," prepared for CANMET.

2. Serata Geomechanics, Inc., March, 1987, "Field/laboratory testing report," prepared for CANMET.

3. Monenco, Ltd., July 1984, "Highvale mine -- 1983 geotechnical report," vol. 1, prepared for TransAlta Utilities.

4. Monenco, Ltd., December 1984, "Highvale mine -- 1984 monitoring program, year end report," prepared for TransAlta Utilities.

5. Monenco, Ltd., February, 1986, "Highvale mine -- 1985 geological and geotechnical data collection report," prepared for TransAlta Utilities.

6. Monenco, Ltd., January, 1987, "Highvale mine -- 1986 geological and geotechnical data collection report," prepared for TransAlta Utilities.

7. Gay, N.C., 1980, "The state of stress in plates," Dynamics of Plate Interiors, Geodynamics Series, vol. 1.

8. Gough, D.I., and Bell, J.S., 1981, "Stress orientations from oil well fractures in Alberta and Texas," National Research Council of Canada.

9. Fordjor, C.K., Bell, J.S., and Gough, D.I., 1983, "Breakouts in Alberta and stress in North American plate," Canadian Journal of Earth Science, vol. 20.

APPENDIX A

RESULTS FROM MODEL APPLICATION

RUN DESIGNATION	-	CN1D05/CN1S05
MATERIAL PROPERTY	-	"Norm"
SLOPE GEOMETRY	-	$\alpha = 45°$, $\beta = 57°$
EXCAVATION TIMING	-	3 months
EXCAVATION SEQUENCE	-	Simultaneous Coal/Overburden Removal
INITIAL STRESS STATE	-	Hydrostatic

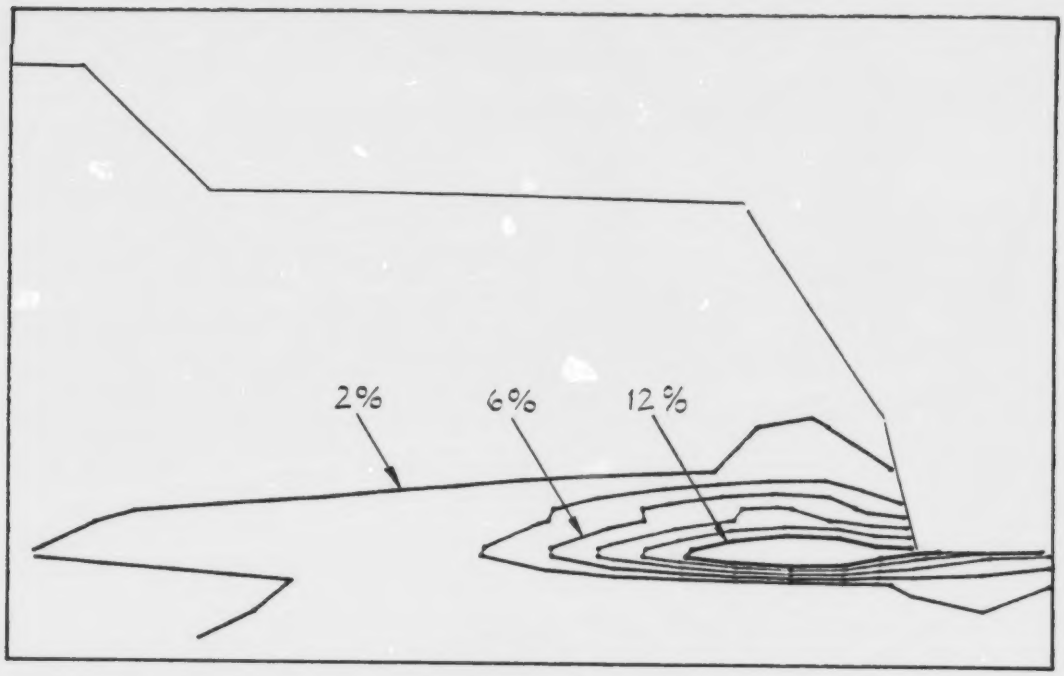

FIG. A.1.1 Octahedral Shear Strain Contour Plot for the Final Slope.

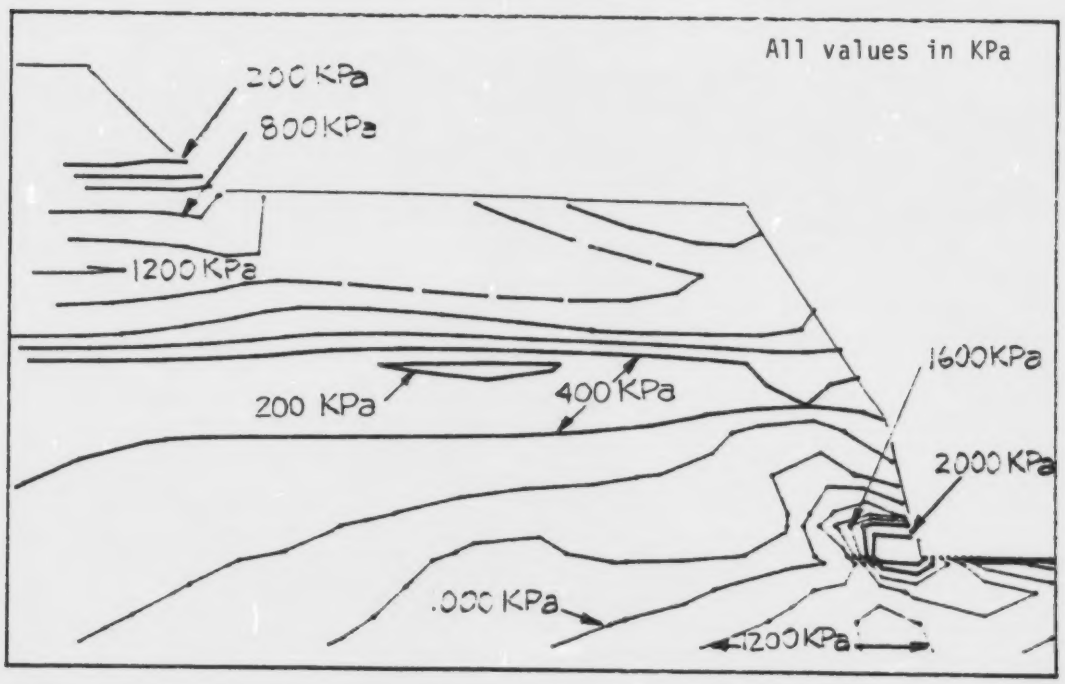

FIG. A.1.2 Octahedral Shear Stress Contour Plot for the Final Slope.

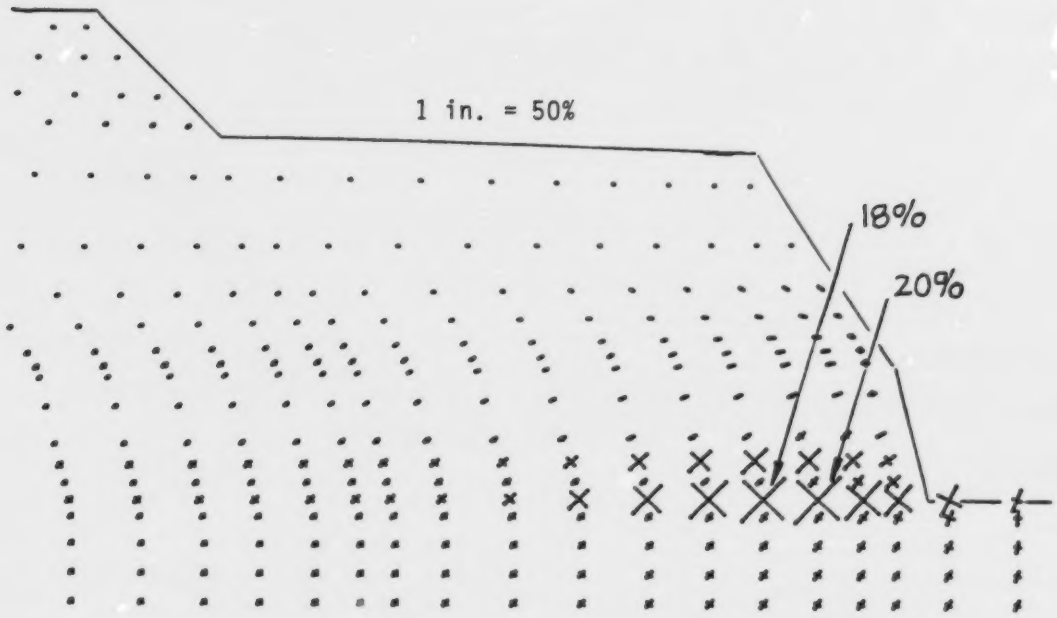

FIG. A.1.3 Principal Strain Distribution Around Final Slope.

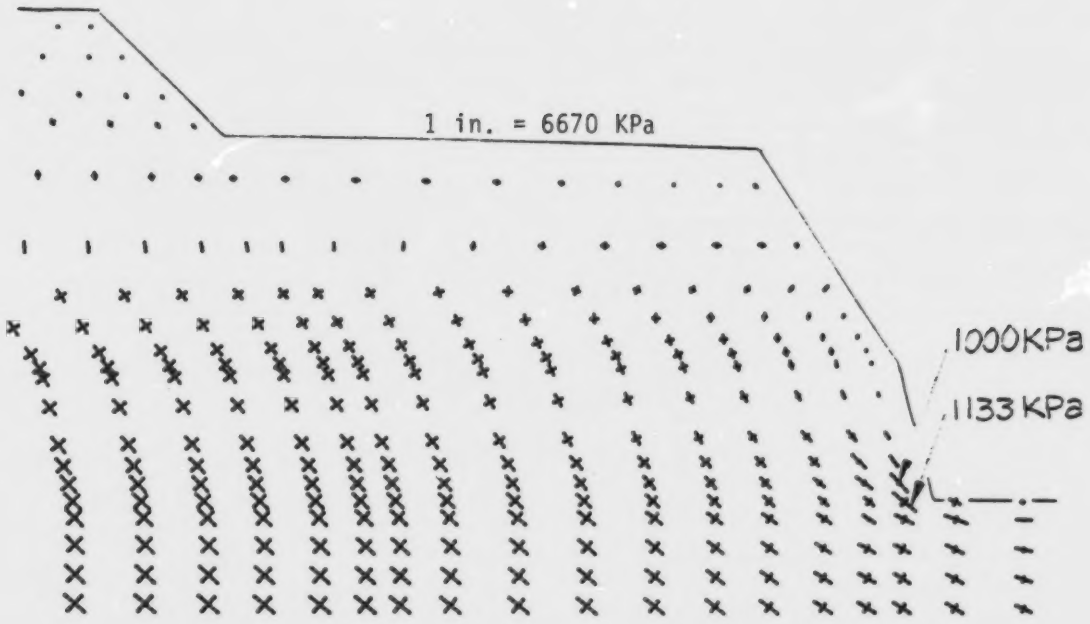

FIG. A.1.4 Principal Stress Distribution Around Final Slope.

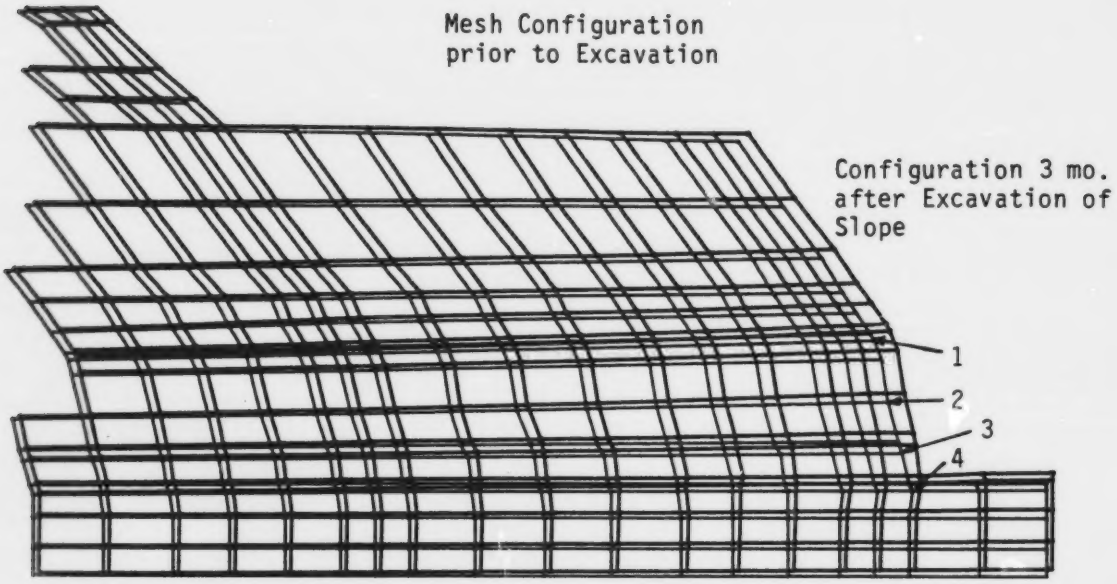

FIG. A.1.5 Deformation of Mesh Corresponding to Final Slope.

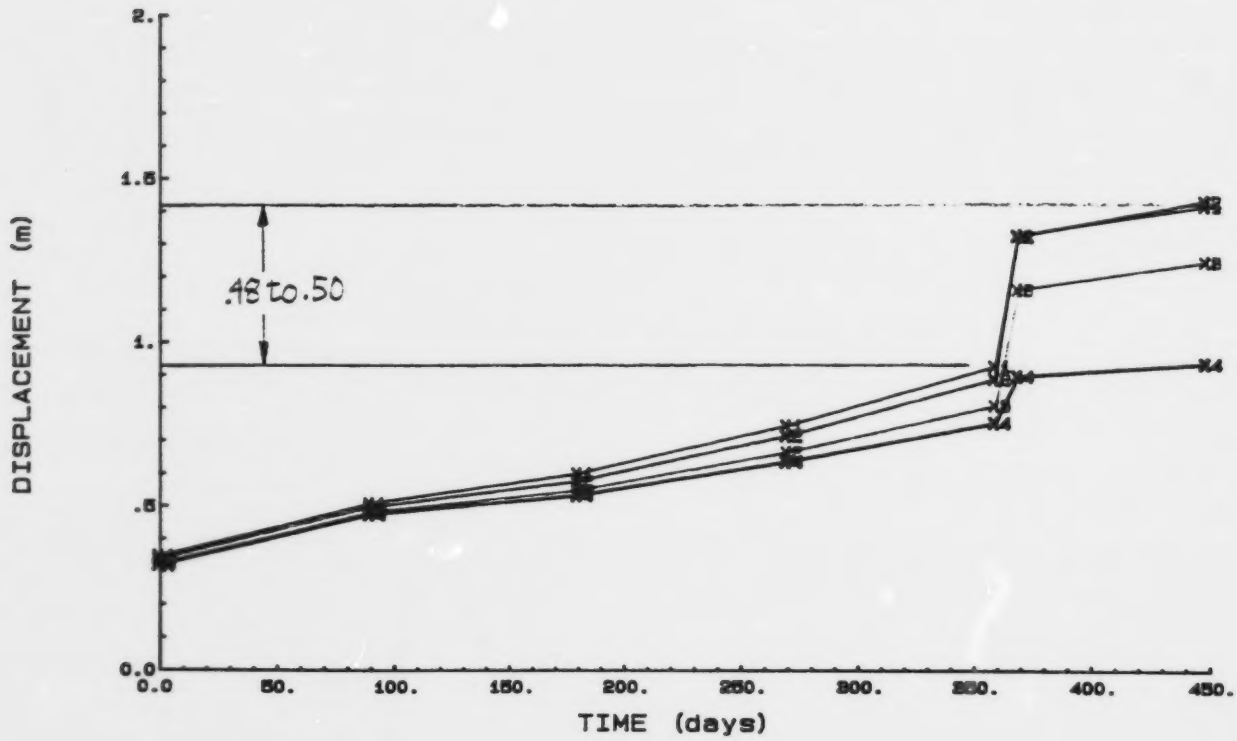

FIG. A.1.6 Displacement of Critical Nodes in the Final Slope as a Function of Time.

RUN DESIGNATION	-	CN1D06/CN1S06
MATERIAL PROPERTY	-	"Weak"
SLOPE GEOMETRY	-	$\alpha = 45°, \beta = 57°$
EXCAVATION TIMING	-	3 months
EXCAVATION SEQUENCE	-	Simultaneous Coal/Overburden Removal
INITIAL STRESS STATE	-	Hydrostatic

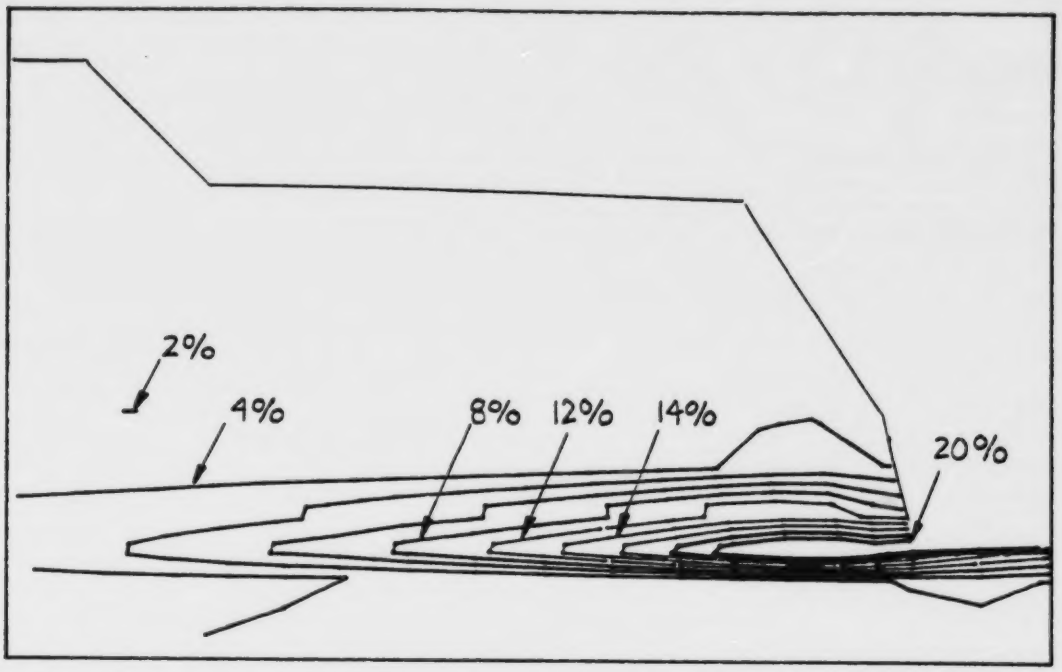

FIG. A.2.1 Octahedral Shear Strain Contour Plot for the Final Slope.

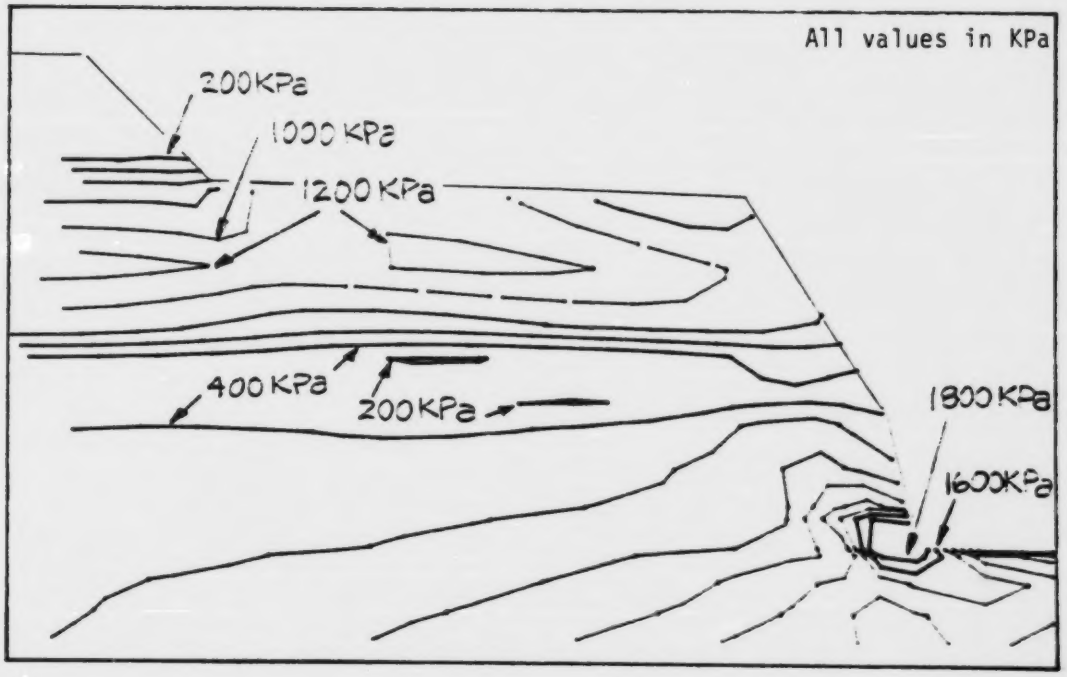

FIG. A.2.2 Octahedral Shear Stress Contour Plot for the Final Slope.

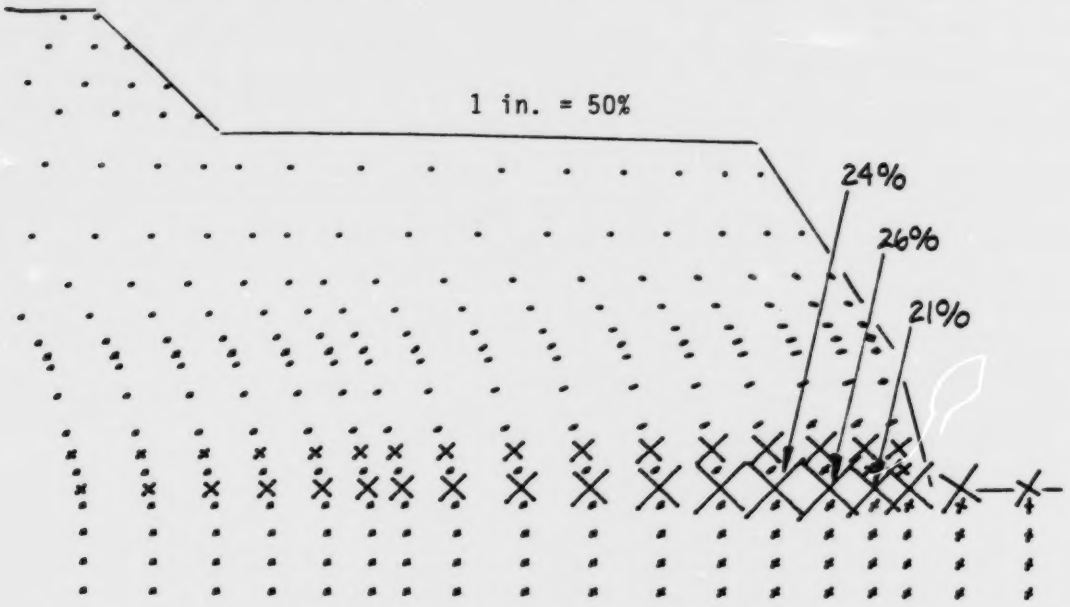

FIG. A.2.3 Principal Strain Distribution Around Final Slope.

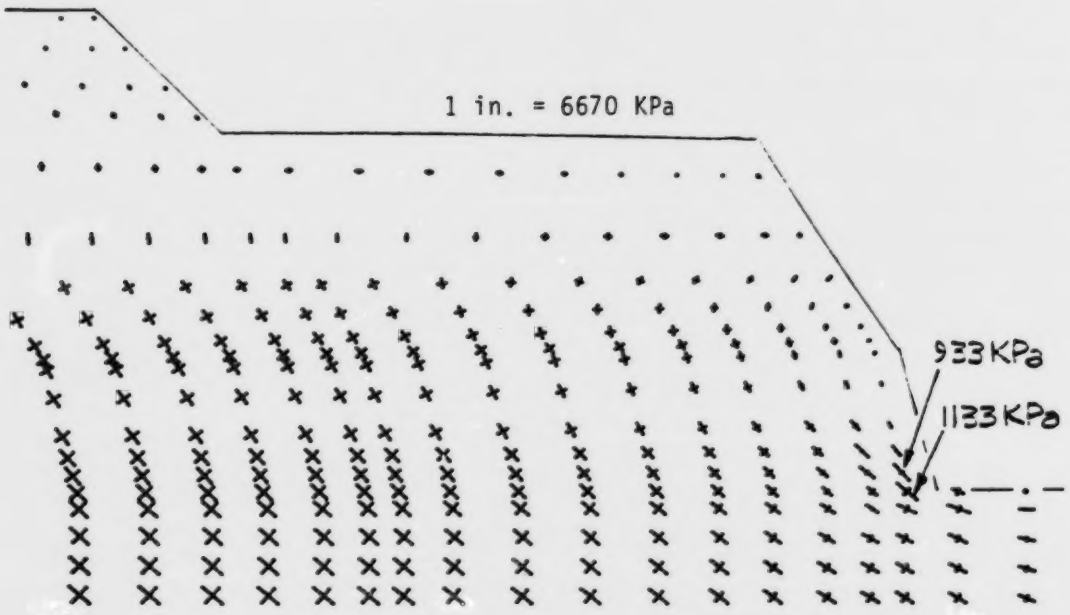

FIG. A.2.4 Principal Stress Distribution Around Final Slope.

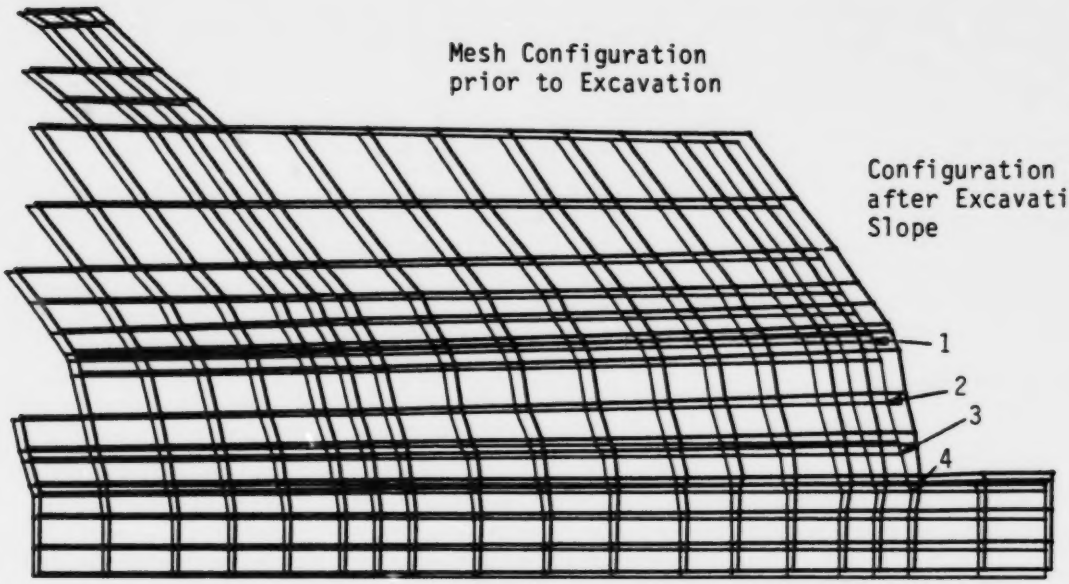

FIG. A.2.5 Deformation of Mesh Corresponding to Final Slope.

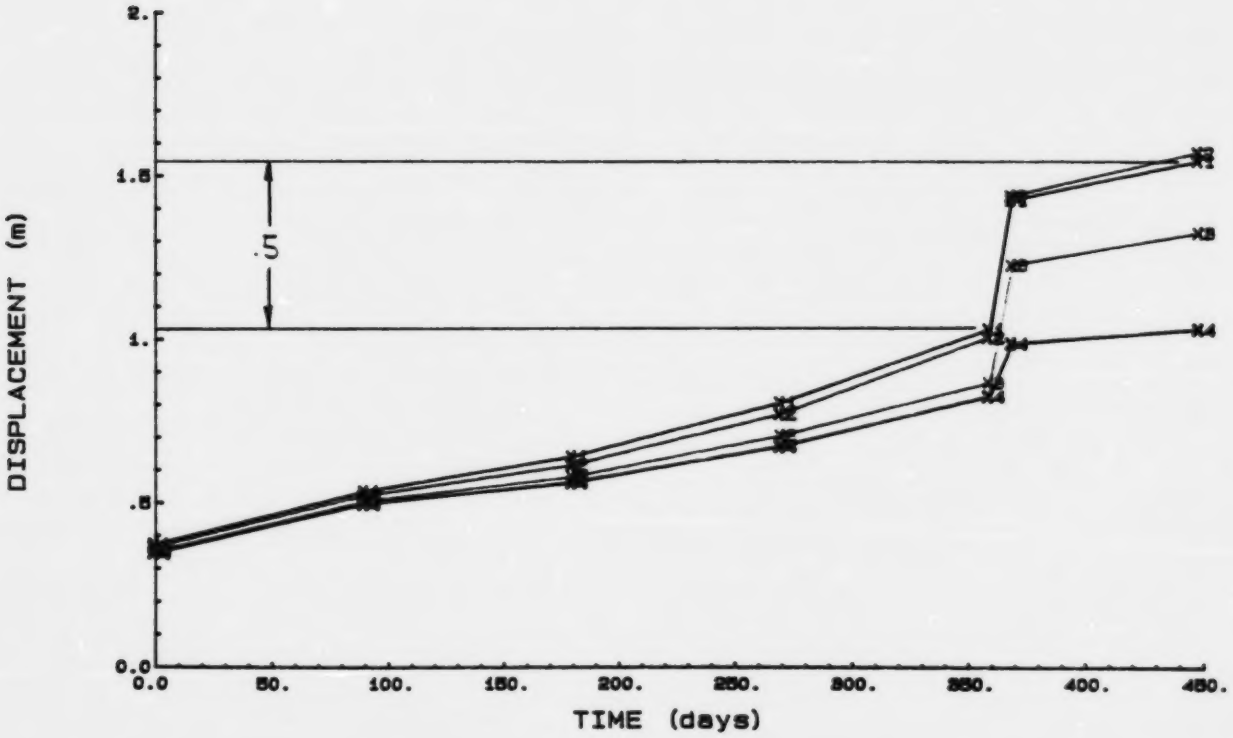

FIG. A.2.6 Displacement of Critical Nodes in the Final Slope as a Function of Time.

RUN DESIGNATION	-	CN1DO8/CN1SO8
MATERIAL PROPERTY	-	"Strong"
SLOPE GEOMETRY	-	$\alpha = 45°$, $\beta = 57°$
EXCAVATION TIMING	-	3 months
EXCAVATION SEQUENCE	-	Simultaneous Coal/Overburden Removal
INITIAL STRESS STATE	-	Hydrostatic

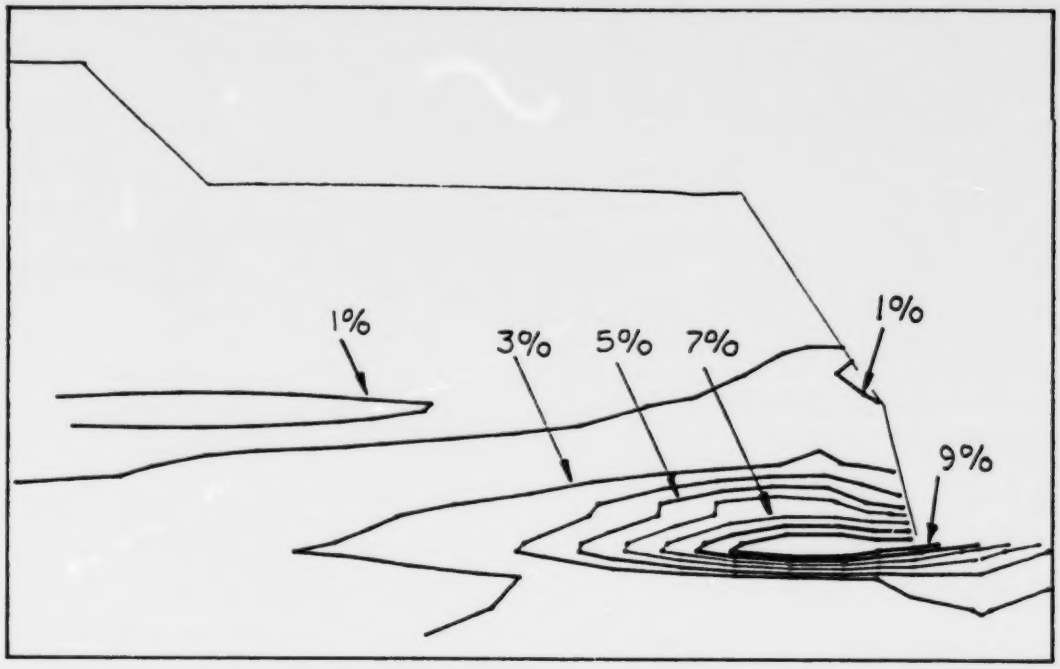

FIG. A.3.1 Octahedral Shear Strain Contour Plot for the Final Slope.

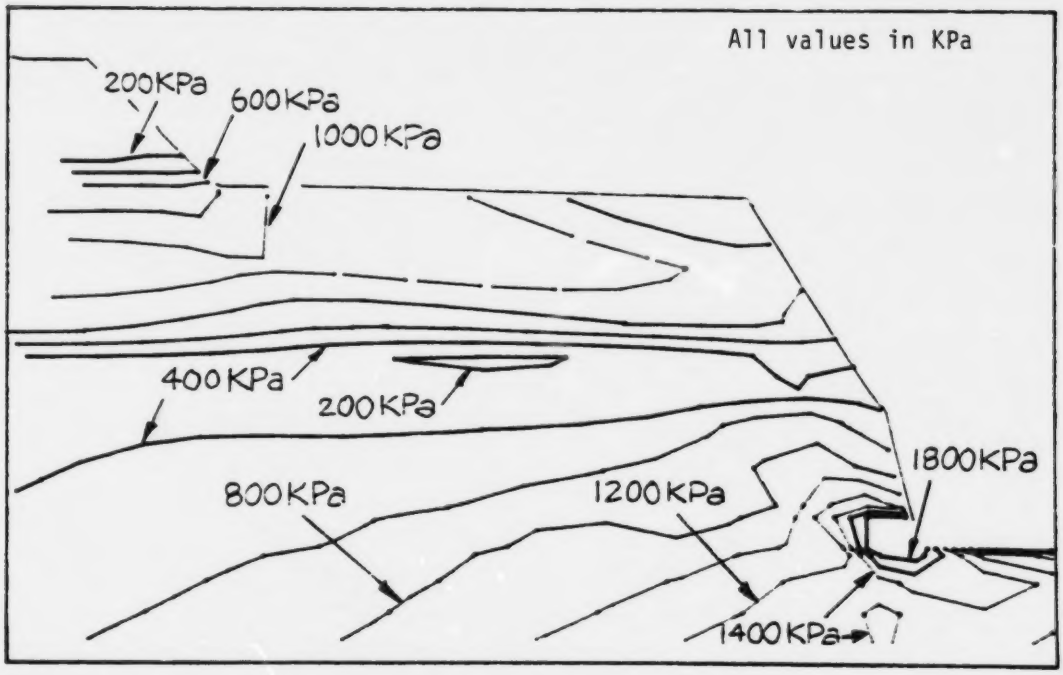

FIG. A.3.2 Octahedral Shear Stress Contour Plot for the Final Slope.

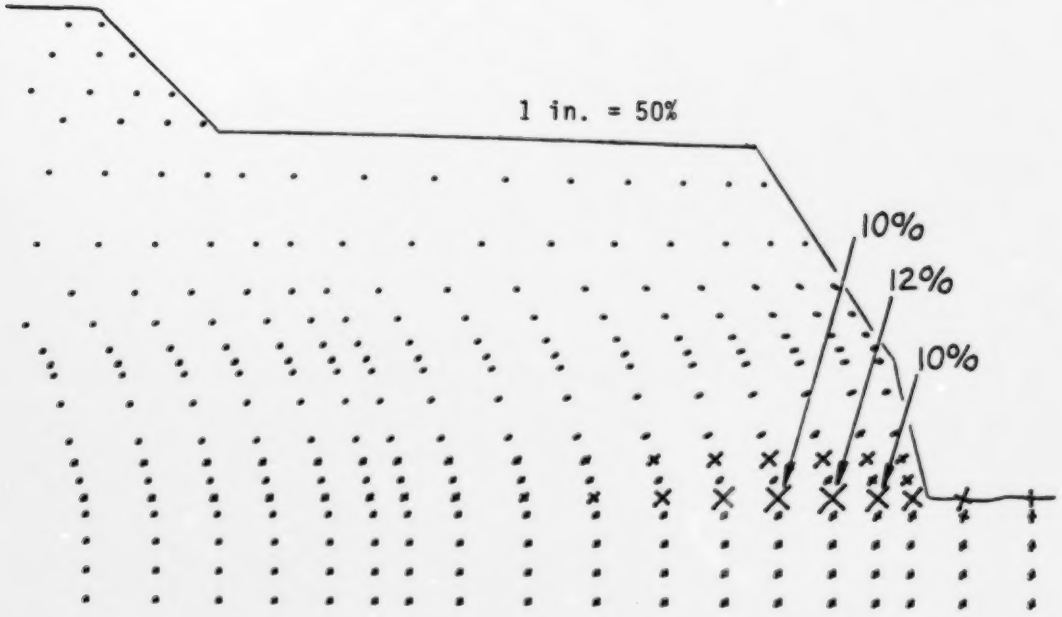

FIG. A.3.3 Principal Strain Distribution Around Final Slope.

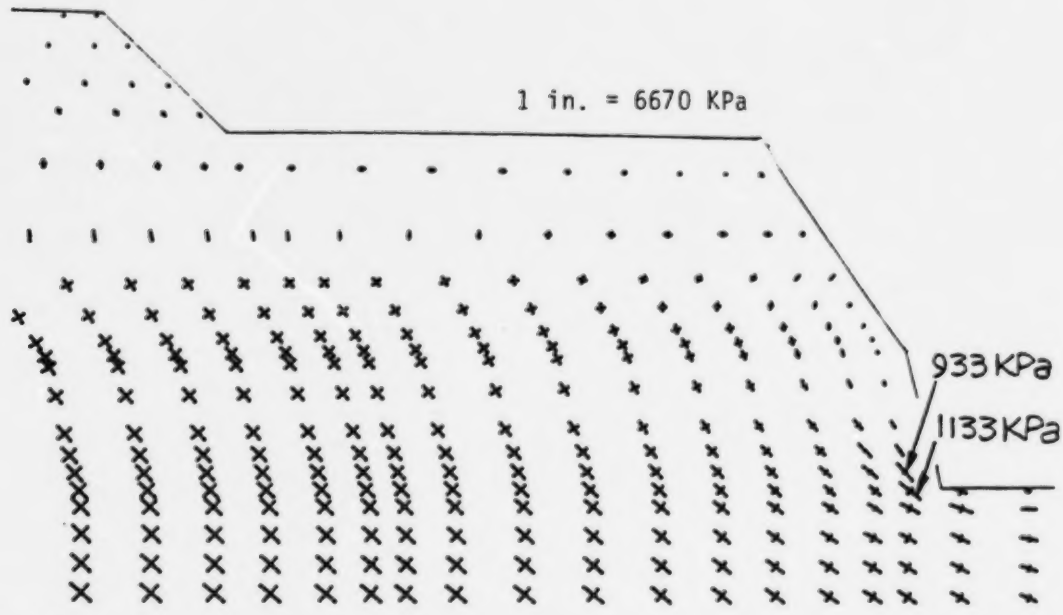

FIG. A.3.4 Principal Stress Distribution Around Final Slope.

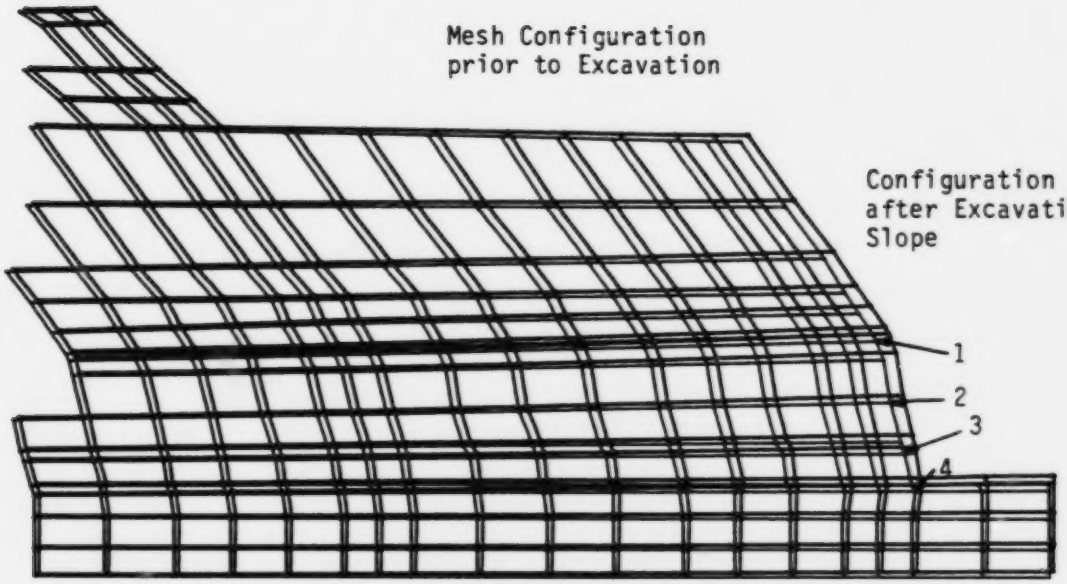

FIG. A.3.5 Deformation of Mesh Corresponding to Final Slope.

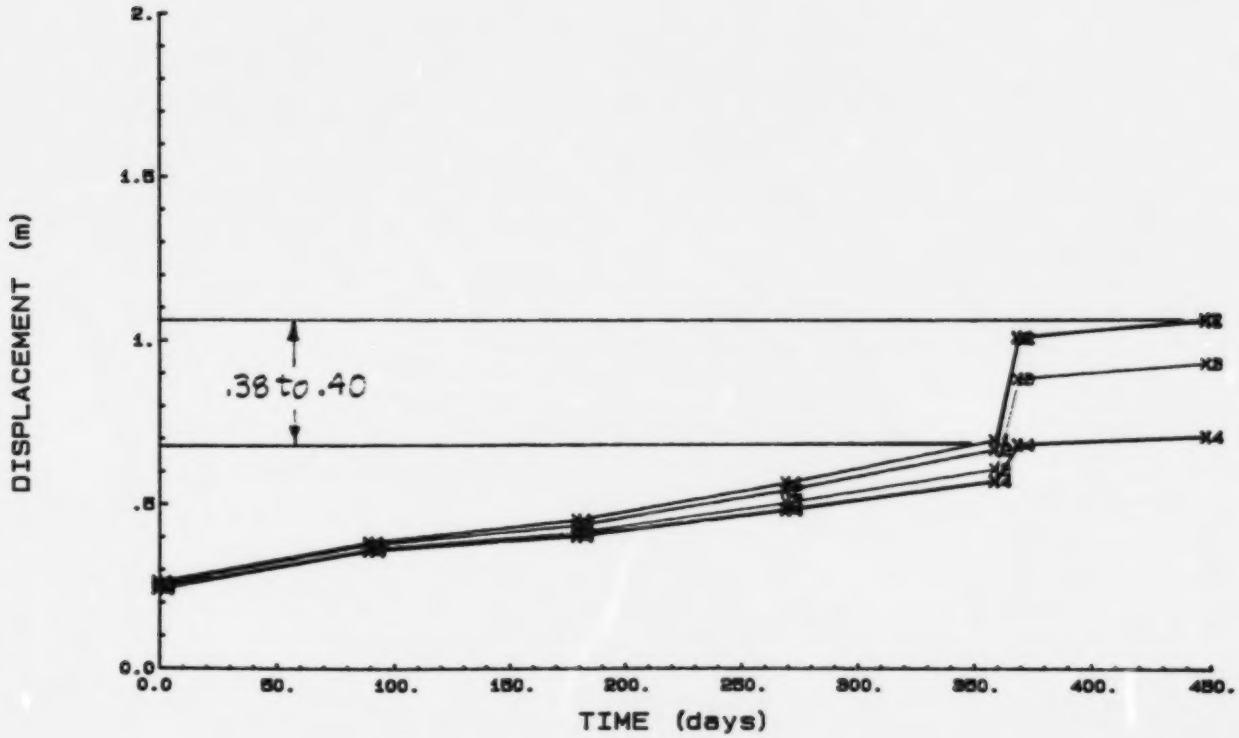

FIG. A.3.6 Displacement of Critical Nodes in the Final Slope as a Function of Time.

RUN DESIGNATION	-	CN1DG6/CN1SG6
MATERIAL PROPERTY	-	"Norm"
SLOPE GEOMETRY	-	$\alpha = 50°$ $\beta = 65°$
EXCAVATION TIMING	-	3 months
EXCAVATION SEQUENCE	-	Simultaneous Coal/Overburden Removal
INITIAL STRESS STATE	-	Hydrostatic

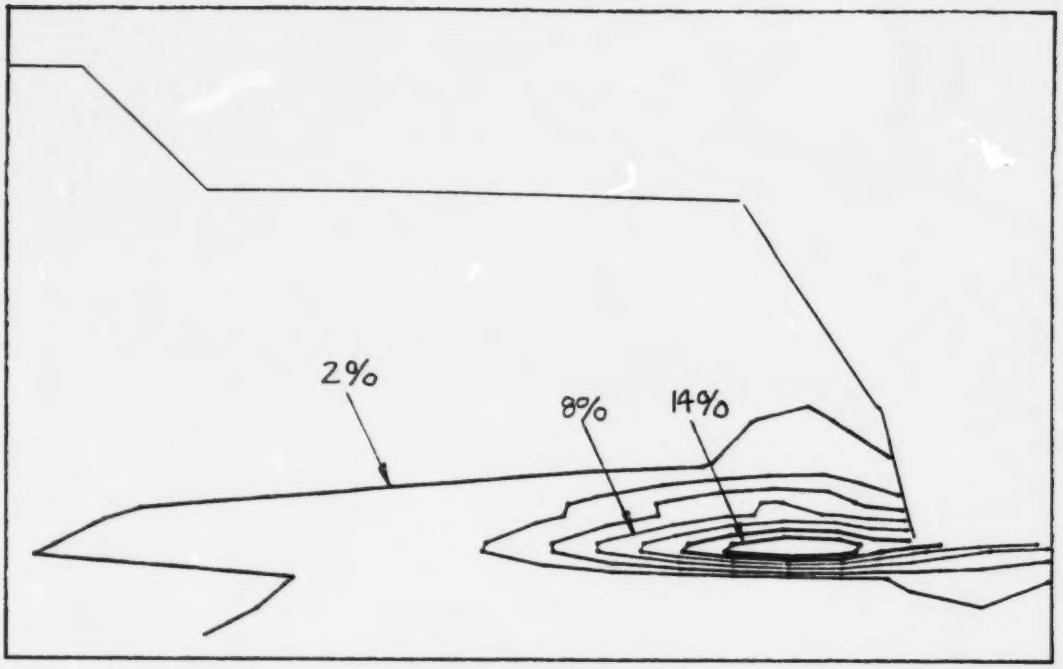

FIG. A.4.1 Octahedral Shear Strain Contour Plot for the Final Slope.

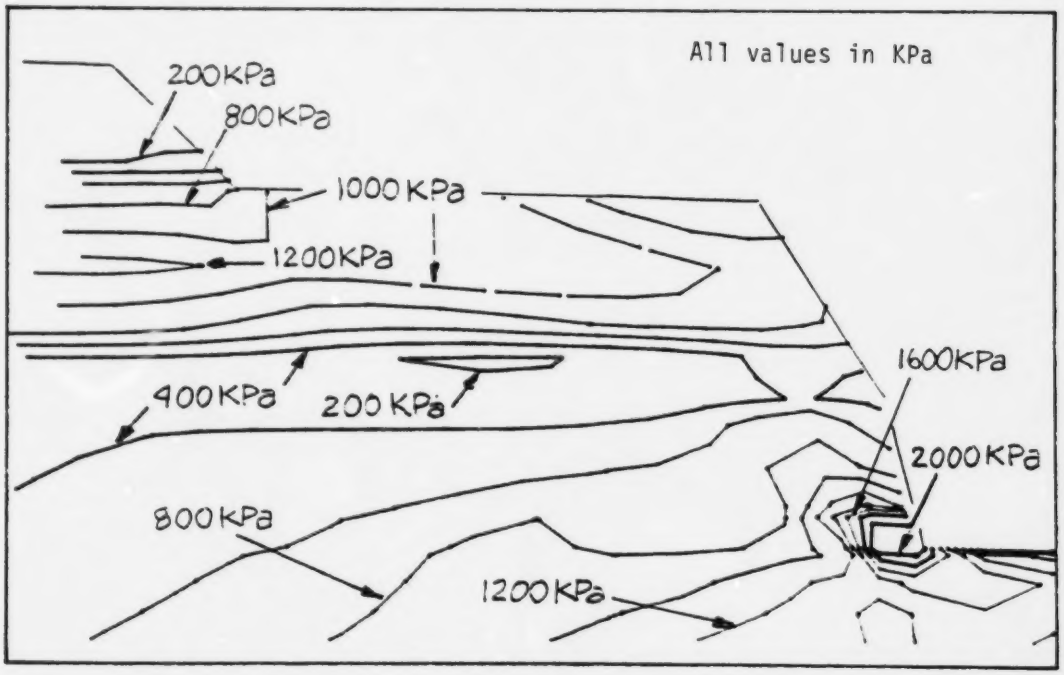

FIG. A.4.2 Octahedral Shear Stress Contour Plot for the Final Slope.

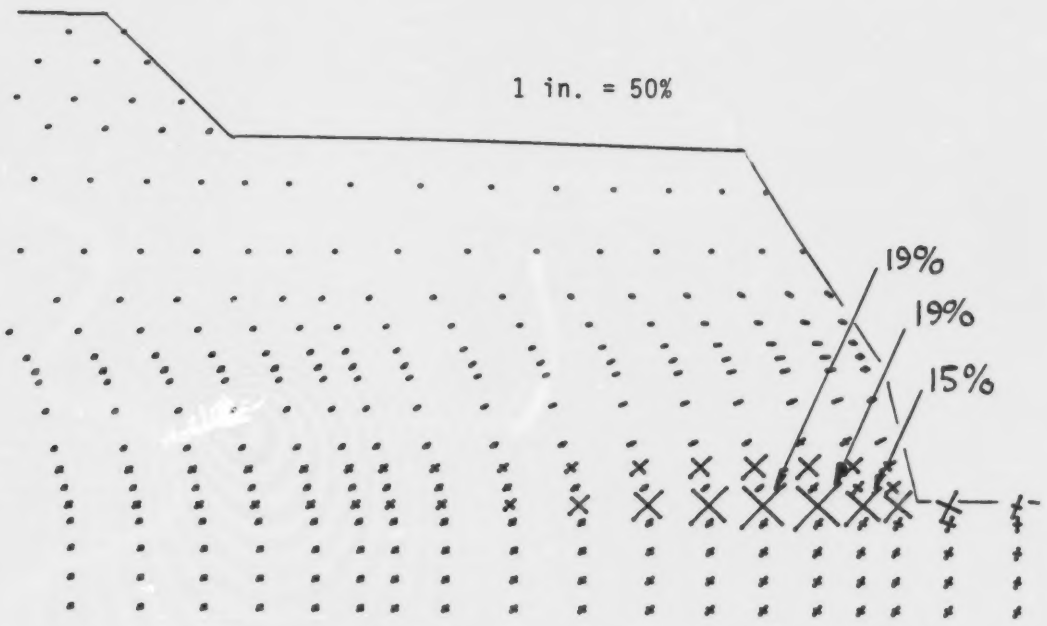

FIG. A.4.3 Principal Strain Distribution Around Final Slope.

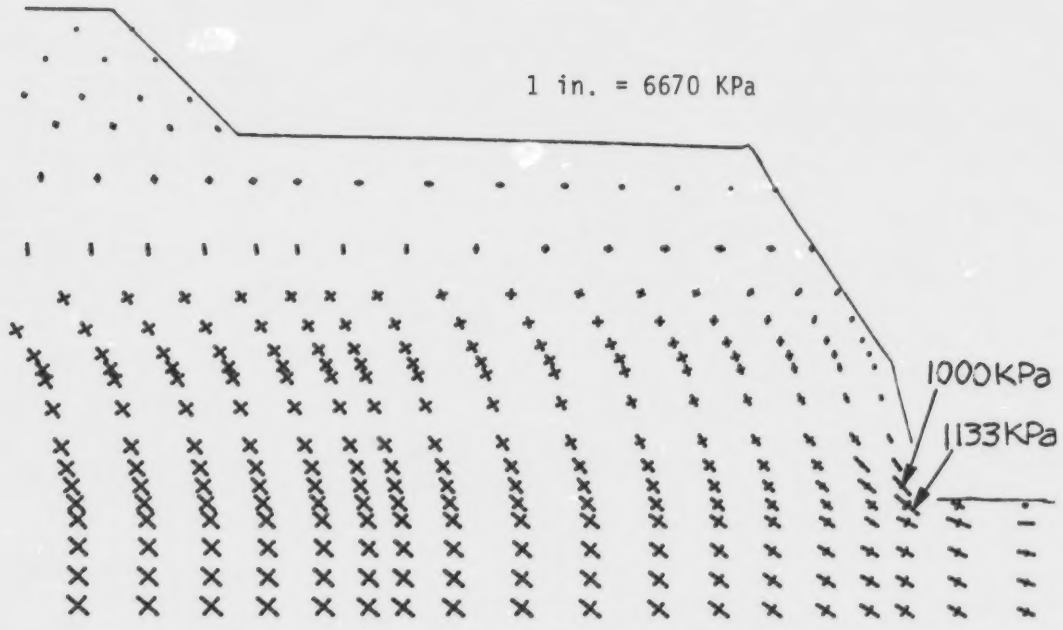

FIG. A.4.4 Principal Stress Distribution Around Final Slope.

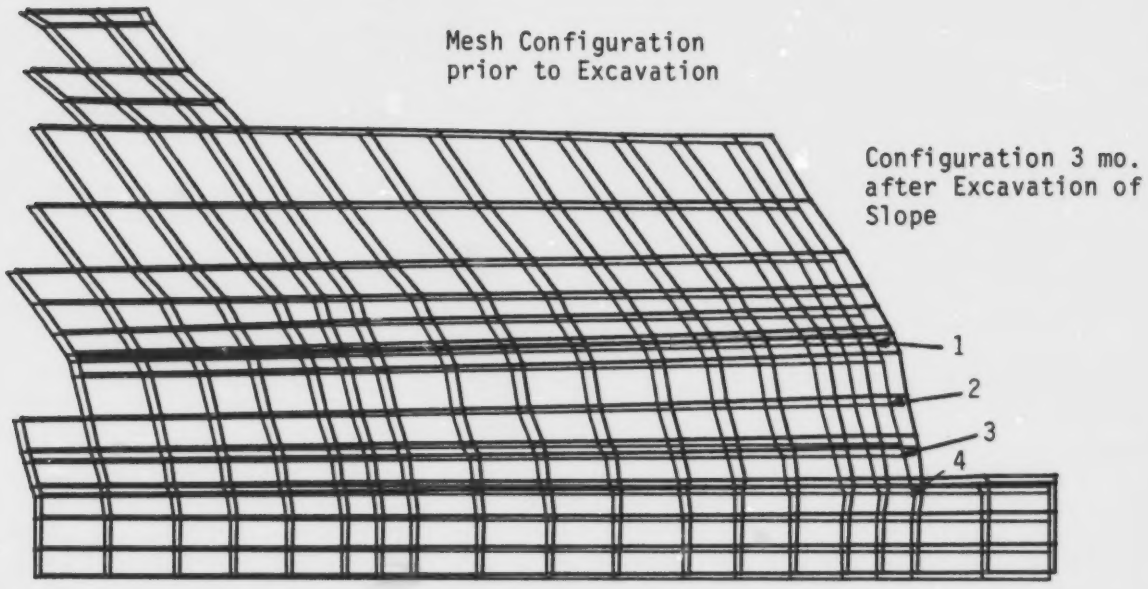

FIG. A.4.5 Deformation of Mesh Corresponding to Final Slope.

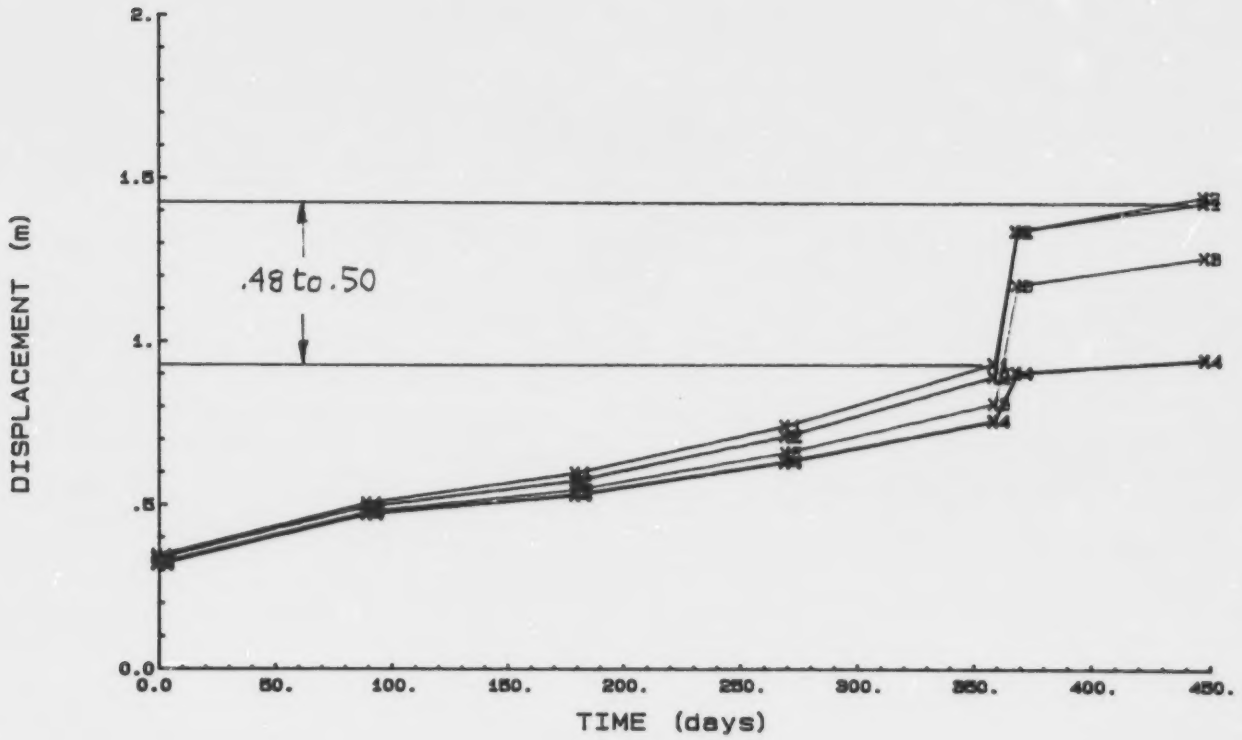

FIG. A.4.6 Displacement of Critical Nodes in the Final Slope as a Function of Time.

RUN DESIGNATION	-	CN1DG7/CN1SG7
MATERIAL PROPERTY	-	"Weak"
SLOPE GEOMETRY	-	$\alpha = 50°$, $\beta = 65°$
EXCAVATION TIMING	-	3 months
EXCAVATION SEQUENCE	-	Simultaneous Coal/Overburden Removal
INITIAL STRESS STATE	-	Hydrostatic

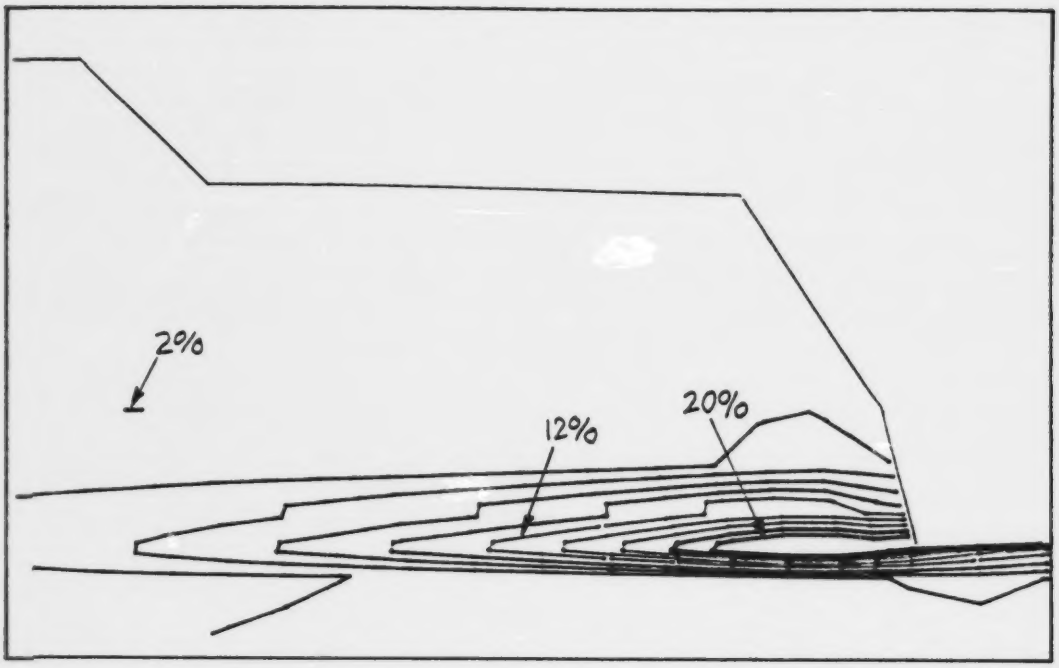

FIG. A.5.1 Octahedral Shear Strain Contour Plot for the Final Slope.

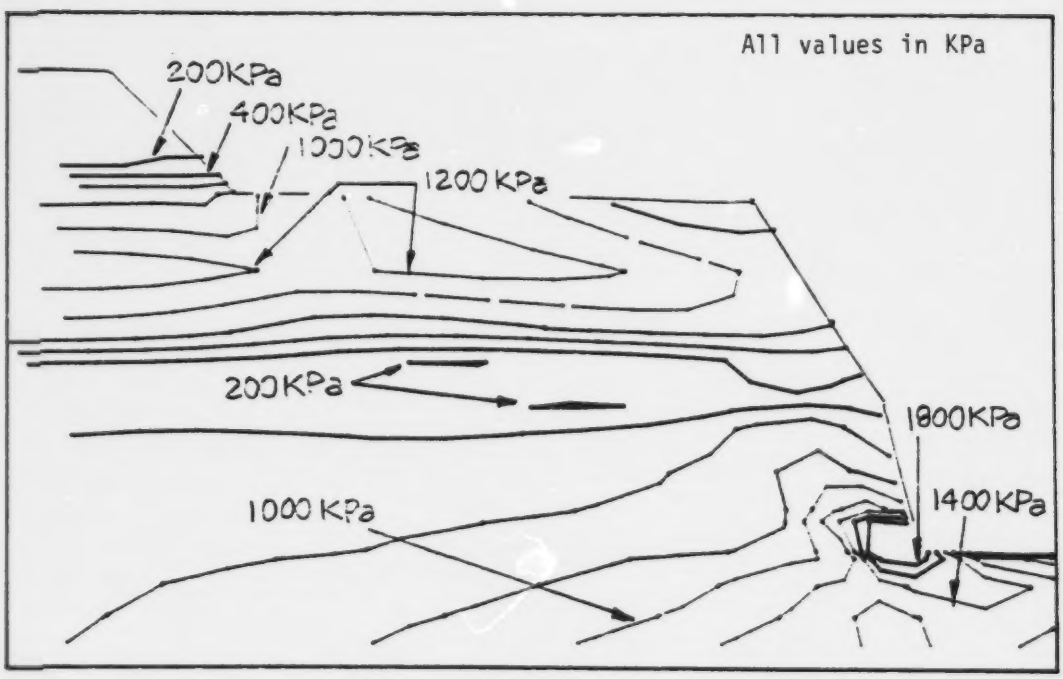

FIG. A.5.2 Octahedral Shear Stress Contour Plot for the Final Slope.

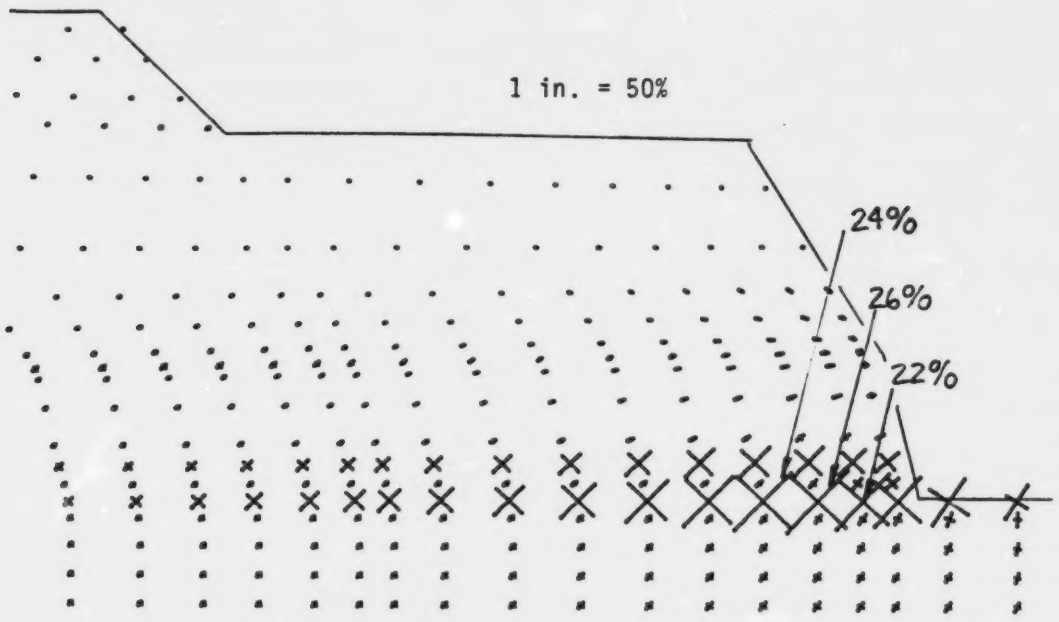

FIG. A.5.3 Principal Strain Distribution Around Final Slope.

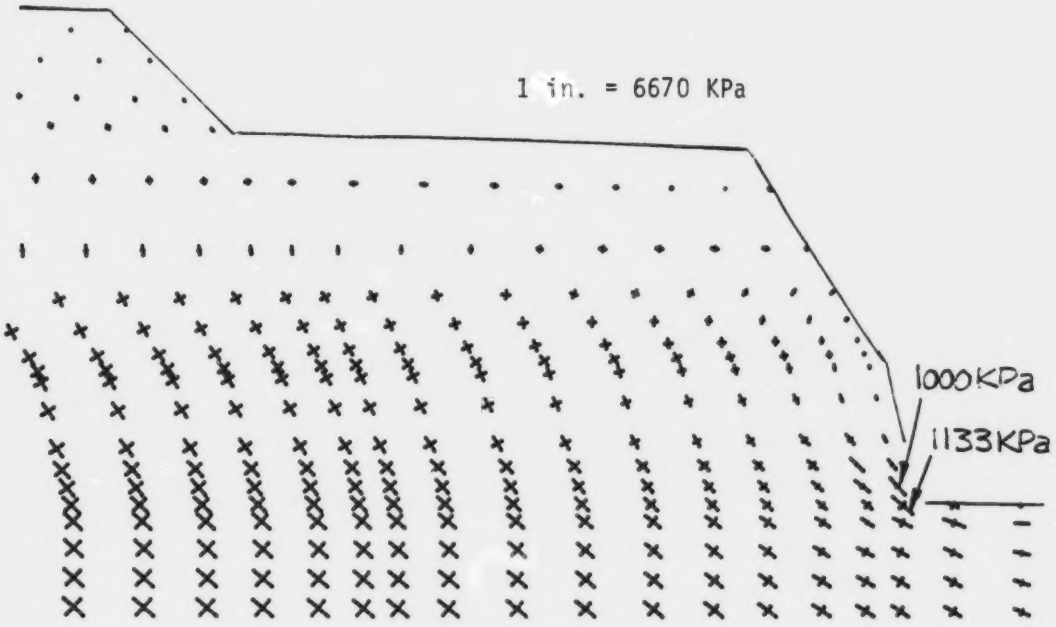

FIG. A.5.4 Principal Stress Distribution Around Final Slope.

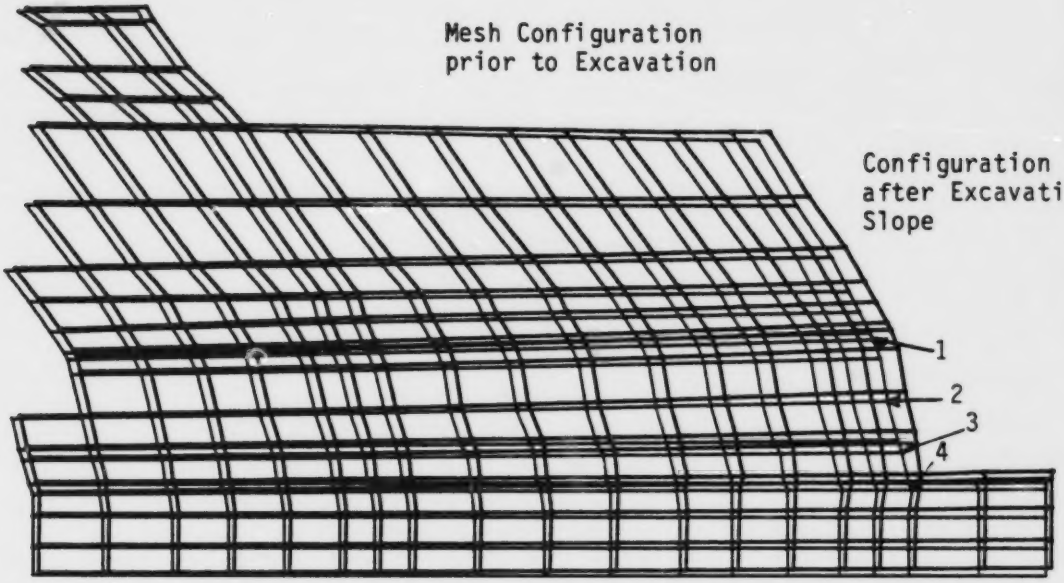

FIG. A.5.5 Deformation of Mesh Corresponding to Final Slope.

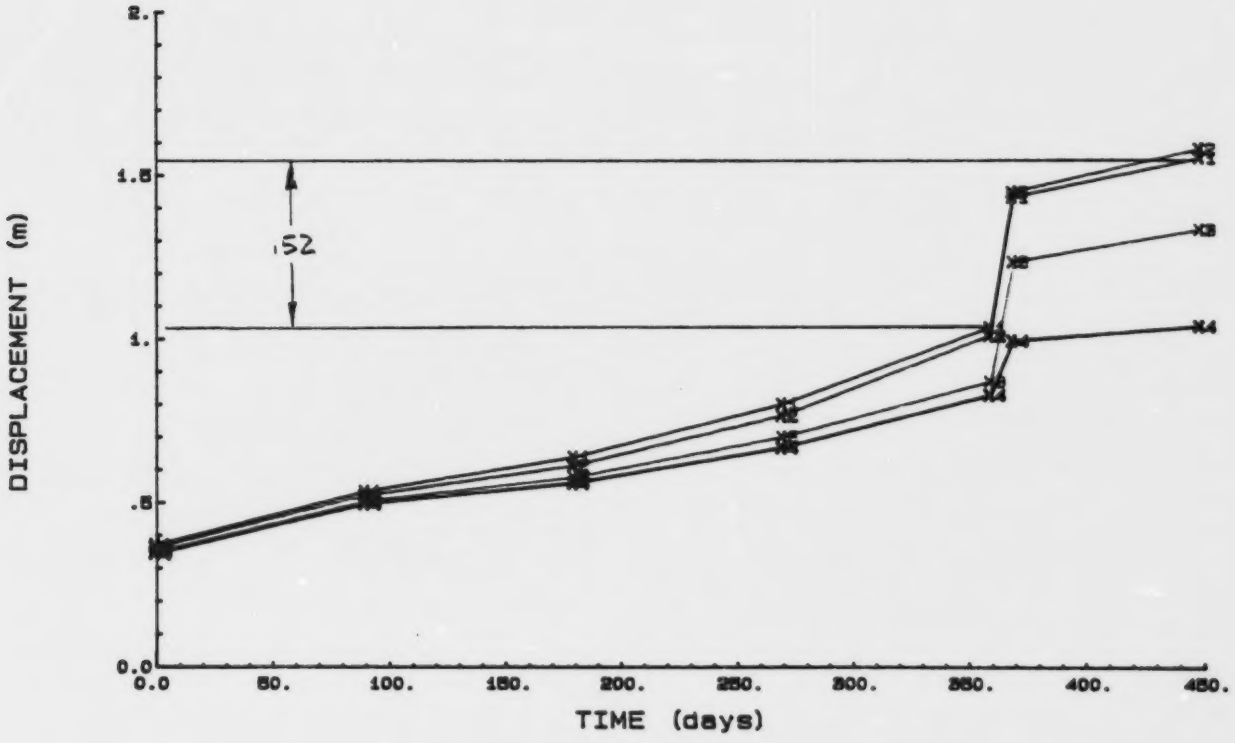

FIG. A.5.6 Displacement of Critical Nodes in the Final Slope as a Function of Time.

RUN DESIGNATION	-	CN1DG3/CN1SG3
MATERIAL PROPERTY	-	"Strong"
SLOPE GEOMETRY	-	$\alpha = 50°$ $\beta = 65°$
EXCAVATION TIMING	-	3 months
EXCAVATION SEQUENCE	-	Simultaneous Coal/Overburden Removal
INITIAL STRESS STATE	-	Hydrostatic

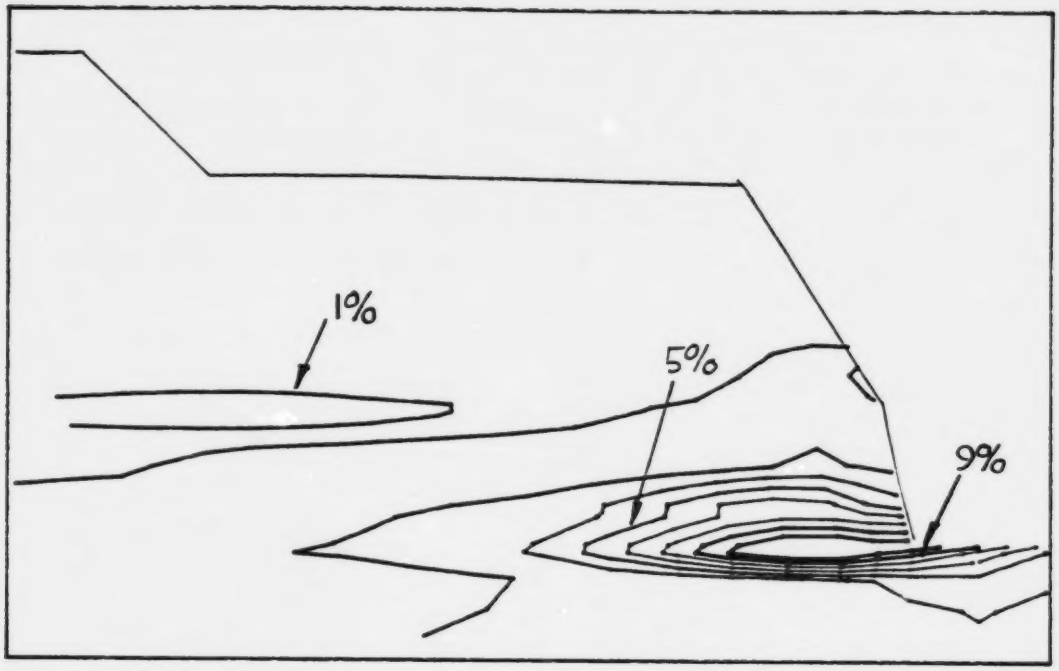

FIG. A.6.1 Octahedral Shear Strain Contour Plot for the Final Slope.

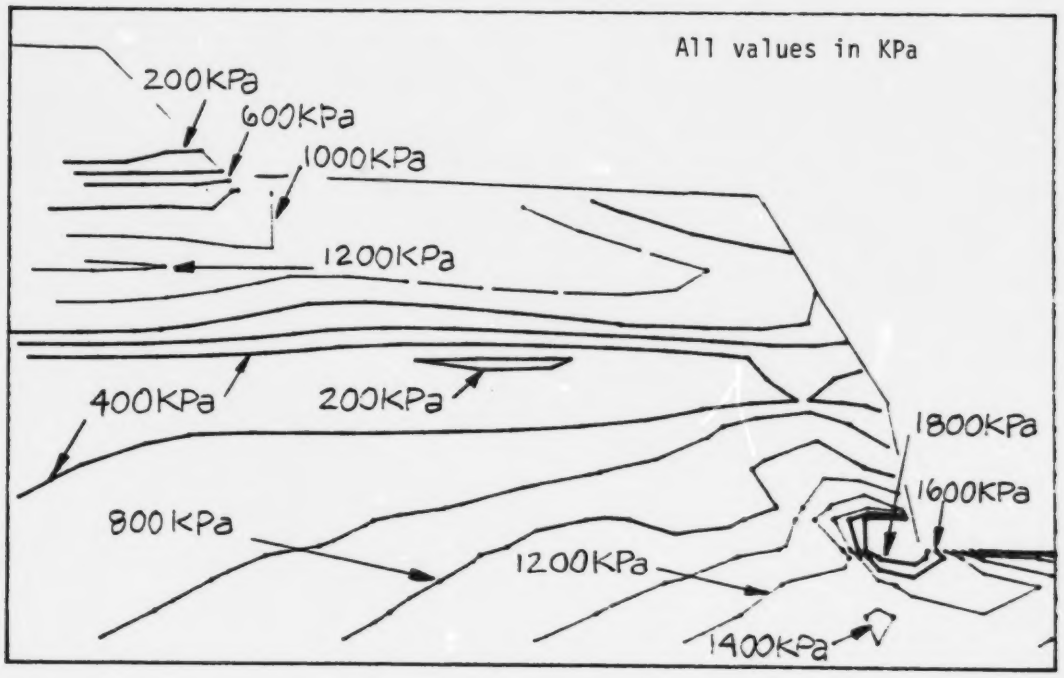

FIG. A.6.2 Octahedral Shear Stress Contour Plot for the Final Slope.

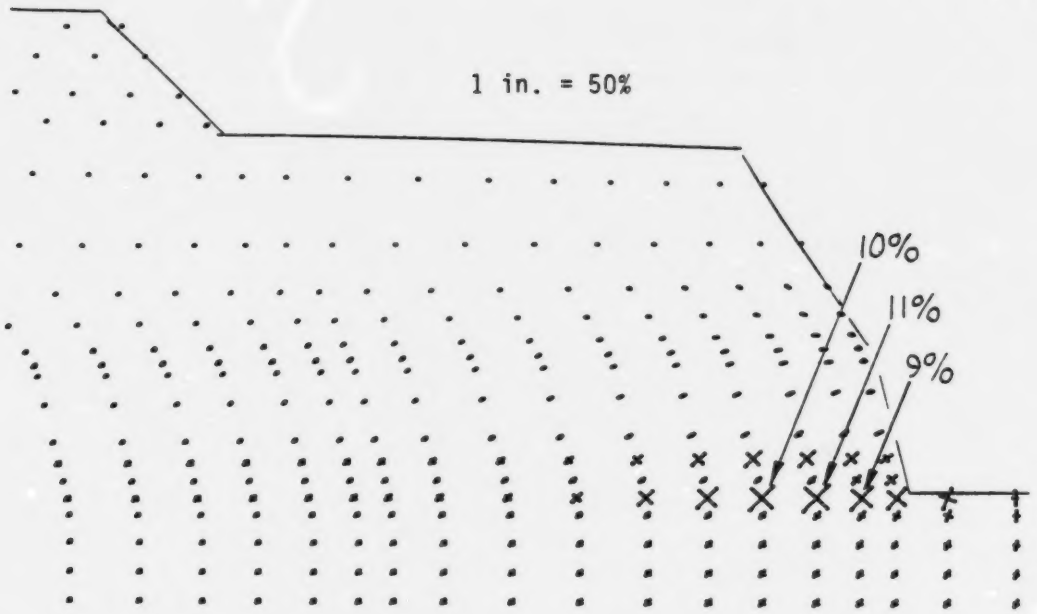

FIG. A.6.3 Principal Strain Distribution Around Final Slope.

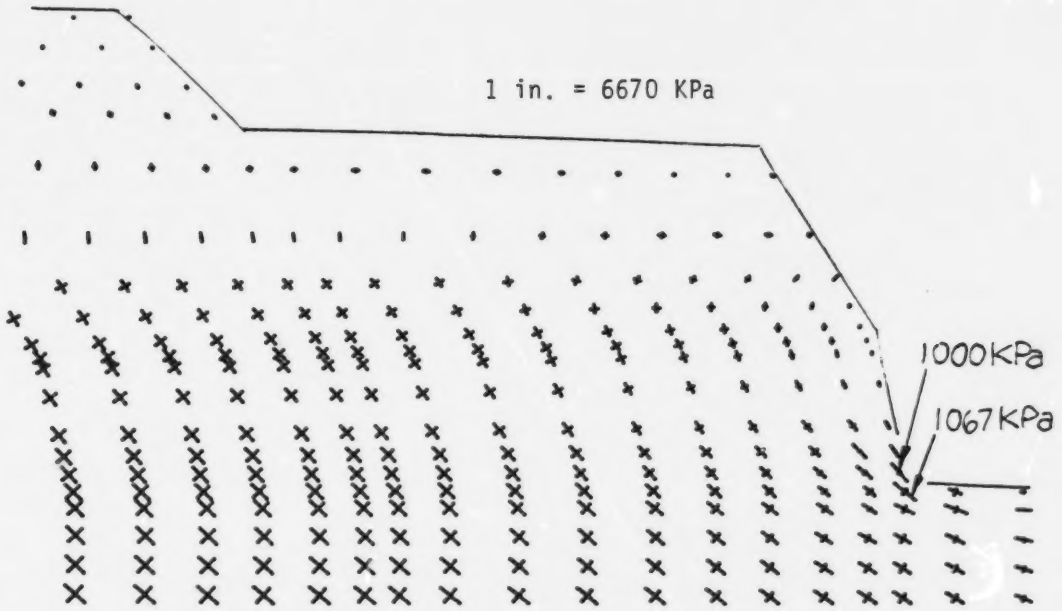

FIG. A.6.4 Principal Stress Distribution Around Final Slope.

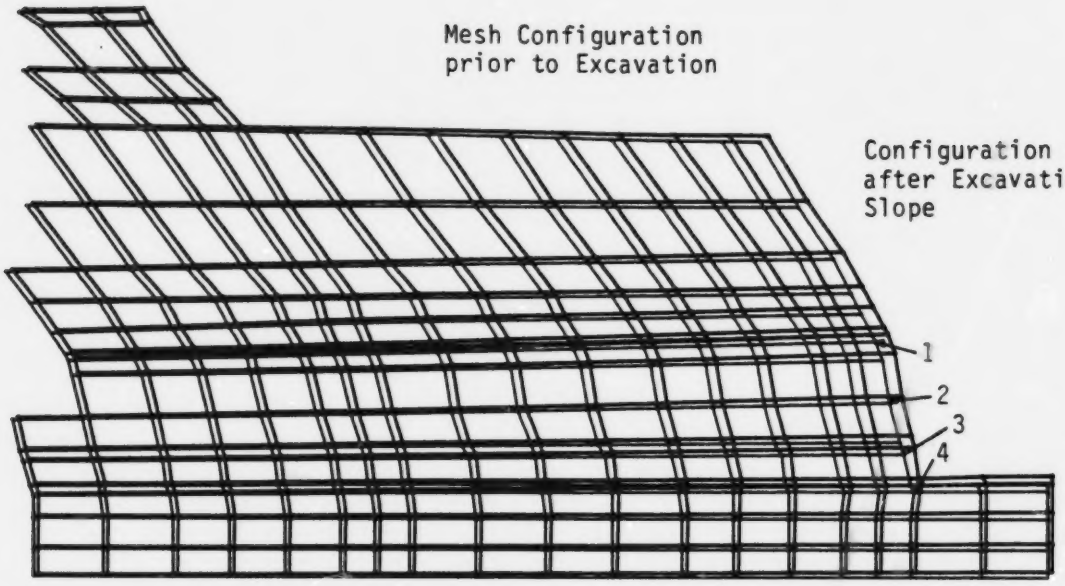

FIG. A.6.5 Deformation of Mesh Corresponding to Final Slope.

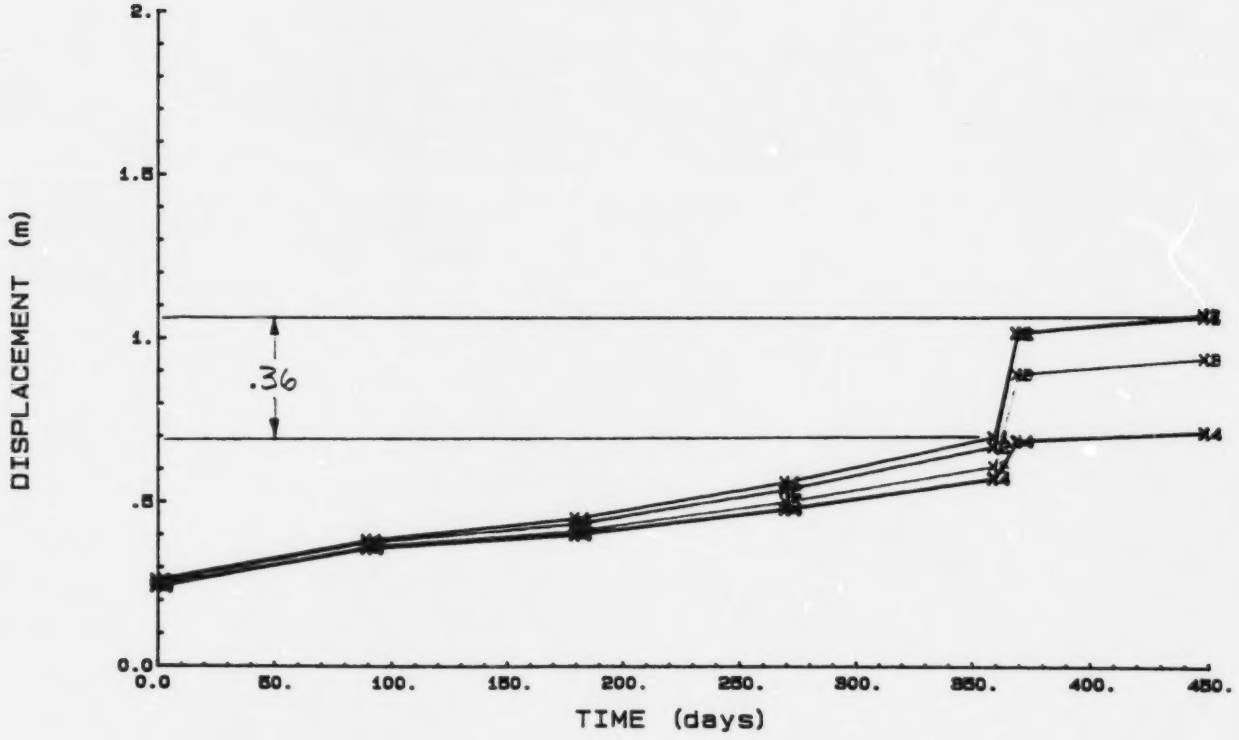

FIG. A.6.6 Displacement of Critical Nodes in the Final Slope as a Function of Time.

RUN DESIGNATION	-	CN1DG8/CN1SG8
MATERIAL PROPERTY	-	"Norm"
SLOPE GEOMETRY	-	$\alpha = 55°$, $\beta = 72°$
EXCAVATION TIMING	-	3 months
EXCAVATION SEQUENCE	-	Simultaneous Coal Overburden Removal
INITIAL STRESS STATE	-	Hydrostatic

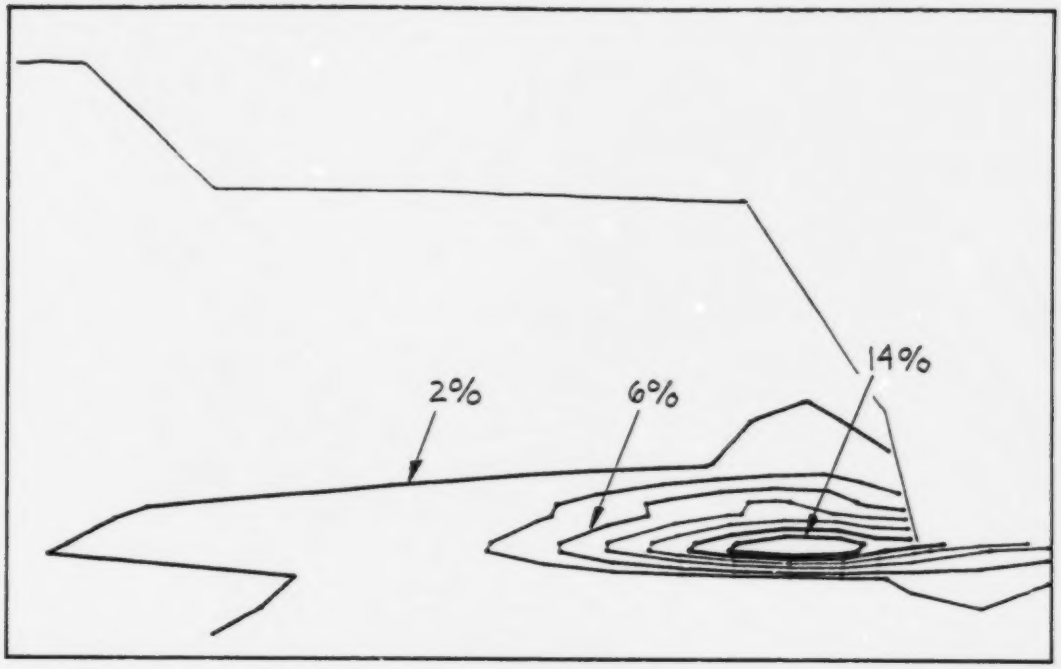

FIG. A.7.1 Octahedral Shear Strain Contour Plot for the Final Slope.

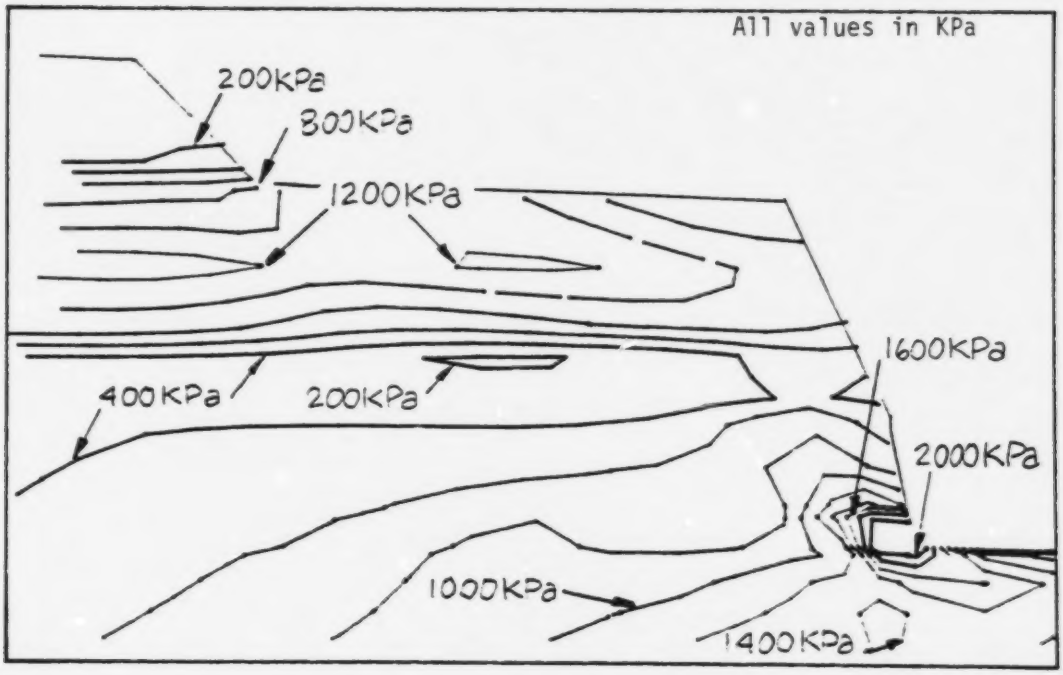

FIG. A.7.2 Octahedral Shear Stress Contour Plot for the Final Slope.

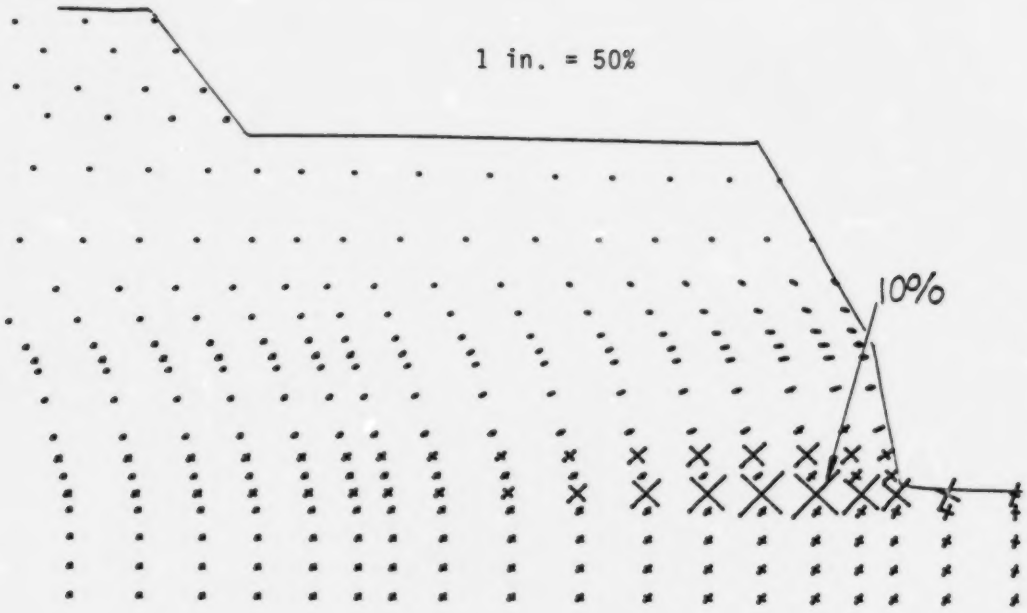

FIG. A.7.3 Principal Strain Distribution Around Final Slope.

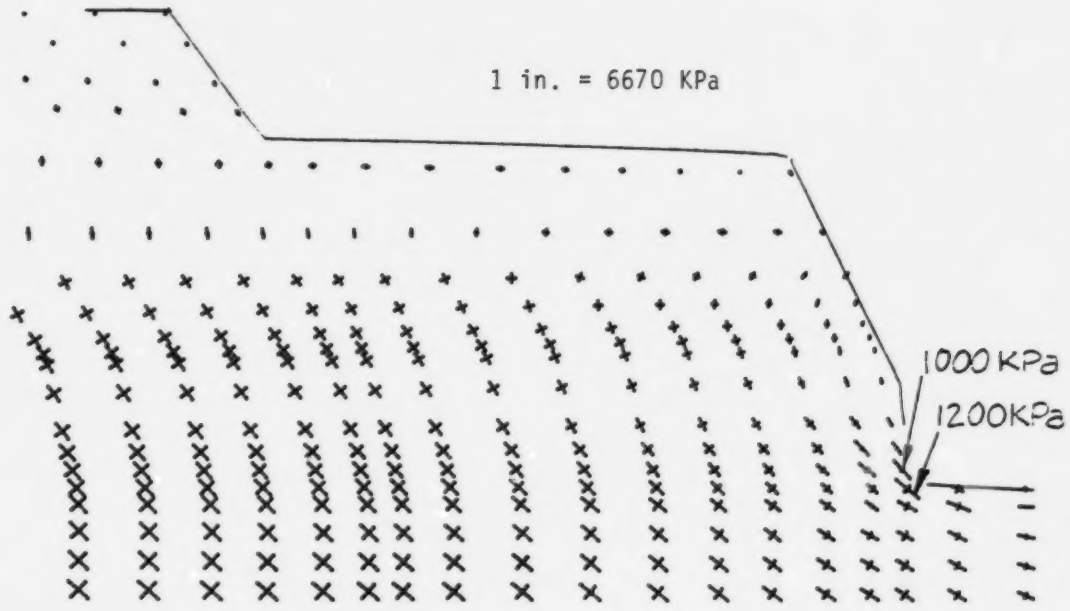

FIG. A.7.4 Principal Stress Distribution Around Final Slope.

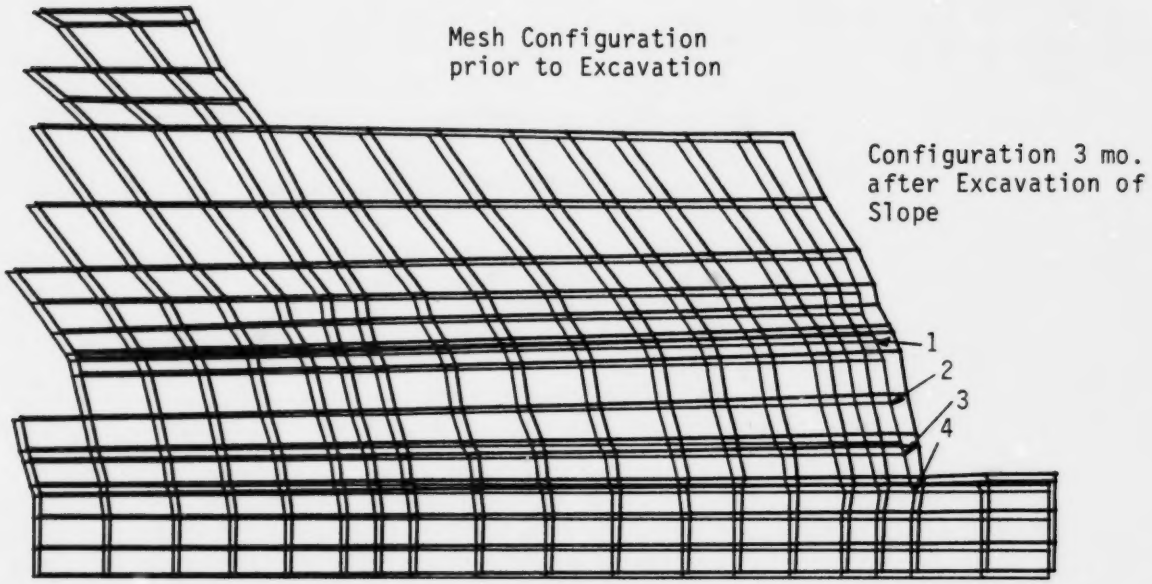

FIG. A.7.5 Deformation of Mesh Corresponding to Final Slope.

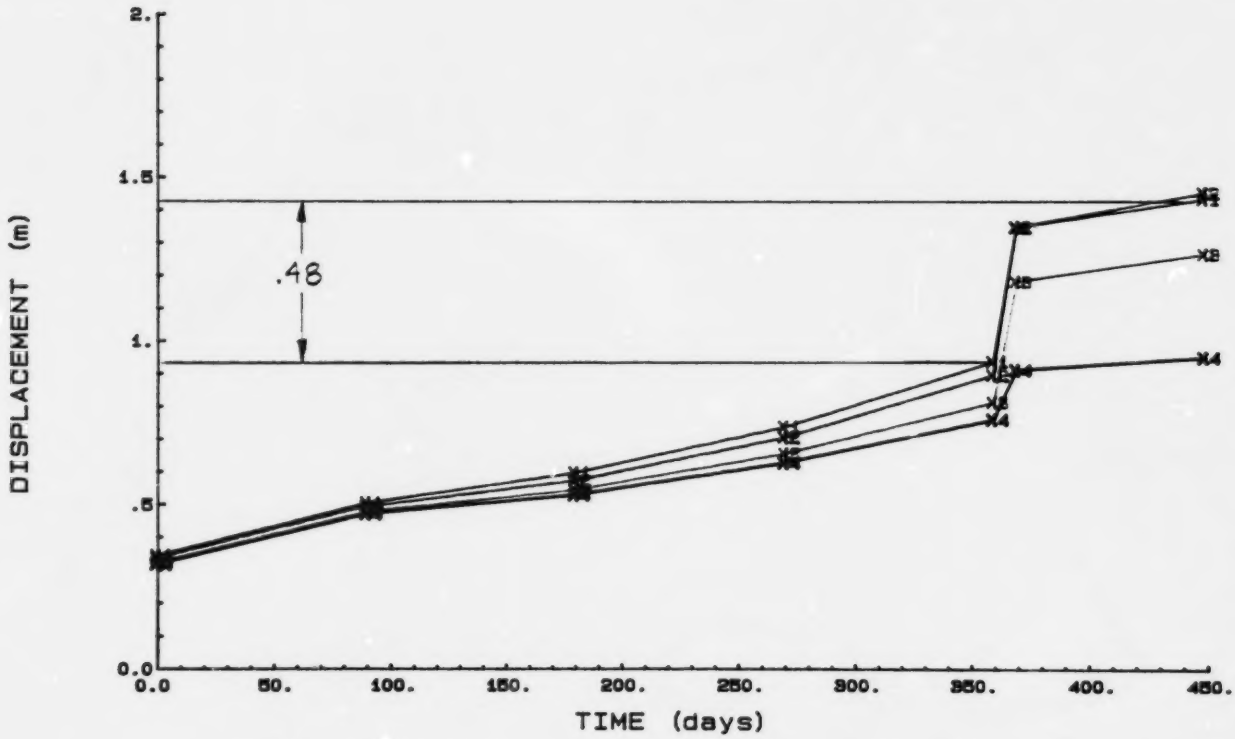

FIG. A.7.6 Displacement of Critical Nodes in the Final Slope as a Function of Time.

RUN DESIGNATION	-	CN1DG9/CN1SG9
MATERIAL PROPERTY	-	"Weak"
SLOPE GEOMETRY	-	$\alpha = 55°$, $\beta = 72°$
EXCAVATION TIMING	-	3 months
EXCAVATION SEQUENCE	-	Simultaneous Coal/Overburden Removal
INITIAL STRESS STATE	-	Hydrostatic

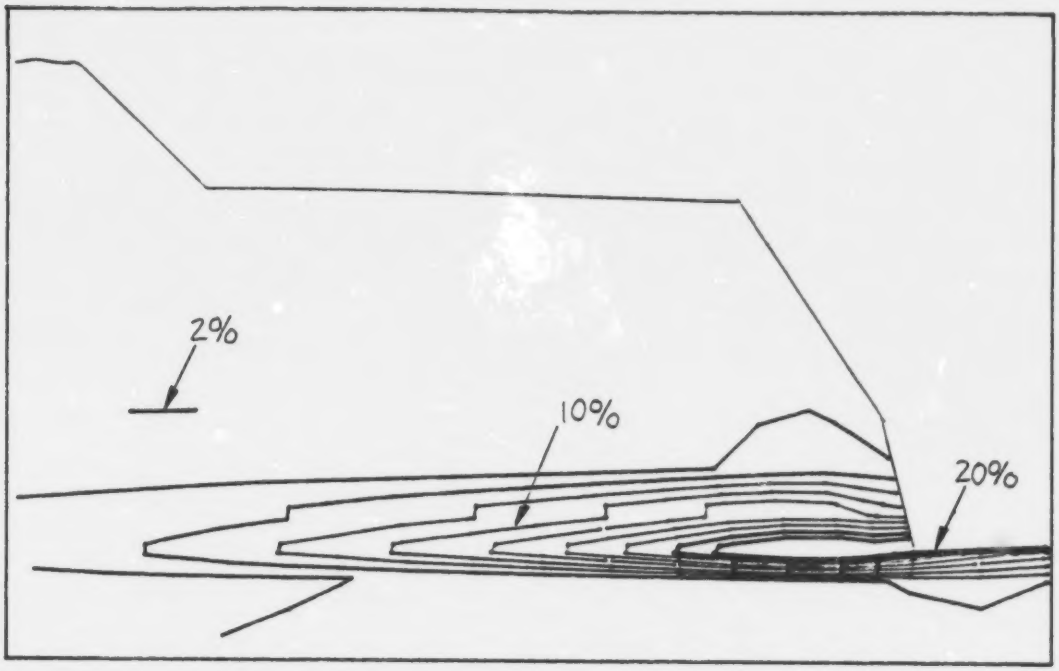

FIG. A.8.1 Octahedral Shear Strain Contour Plot for the Final Slope.

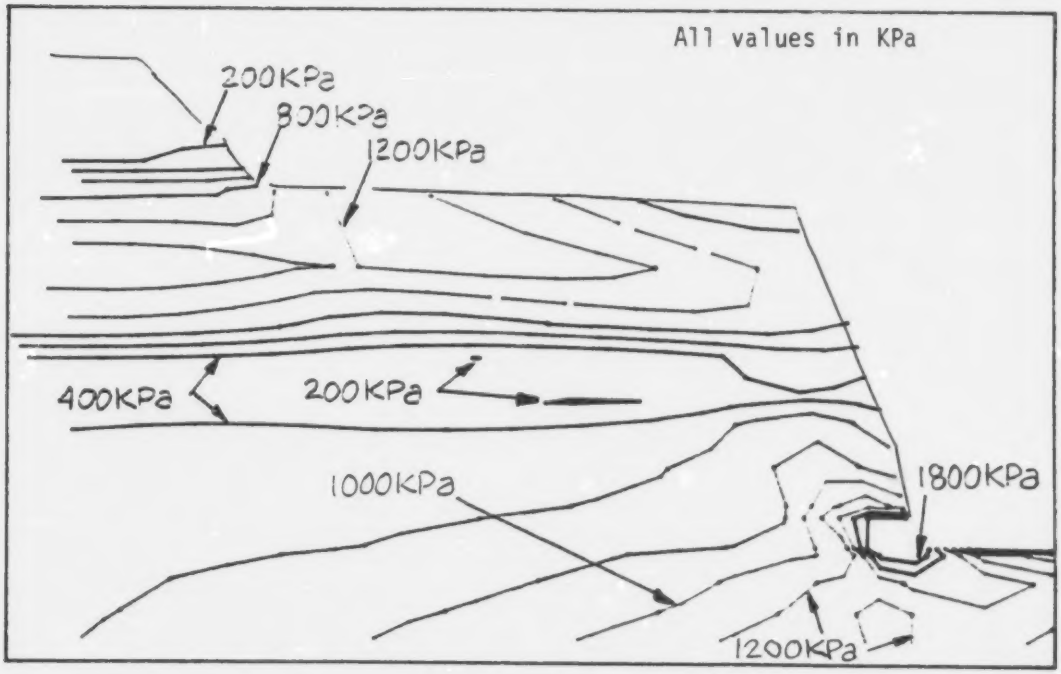

FIG. A.8.2 Octahedral Shear Stress Contour Plot for the Final Slope.

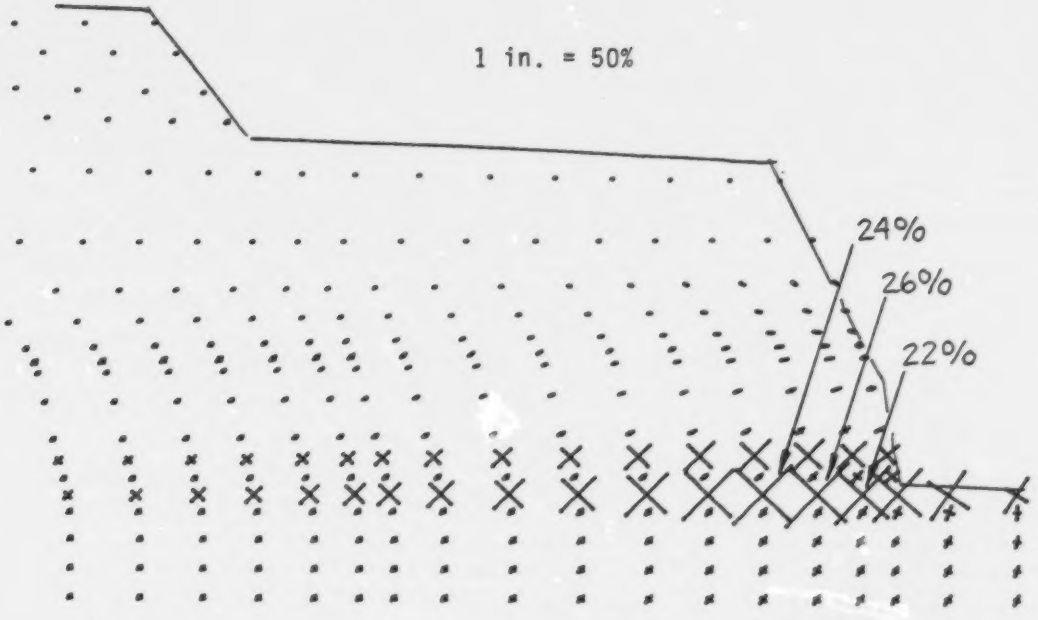

FIG. A.8.3 Principal Strain Distribution Around Final Slope.

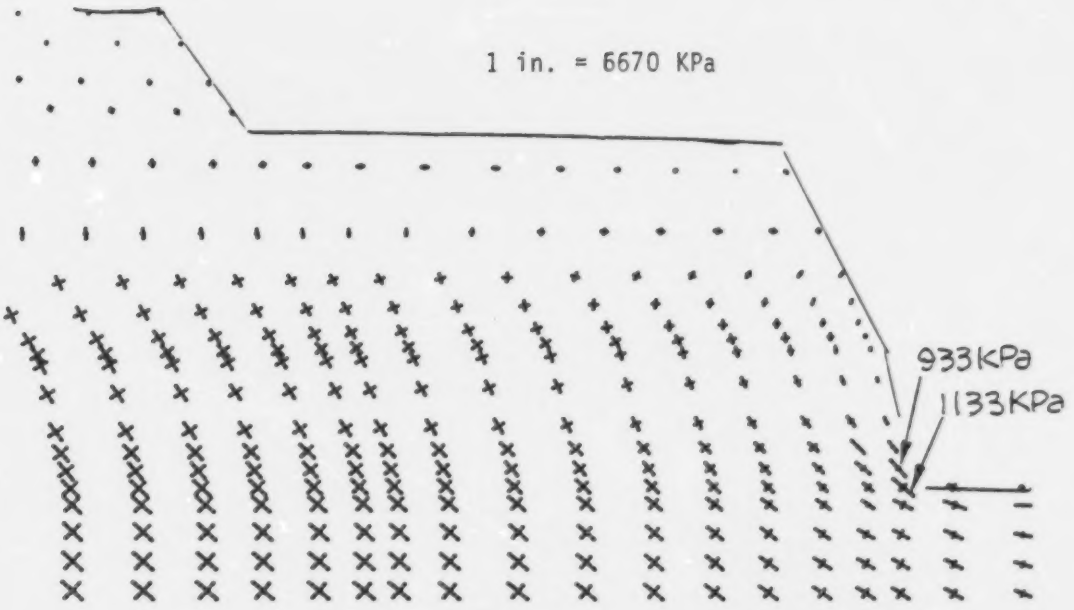

FIG. A.8.4 Principal Stress Distribution Around Final Slope.

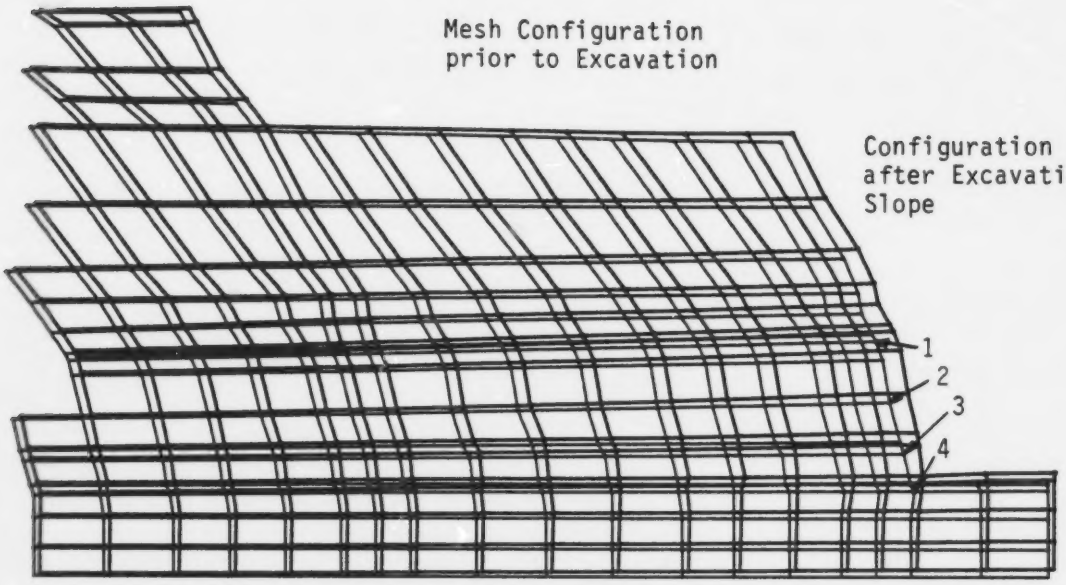

FIG. A.8.5 Deformation of Mesh Corresponding to Final Slope.

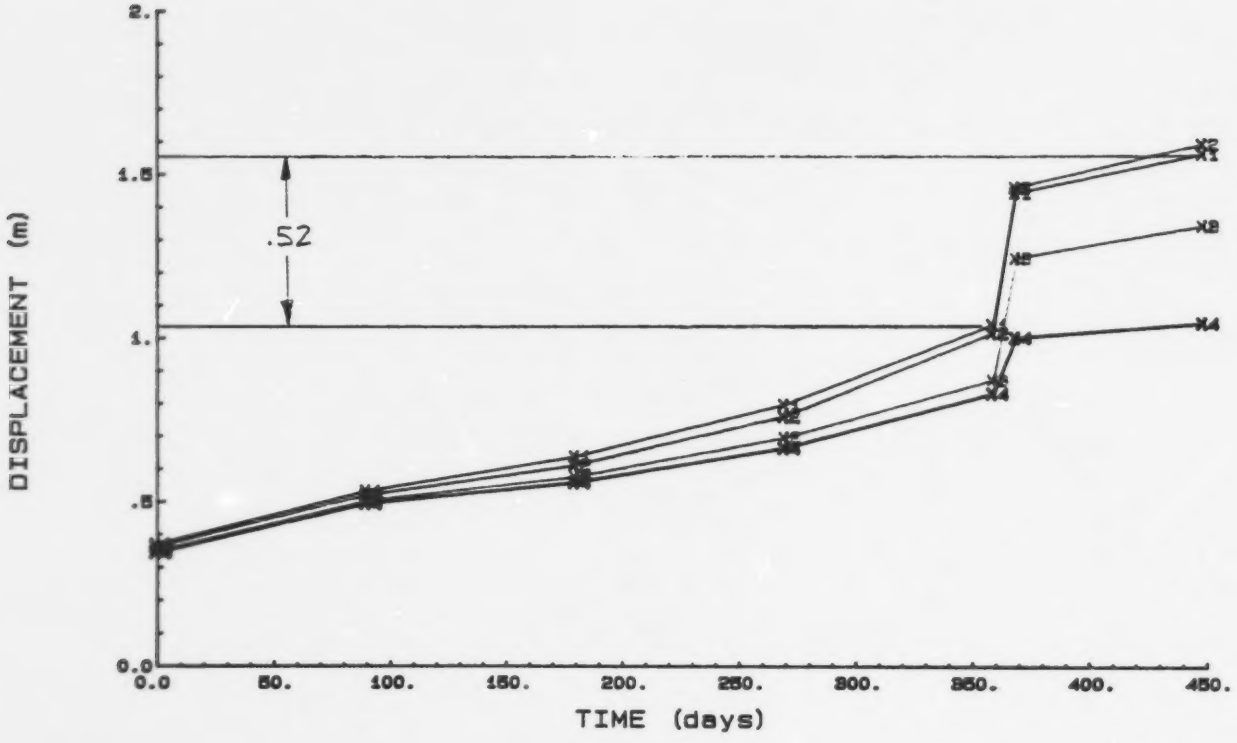

FIG. A.8.6 Displacement of Critical Nodes in the Final Slope as a Function of Time.

RUN DESIGNATION	-	CN1DG5/CN1SG5
MATERIAL PROPERTY	-	"Strong"
SLOPE GEOMETRY	-	$\alpha = 55°$, $\beta = 72°$
EXCAVATION TIMING	-	3 months
EXCAVATION SEQUENCE	-	Simultaneous Coal/Overburden Removal
INITIAL STRESS STATE	-	Hydrostatic

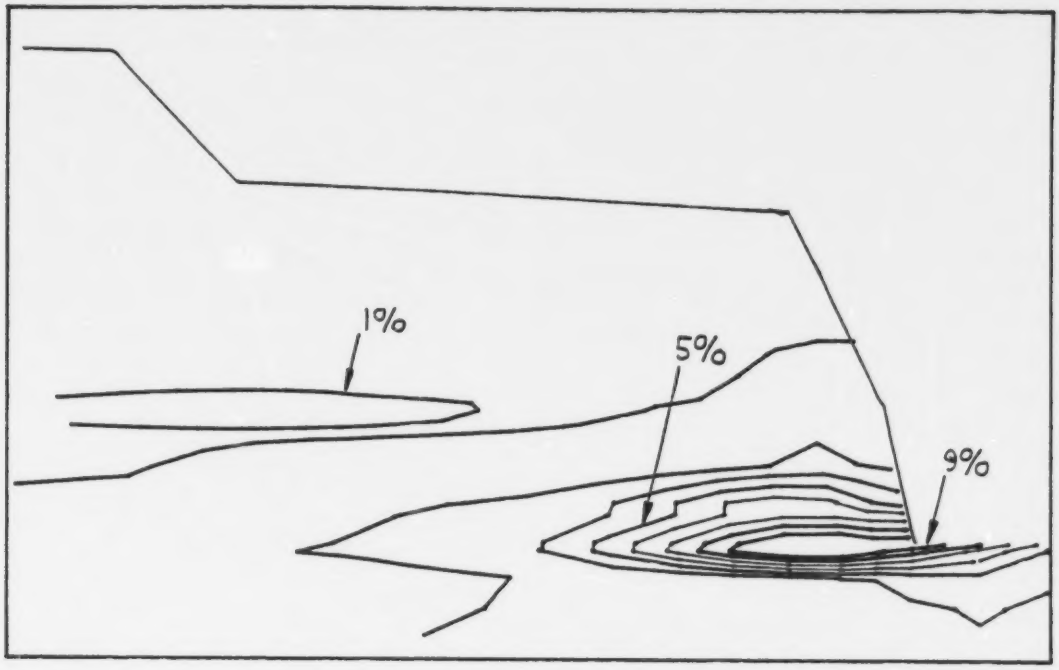

FIG. A.9.1 Octahedral Shear Strain Contour Plot for the Final Slope.

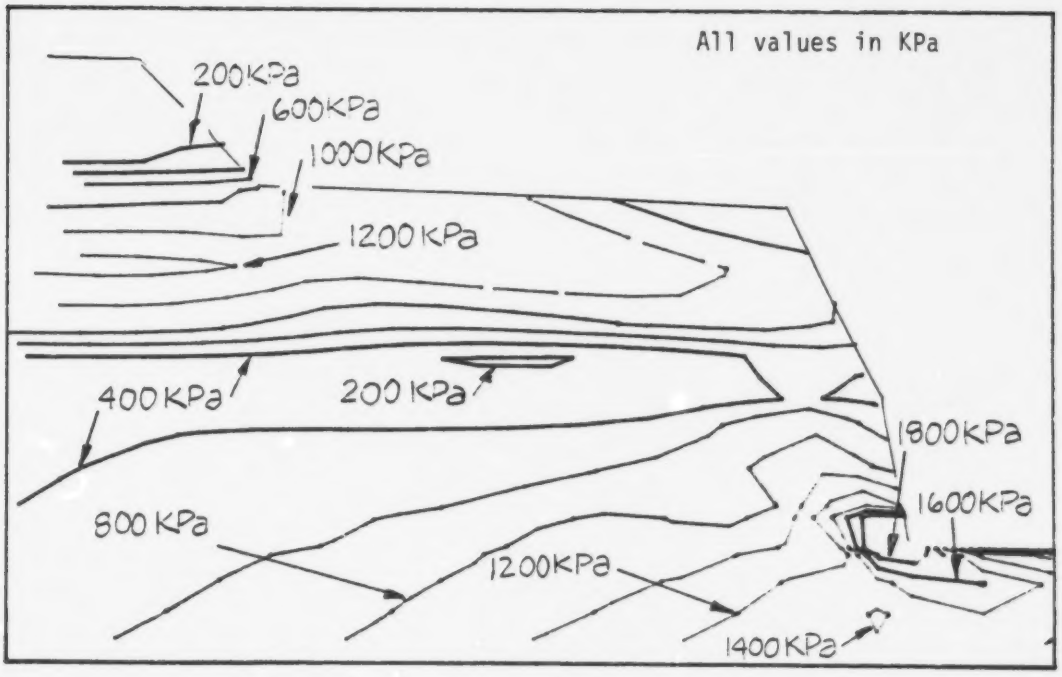

FIG. A.9.2 Octahedral Shear Stress Contour Plot for the Final Slope.

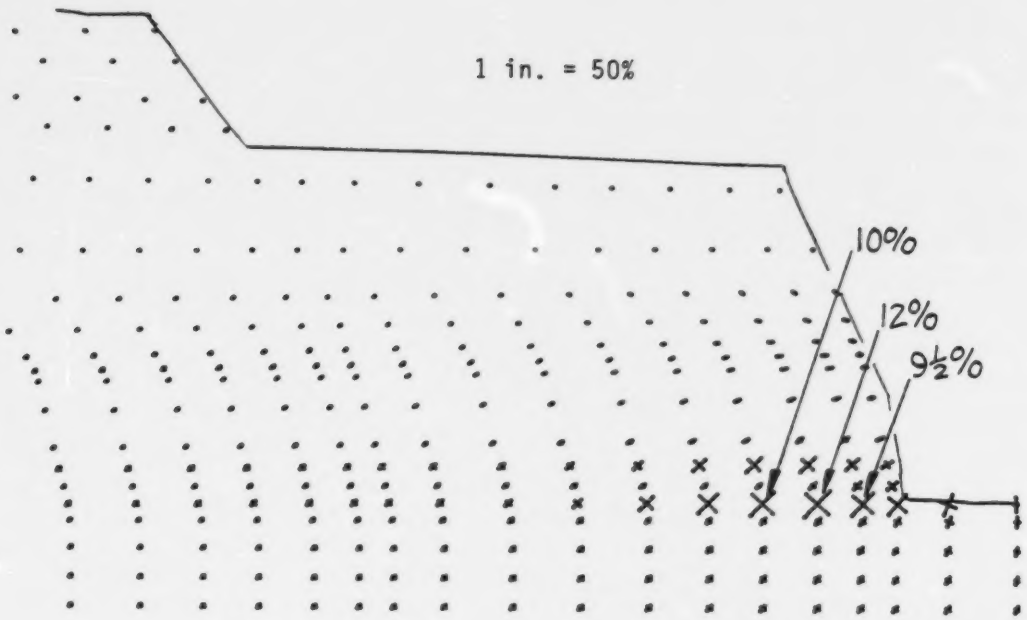

FIG. A.9.3 Principal Strain Distribution Around Final Slope.

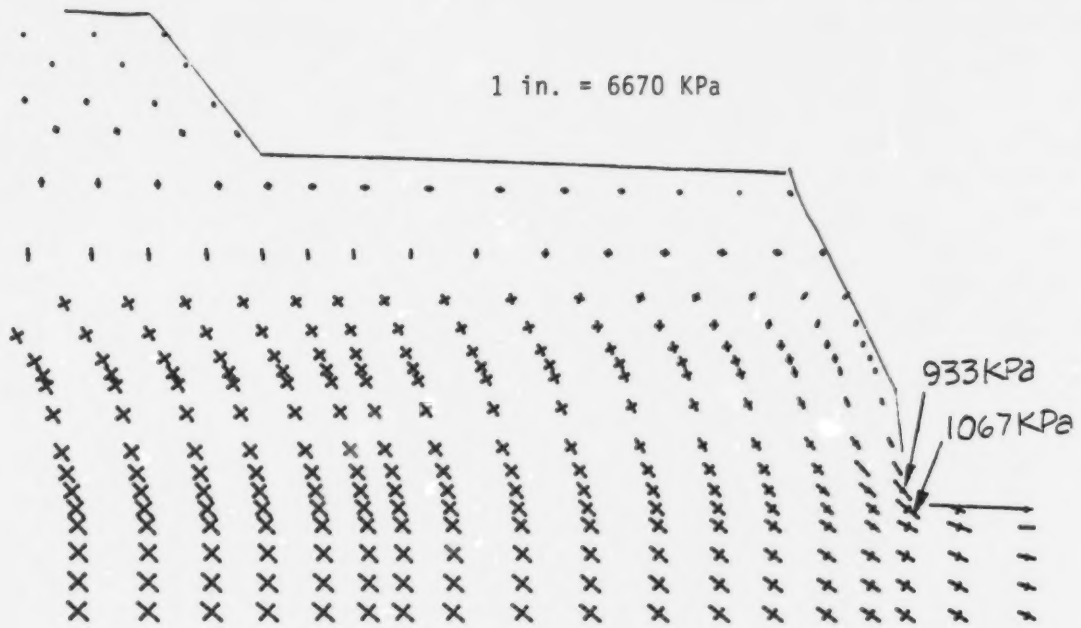

FIG. A.9.4 Principal Stress Distribution Around Final Slope.

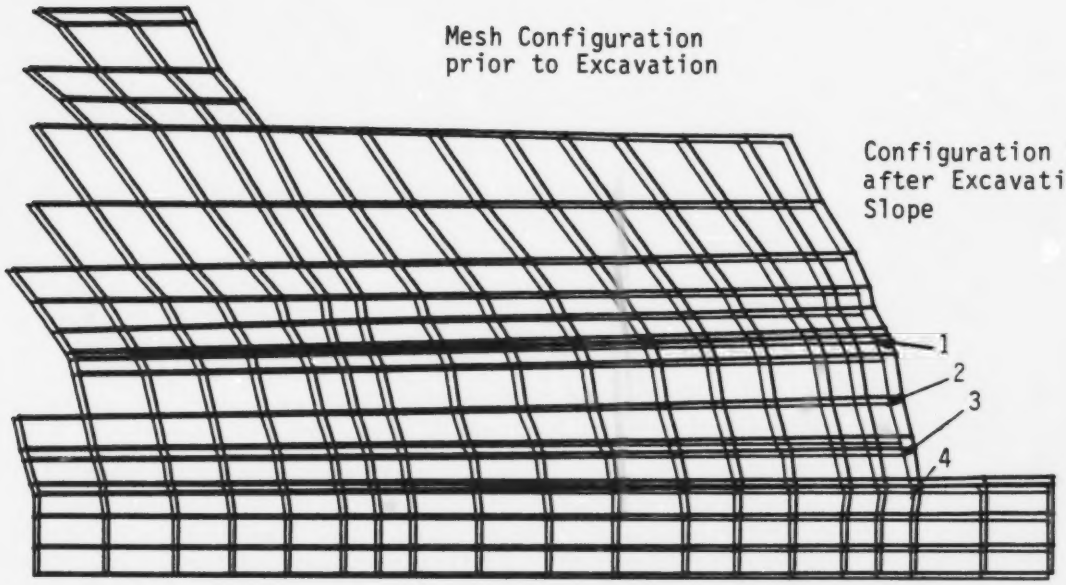

FIG. A.9.5 Deformation of Mesh Corresponding to Final Slope.

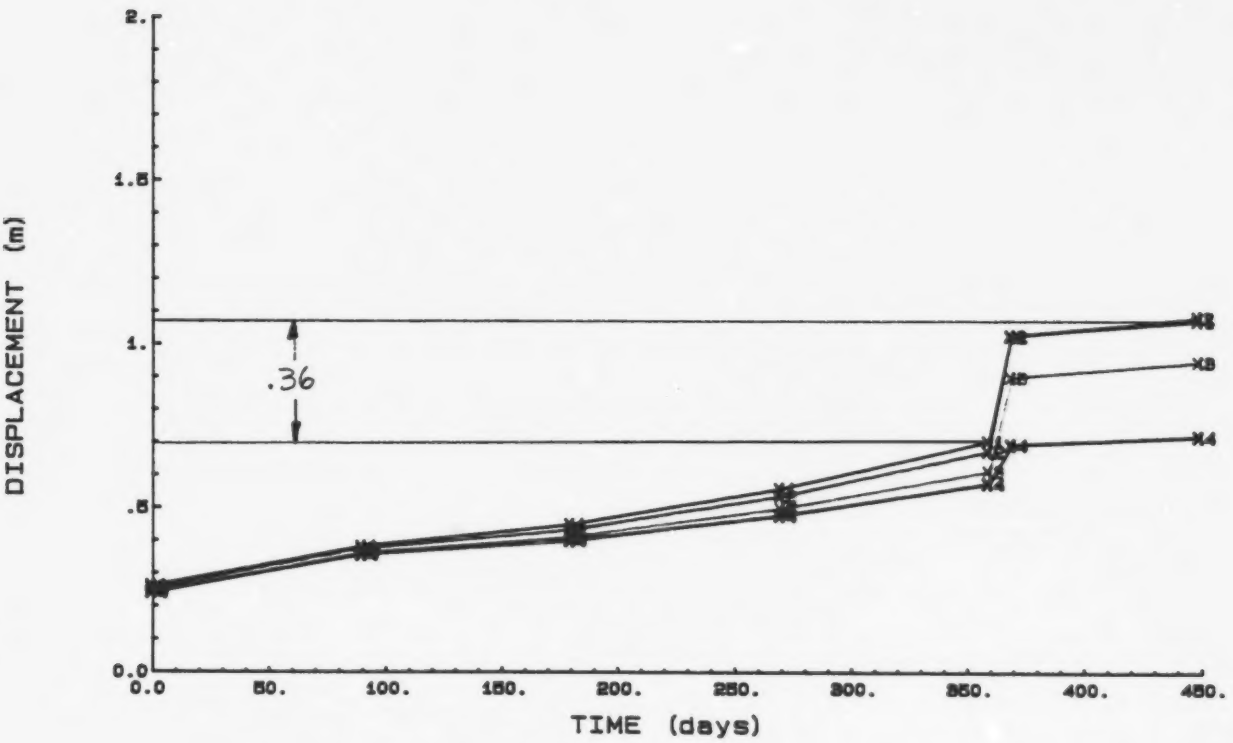

FIG. A.9.6 Displacement of Critical Nodes in the Final Slope as a Function of Time.

RUN DESIGNATION	-	CN1DT1/CN1ST1
MATERIAL PROPERTY	-	"Norm"
SLOPE GEOMETRY	-	$\alpha = 45°$, $\beta = 57°$
EXCAVATION TIMING	-	6 months
EXCAVATION SEQUENCE	-	Simultaneous Coal/Overburden Removal
INITIAL STRESS STATE	-	Hydrostatic

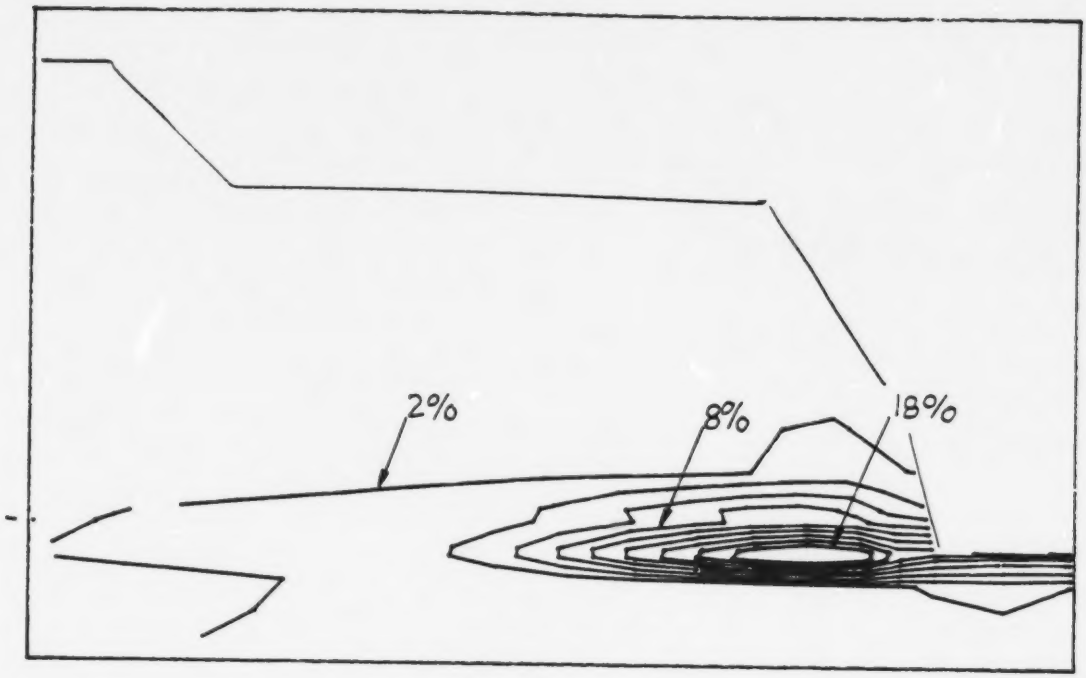

FIG. A.10.1 Octahedral Shear Strain Contour Plot for the Final Slope.

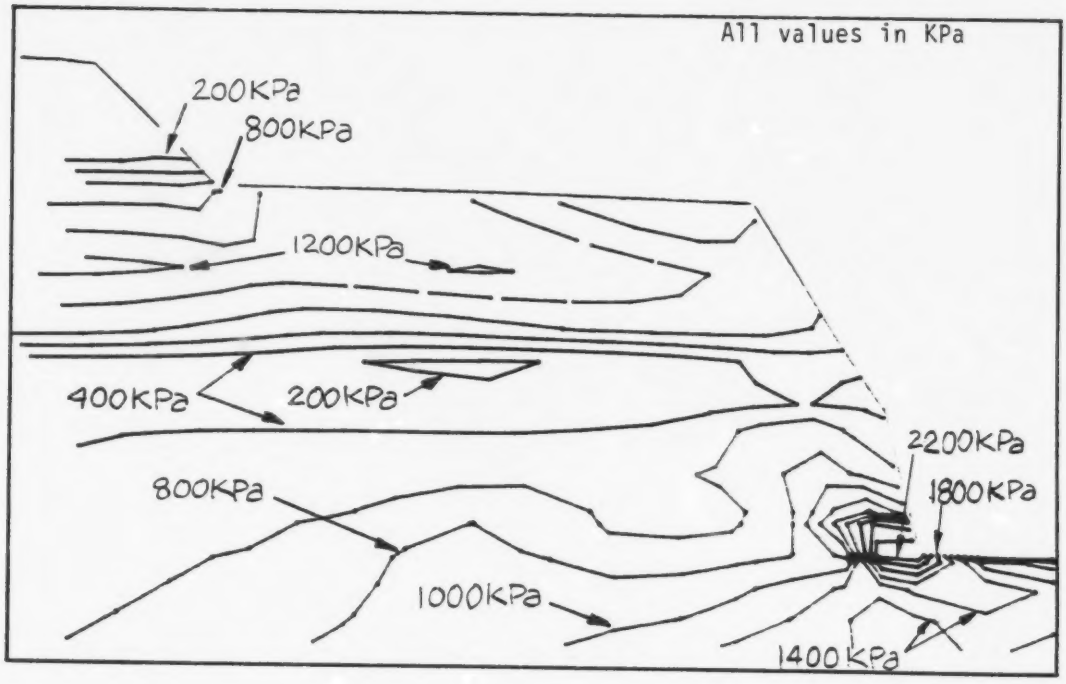

FIG. A.10.2 Octahedral Shear Stress Contour Plot for the Final Slope.

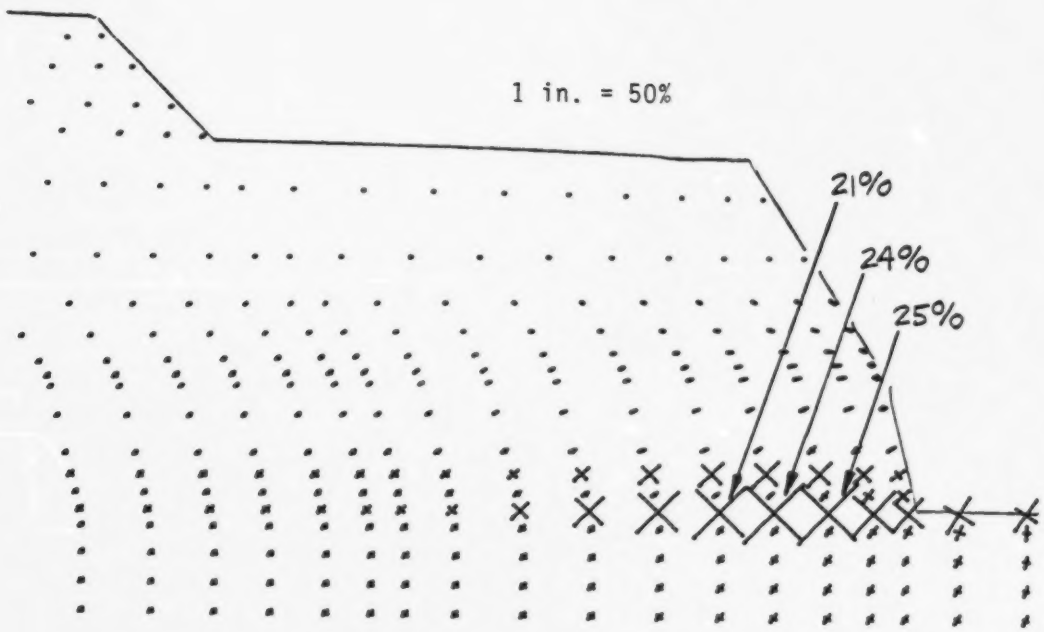

FIG. A.10.3 Principal Strain Distribution Around Final Slope.

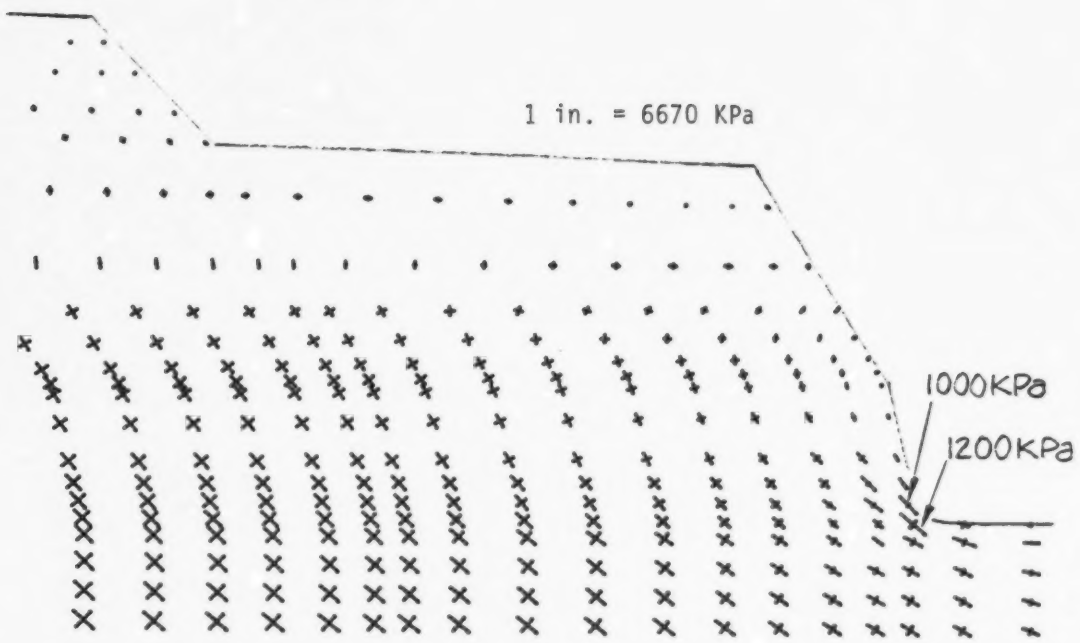

FIG. A.10.4 Principal Stress Distribution Around Final Slope.

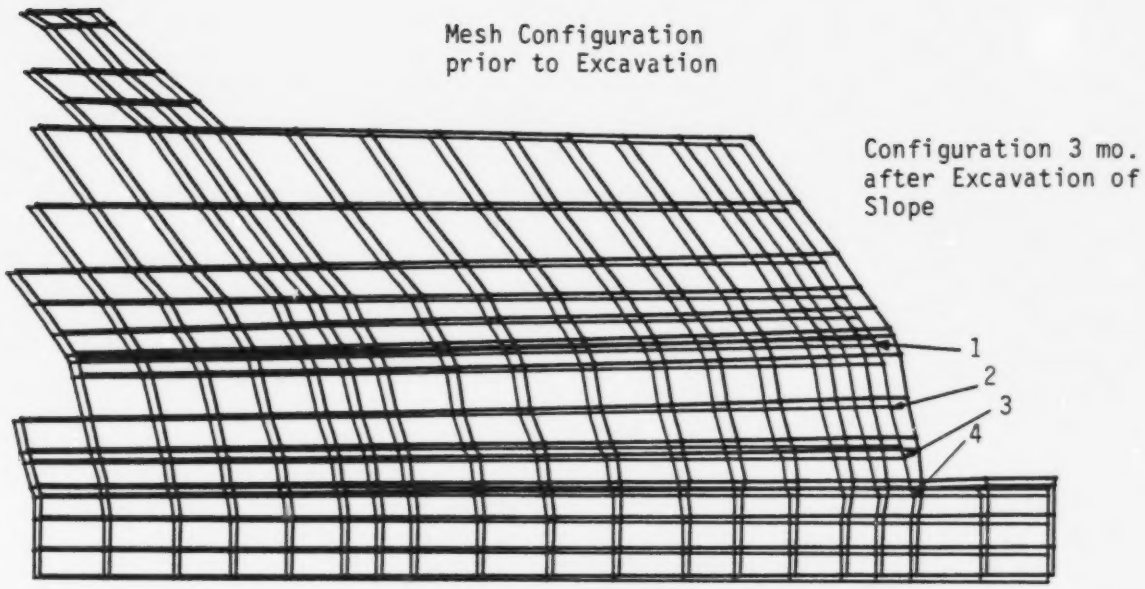

FIG. A.10.5 Deformation of Mesh Corresponding to Final Slope.

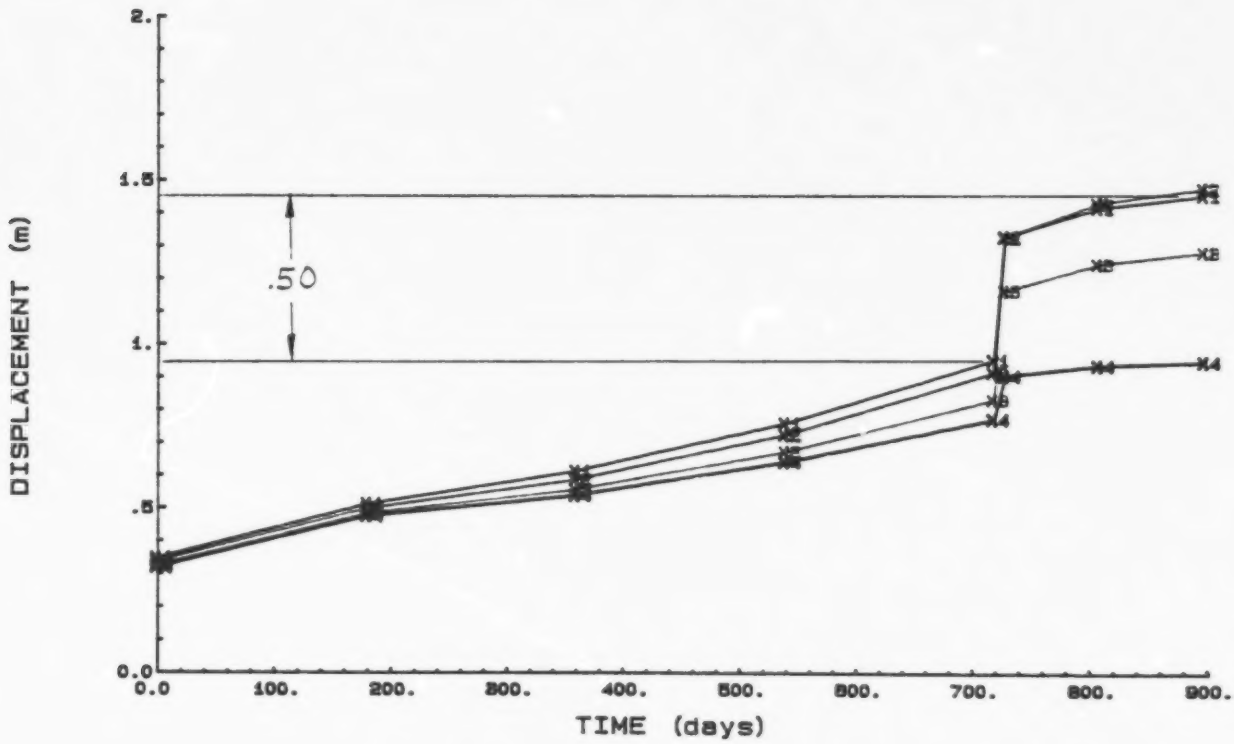

FIG. A.10.6 Displacement of Critical Nodes in the Final Slope as a Function of Time.

RUN DESIGNATION	-	CN1DT2/CN1ST2
MATERIAL PROPERTY	-	"Strong"
SLOPE GEOMETRY	-	$\alpha = 45°$, $\beta = 57°$
EXCAVATION TIMING	-	6 months
EXCAVATION SEQUENCE	-	Simultaneous Coal/Overburden Removal
INITIAL STRESS STATE	-	Hydrostatic

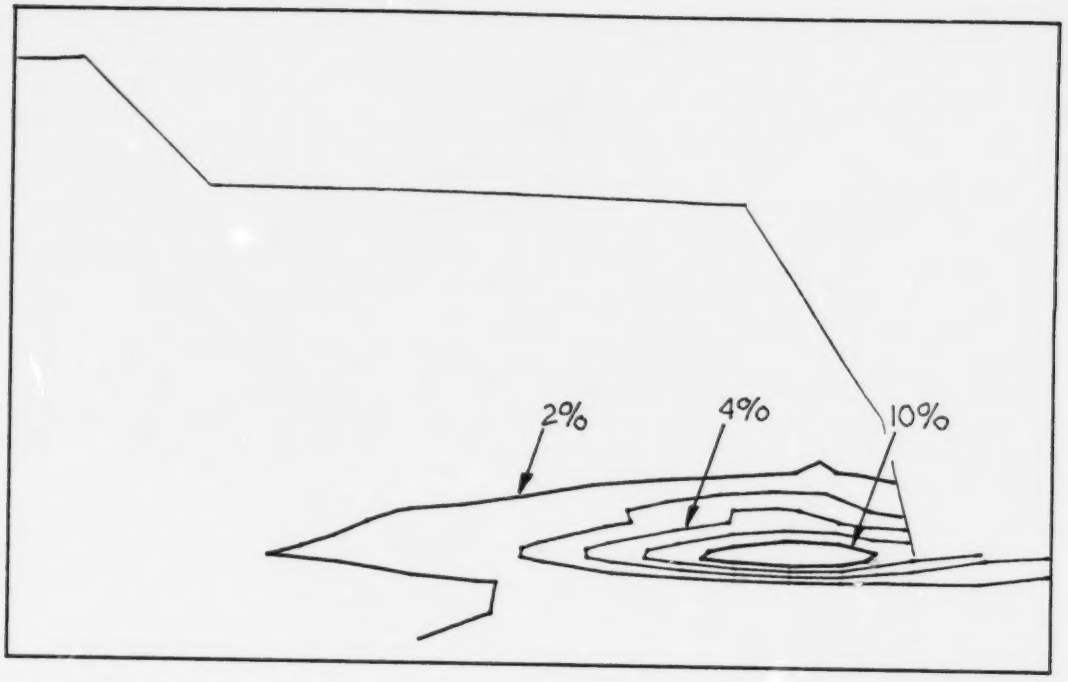

FIG. A.11.1 Octahedral Shear Strain Contour Plot for the Final Slope.

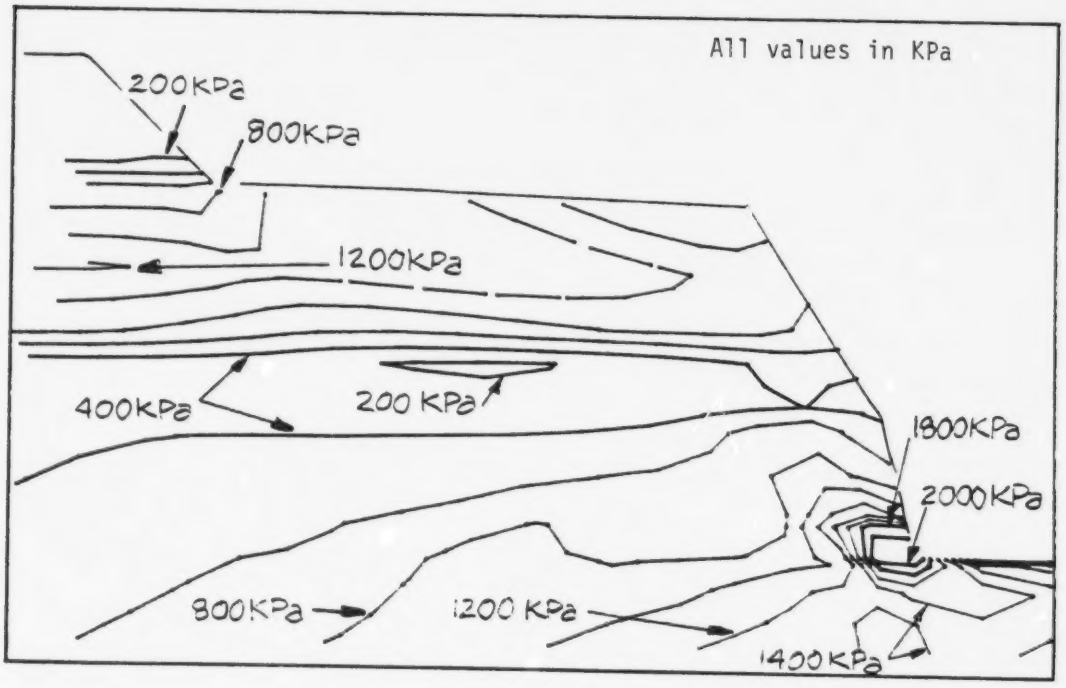

FIG. A.11.2 Octahedral Shear Stress Contour Plot for the Final Slope.

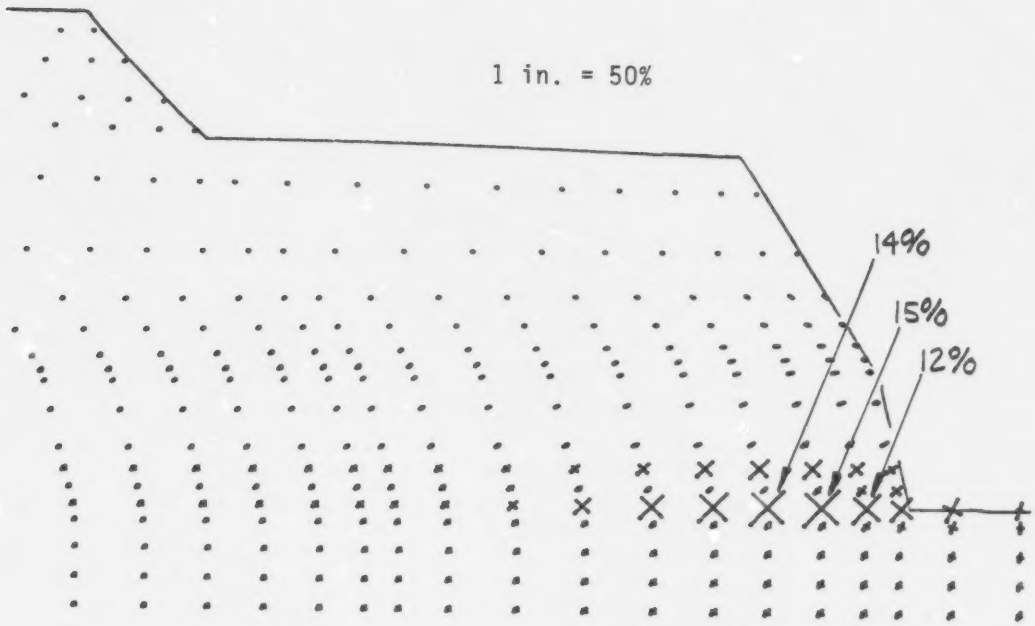

FIG. A.11.3 Principal Strain Distribution Around Final Slope.

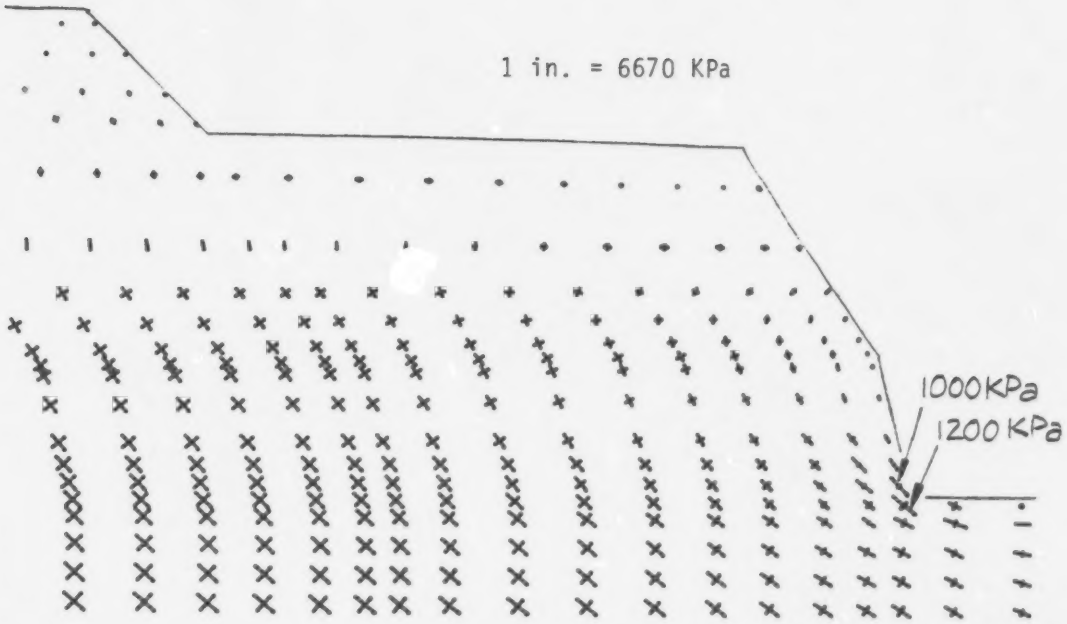

FIG. A.11.4 Principal Stress Distribution Around Final Slope.

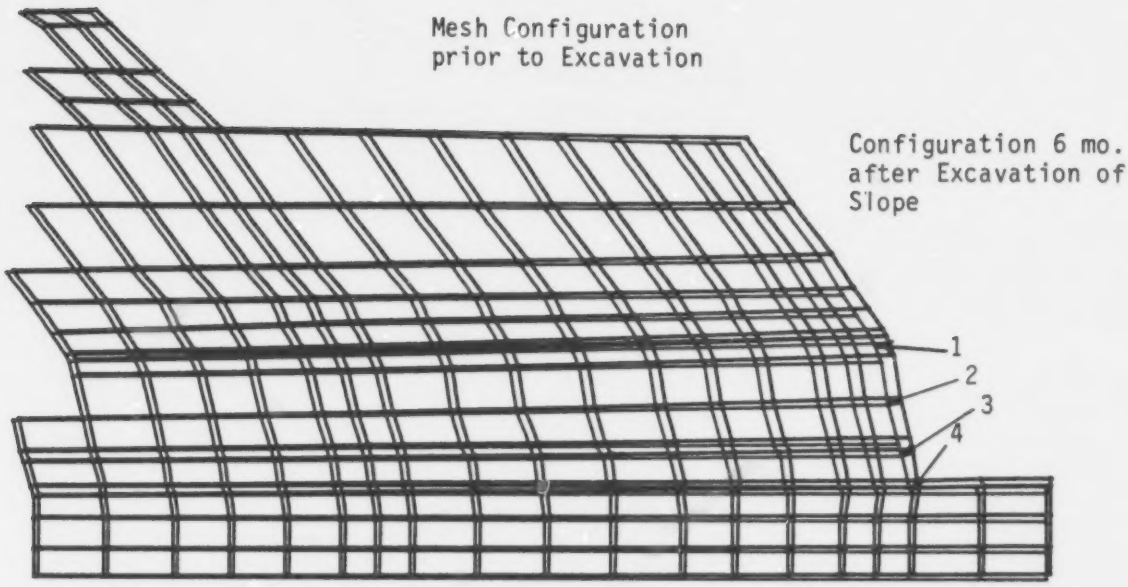

FIG. A.11.5 Deformation of Mesh Corresponding to Final Slope.

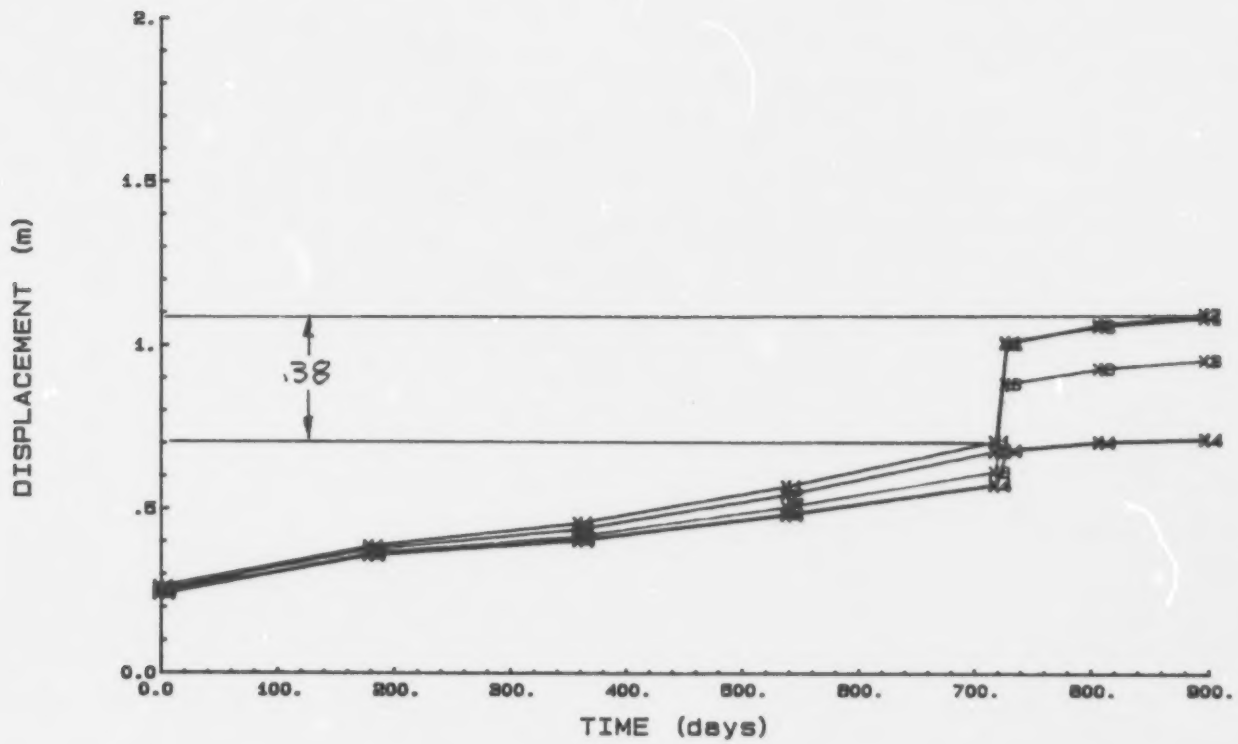

FIG. A.11.6 Displacement of Critical Nodes in the Final Slope as a Function of Time.

RUN DESIGNATION	-	CN1DT3/CN1ST3
MATERIAL PROPERTY	-	"Norm"
SLOPE GEOMETRY	-	$\alpha = 55°$, $\beta = 72°$
EXCAVATION TIMING	-	6 months
EXCAVATION SEQUENCE	-	Simultaneous Coal/Overbruden Removal
INITIAL STRESS STATE	-	Hydrostatic

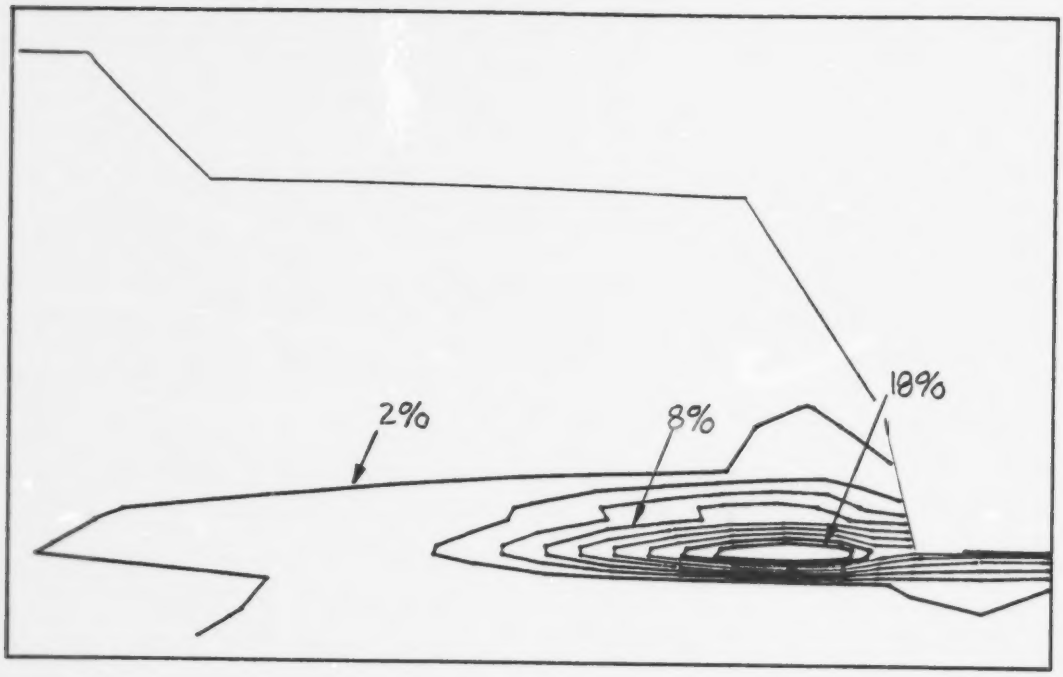

FIG. A.12.1 Octahedral Shear Strain Contour Plot for the Final Slope.

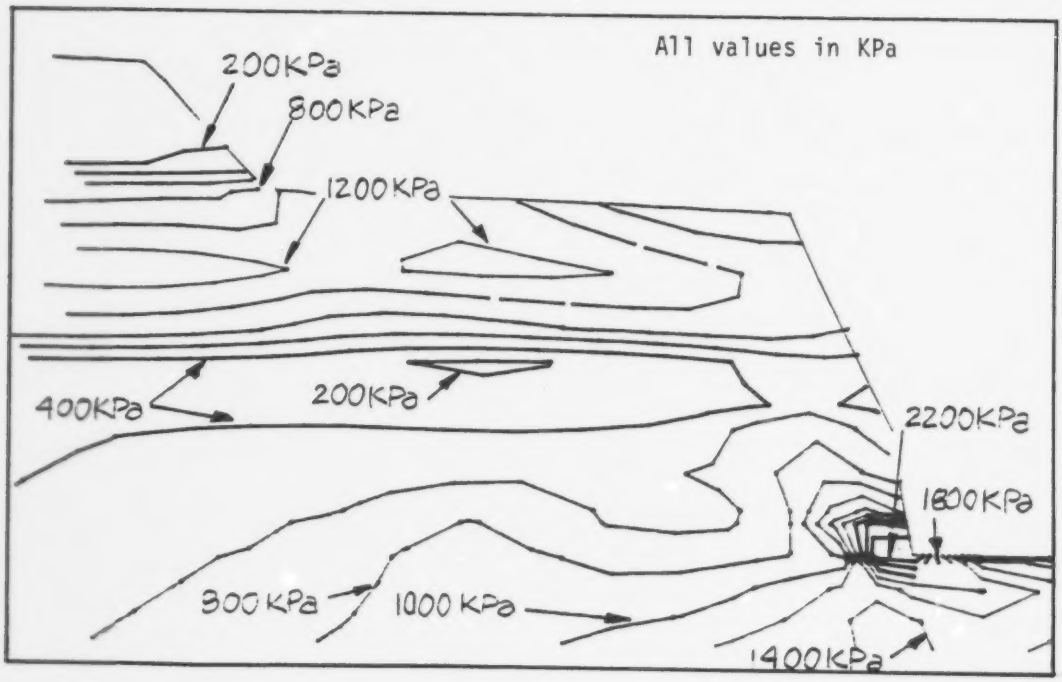

FIG. A.12.2 Octahedral Shear Stress Contour Plot for the Final Slope.

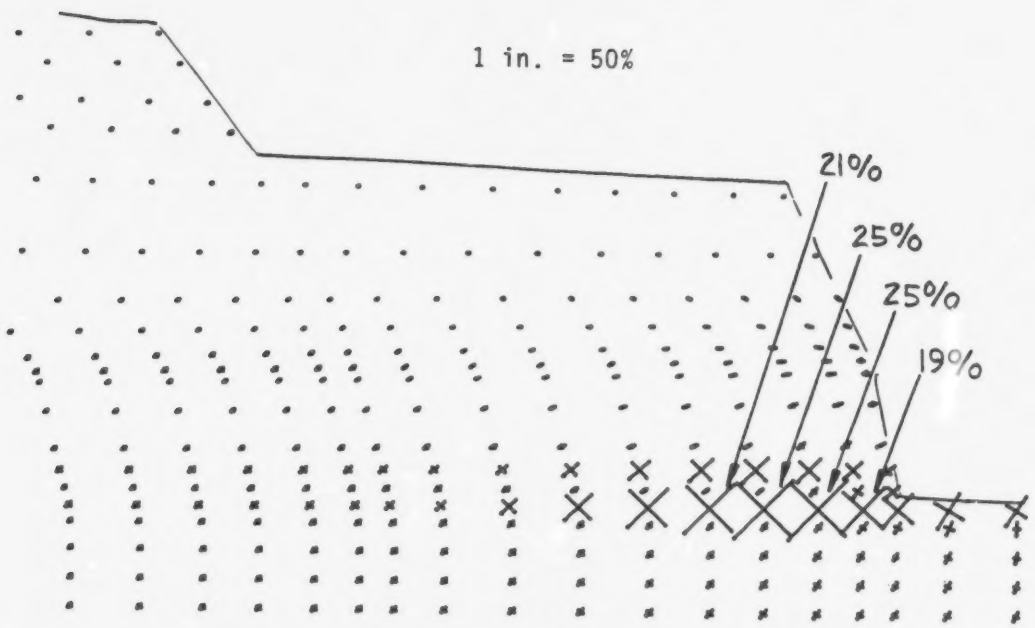

FIG. A.12.3 Principal Strain Distribution Around Final Slope.

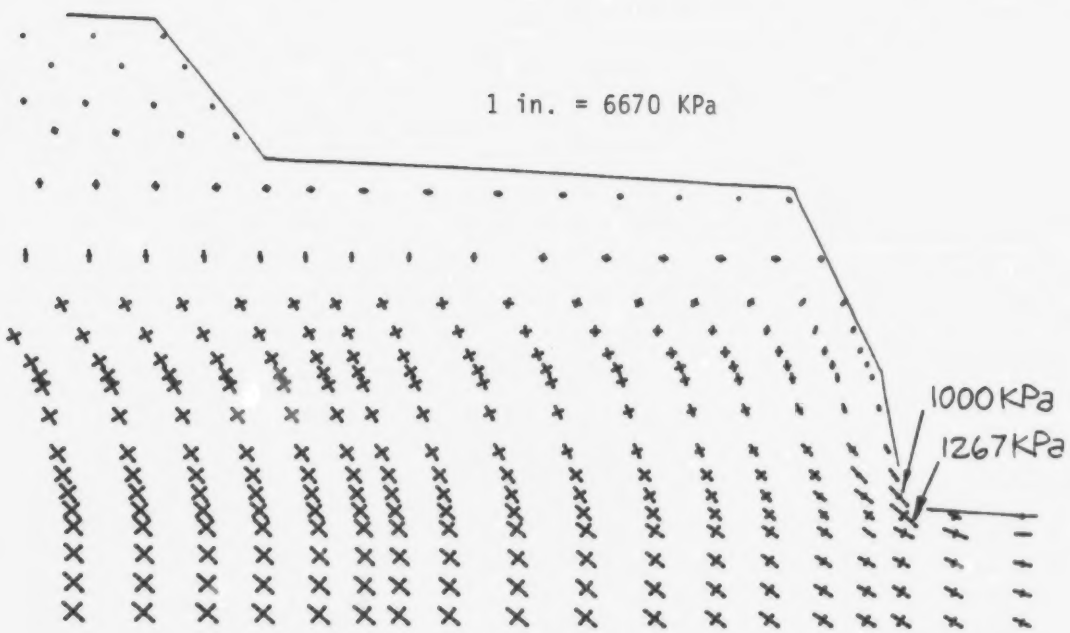

FIG. A.12.4 Principal Stress Distribution Around Final Slope.

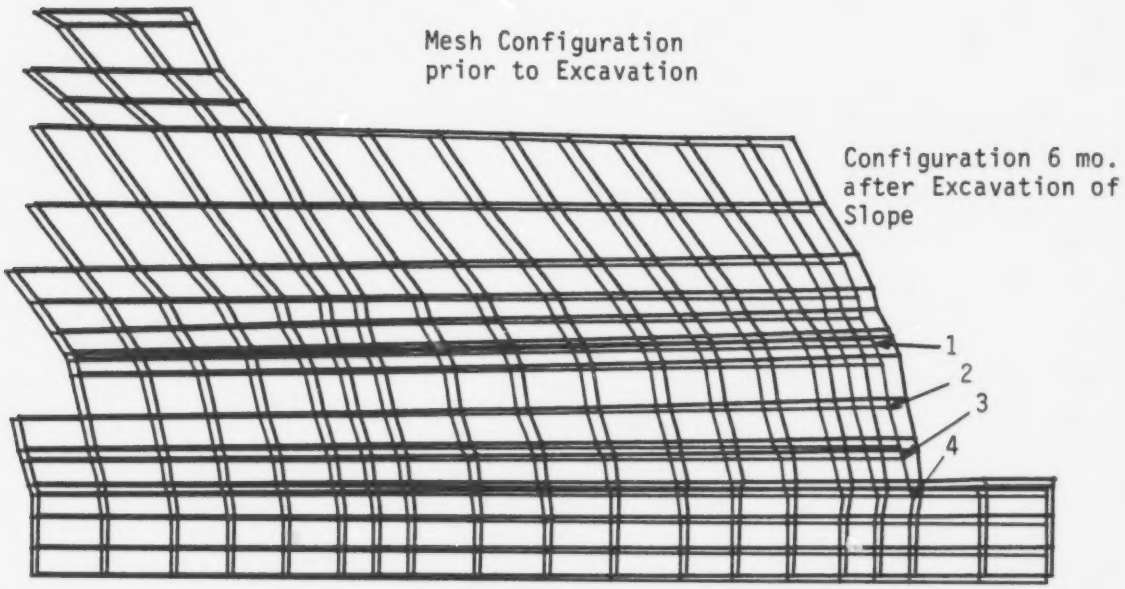

FIG. A.12.5 Deformation of Mesh Corresponding to Final Slope.

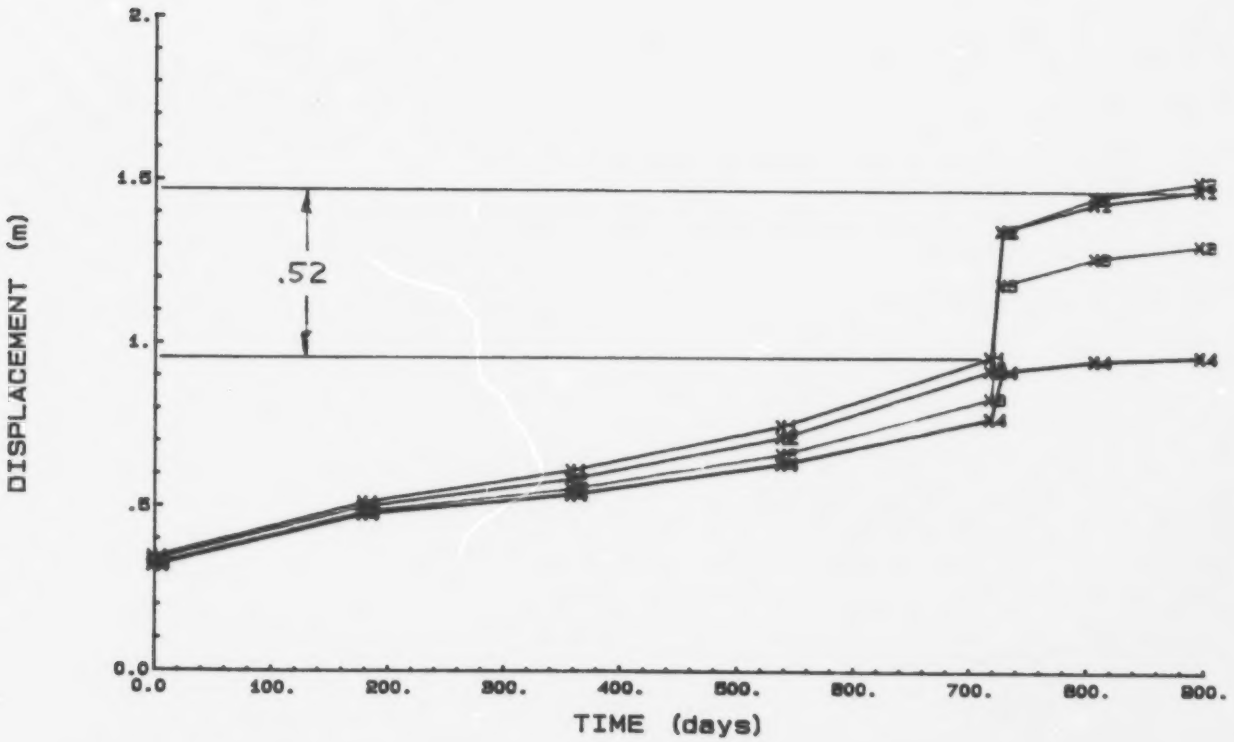

FIG. A.12.6 Displacement of Critical Nodes in the Final Slope as a Function of Time.

RUN DESIGNATION	-	CN1DT4/CN1ST4
MATERIAL PROPERTY	-	"Strong"
SLOPE GEOMETRY	-	$\alpha = 55°$, $\beta = 72°$
EXCAVATION TIMING	-	6 months
EXCAVATION SEQUENCE	-	Simultaneous Coal/Overburden Removal
INITIAL STRESS STATE	-	Hydrostatic

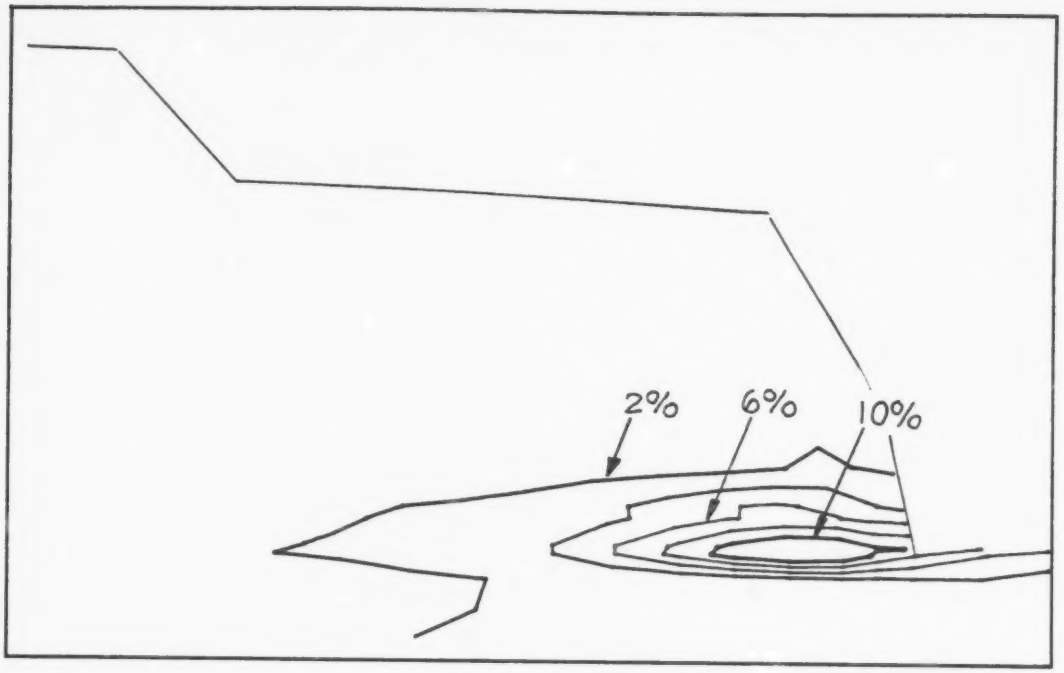

FIG. A.13.1 Octahedral Shear Strain Contour Plot for the Final Slope.

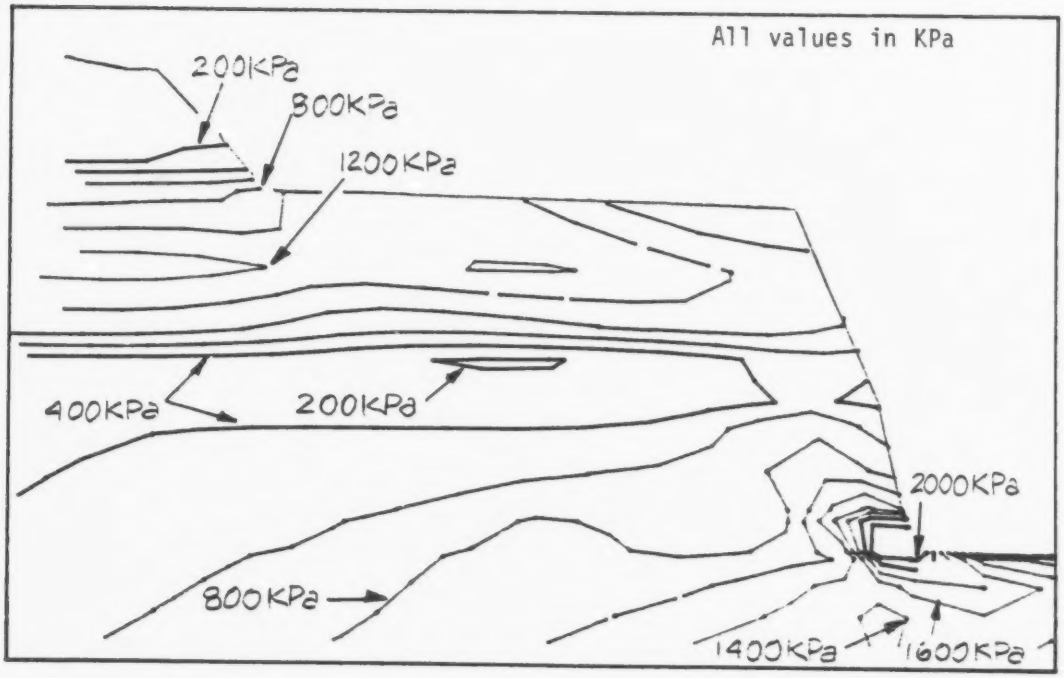

FIG. A.13.2 Octahedral Shear Stress Contour Plot for the Final Slope.

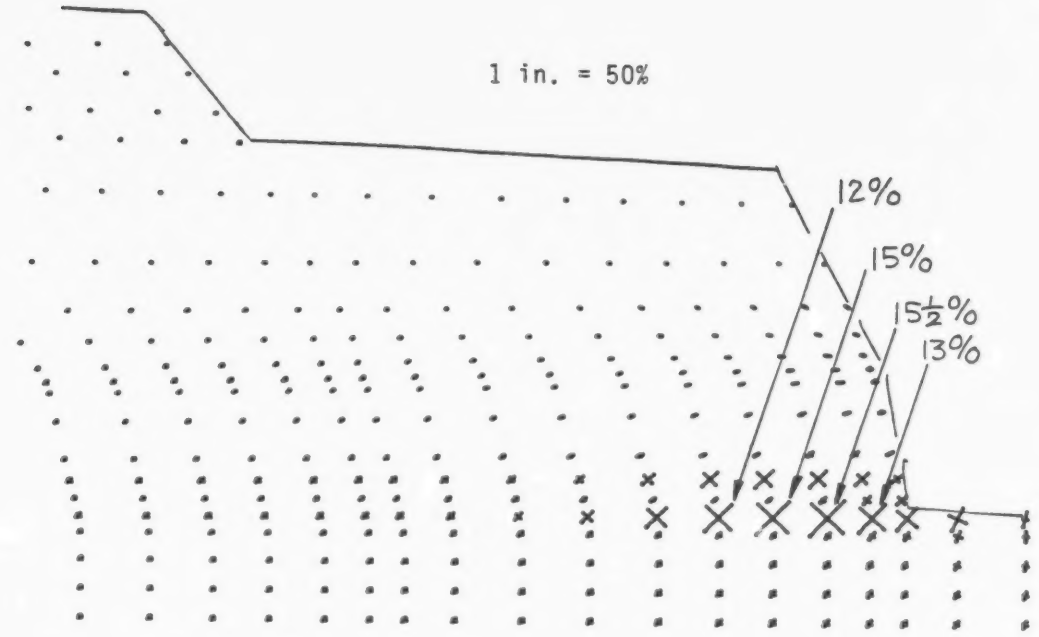

FIG. A.13.3 Principal Strain Distribution Around Final Slope.

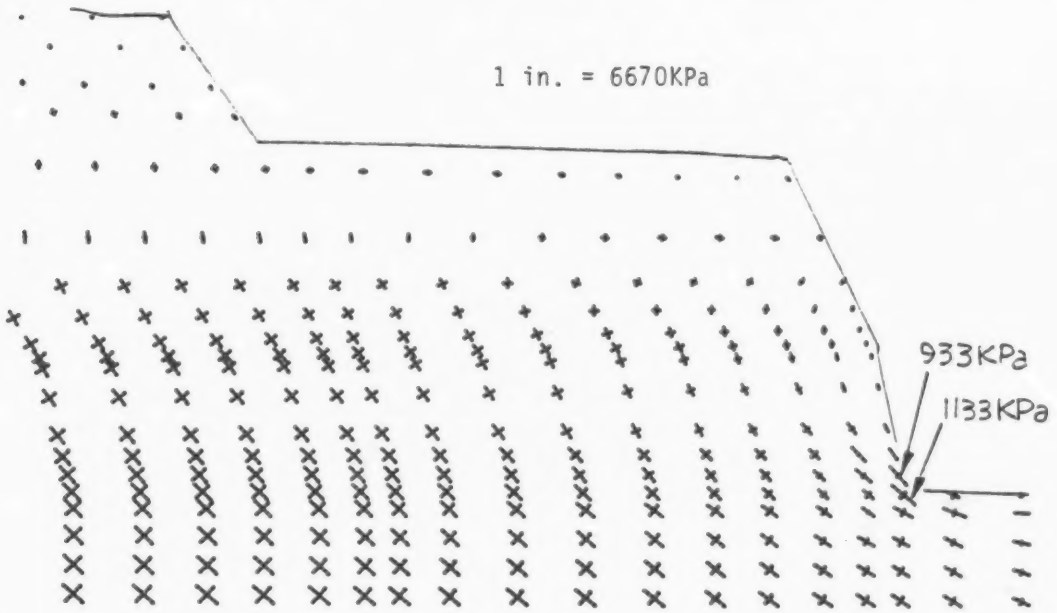

FIG. A.13.4 Principal Stress Distribution Around Final Slope.

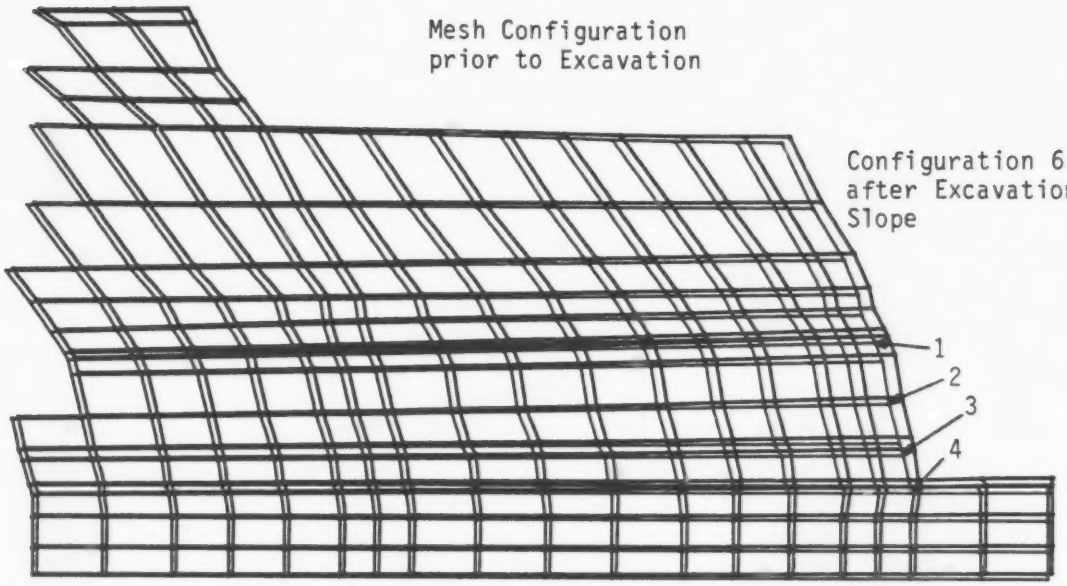

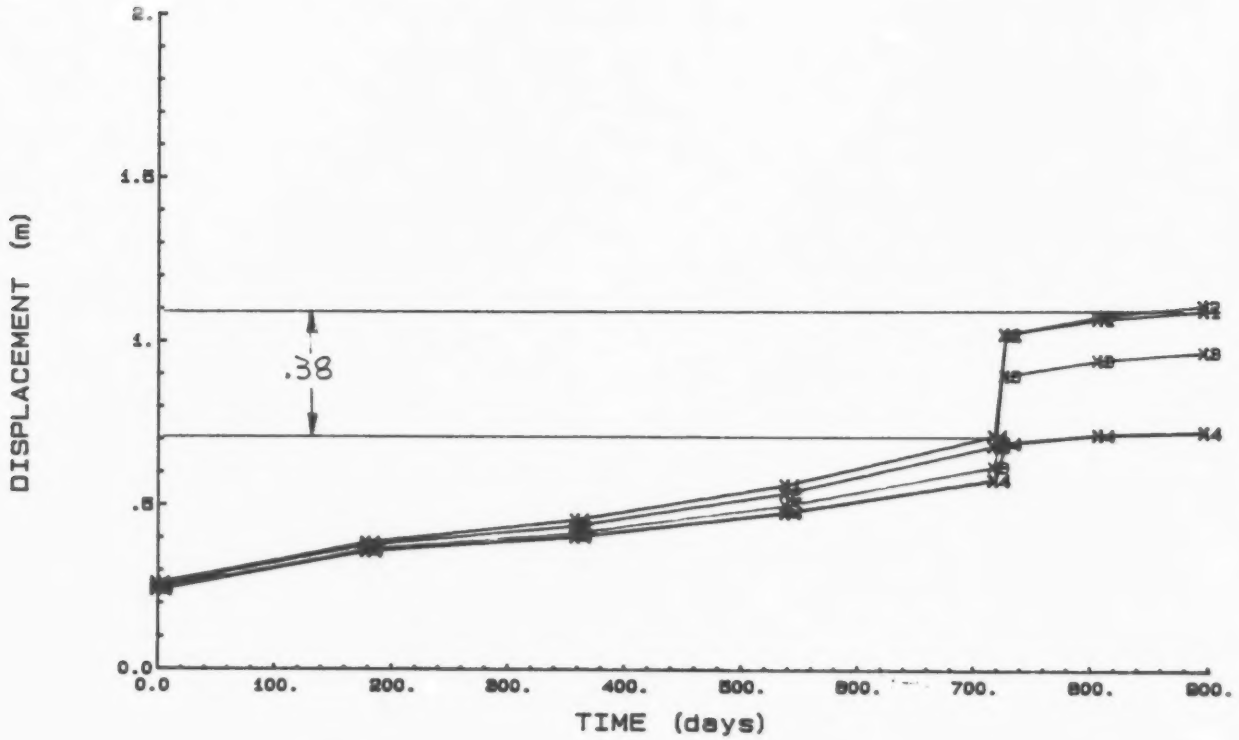

FIG. A.13.6 Displacement of Critical Nodes in the Final Slope as a Function of Time.

RUN DESIGNATION	-	TESD02/TESS02
MATERIAL PROPERTY	-	"Norm"
SLOPE GEOMETRY	-	$\alpha = 45°$, $\beta = 57°$
EXCAVATION TIMING	-	3 months
EXCAVATION SEQUENCE	-	Delayed Coal Removal
INITIAL STRESS STATE	-	Hydrostatic

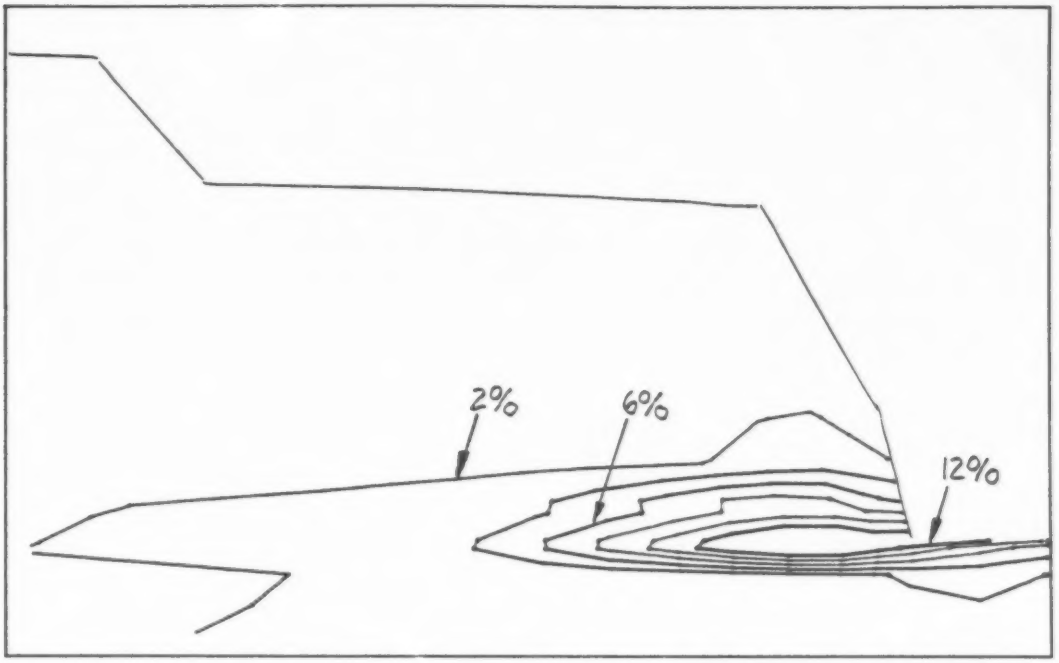

FIG. A.14.1 Octahedral Shear Strain Contour Plot for the Final Slope.

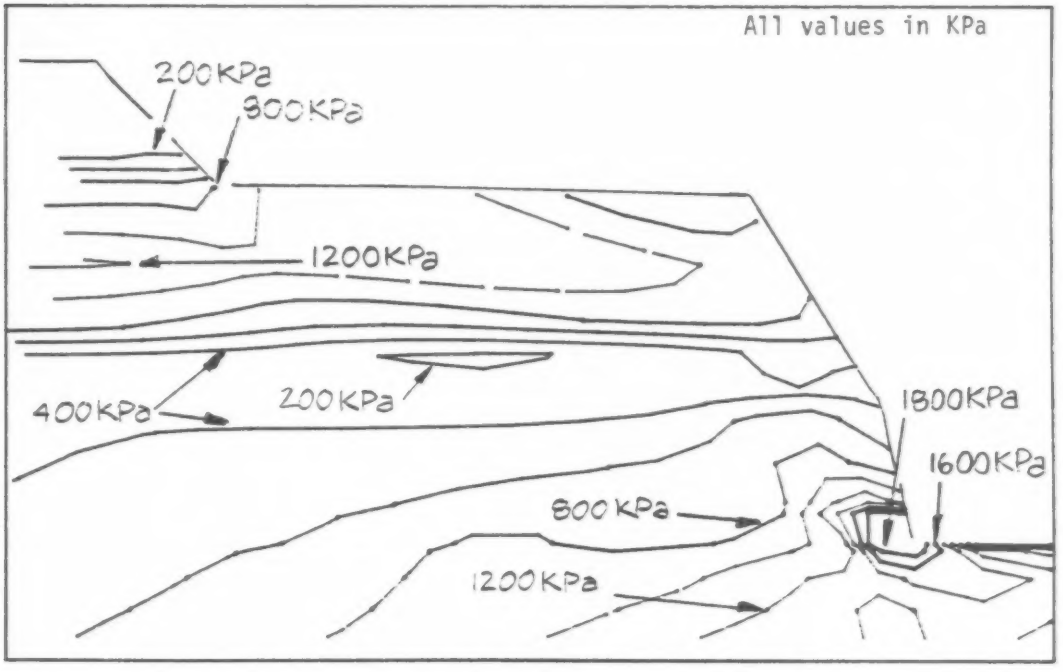

FIG. A.14.2 Octahedral Shear Stress Contour Plot for the Final Slope.

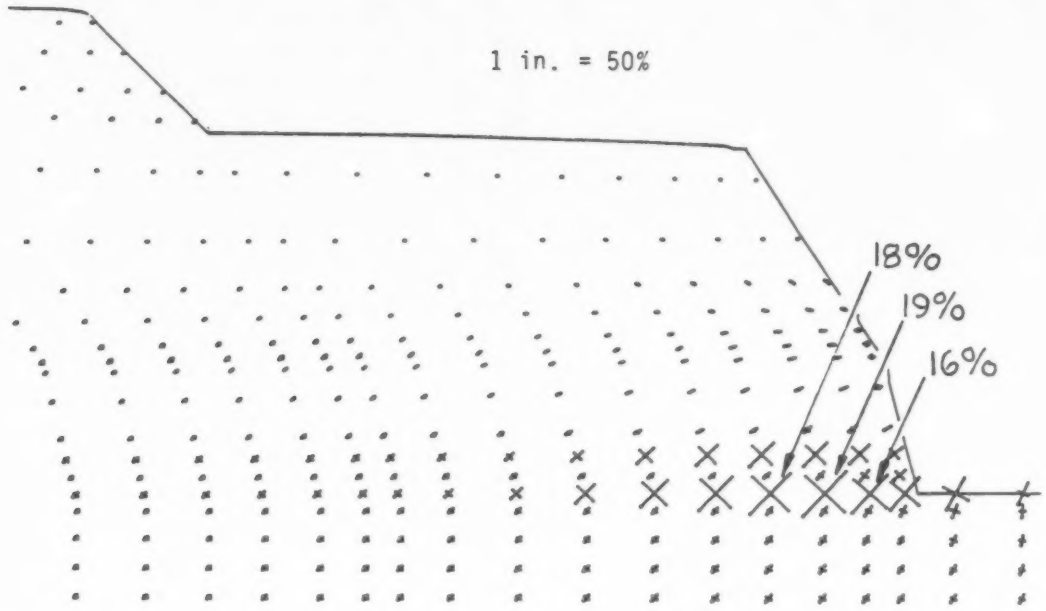

FIG. A.14.3 Principal Strain Distribution Around Final Slope.

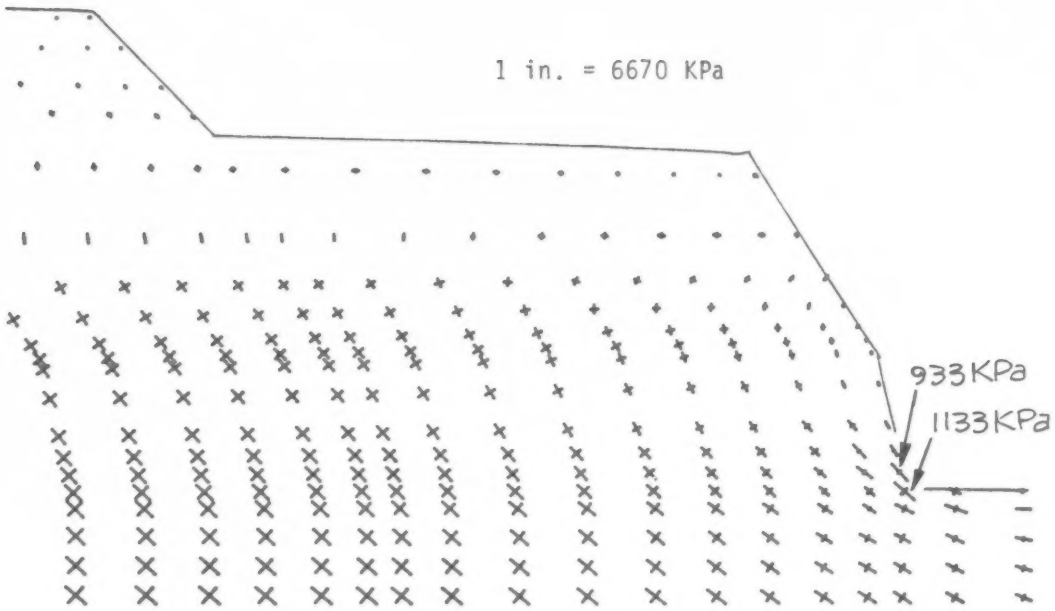

FIG. A.14.4 Principal Stress Distribution Around Final Slope.

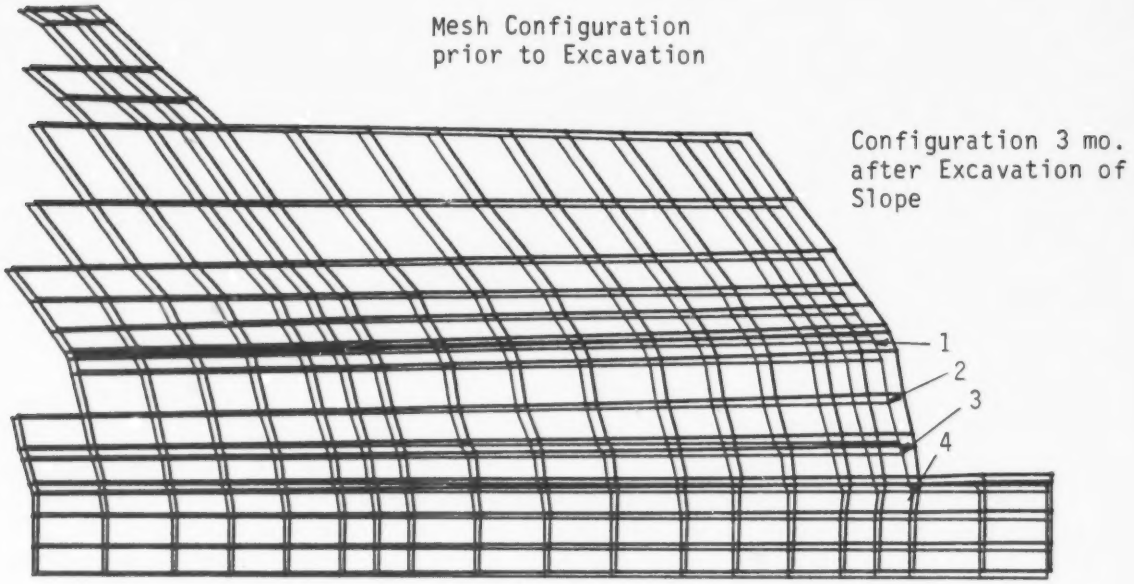

FIG. A.14.5 Deformation of Mesh Corresponding to Final Slope.

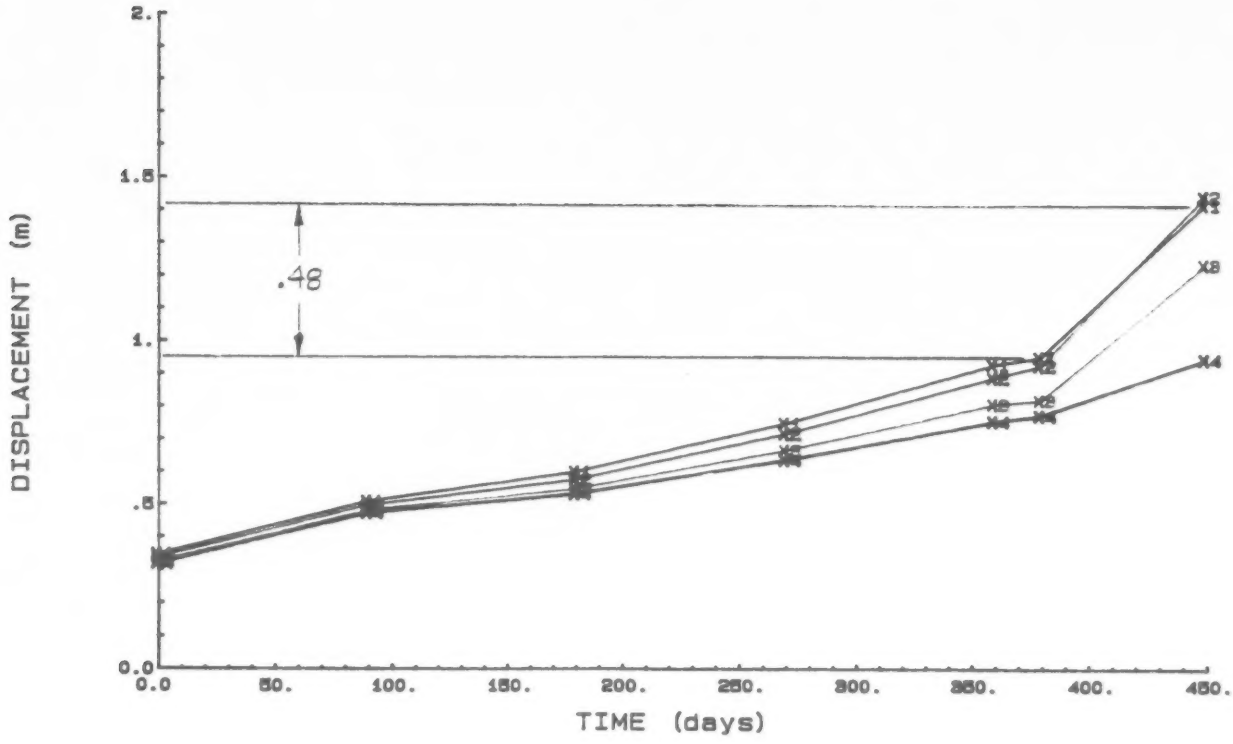

FIG. A.14.6 Displacement of Critical Nodes in the Final Slope as a Function of Time.

RUN DESIGNATION	-	TESD05/TESS05
MATERIAL PROPERTY	-	"Weak"
SLOPE GEOMETRY	-	$\alpha = 45°$, $\beta = 57°$
EXCAVATION TIMING	-	3 months
EXCAVATION SEQUENCE	-	Delayed Coal Removal
INITIAL STRESS STATE	-	Hydrostatic

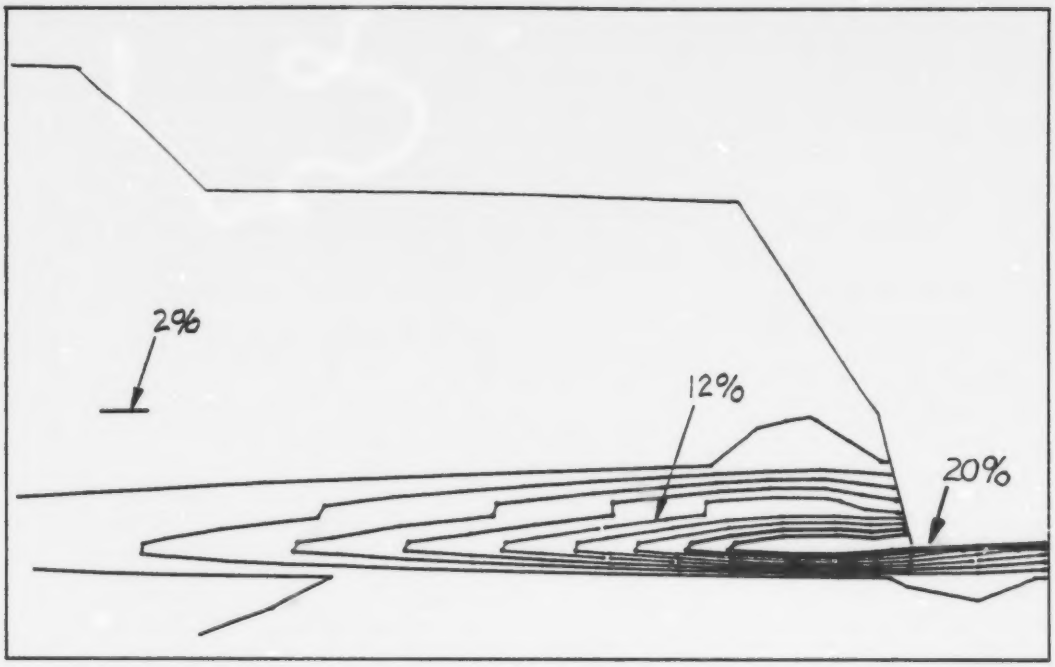

FIG. A.15.1 Octahedral Shear Strain Contour Plot for the Final Slope.

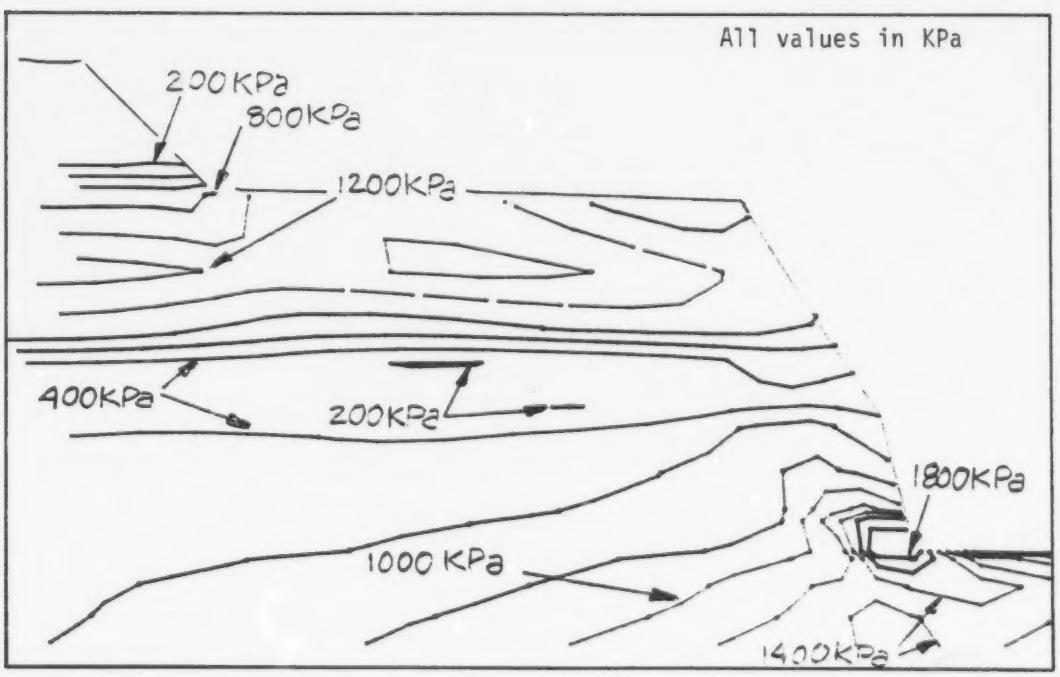

FIG. A.15.2 Octahedral Shear Stress Contour Plot for the Final Slope.

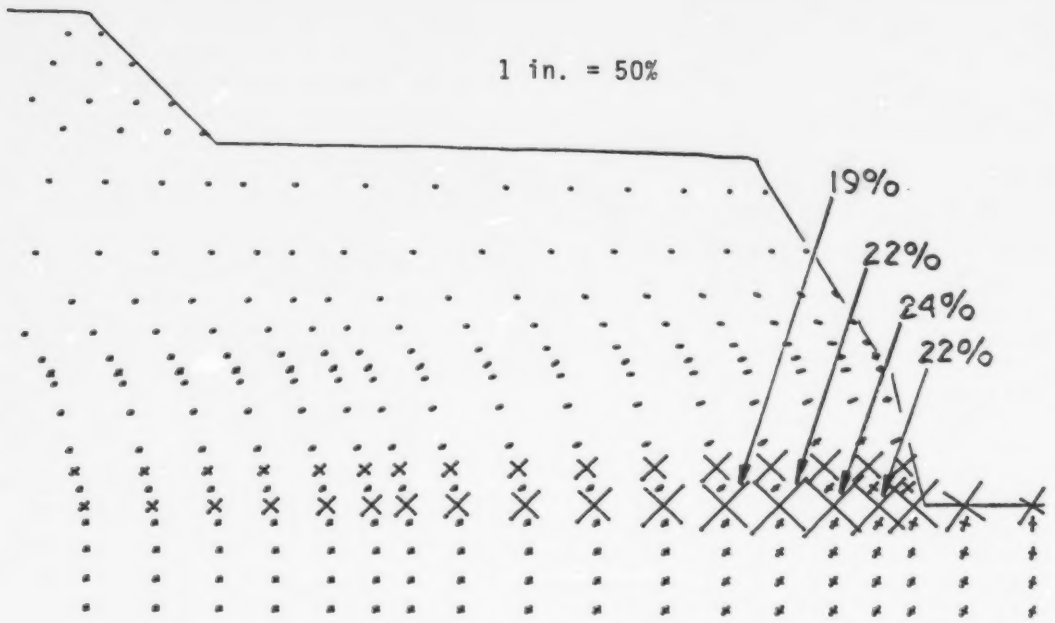

FIG. A.15.3 Principal Strain Distribution Around Final Slope.

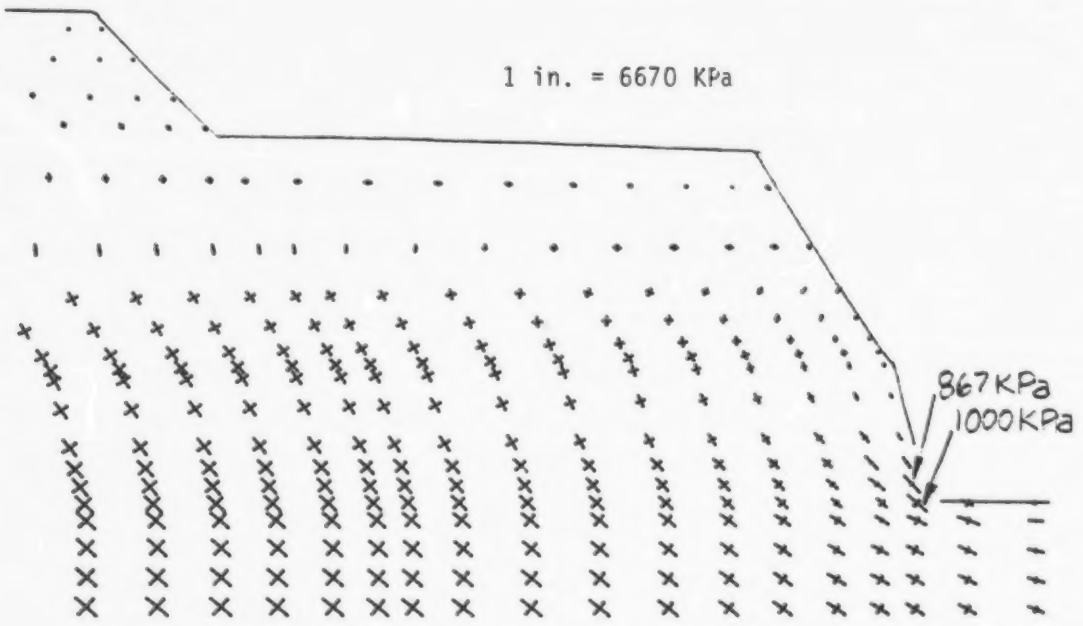

FIG. A.15.4 Principal Stress Distribution Around Final Slope.

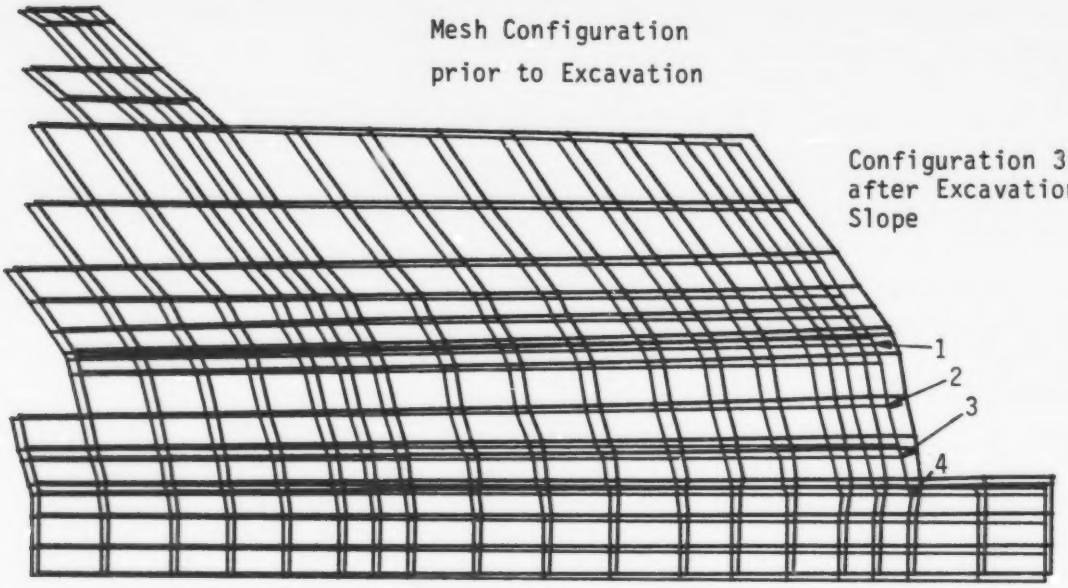

FIG. A.15.5 Deformation of Mesh Corresponding to Final Slope.

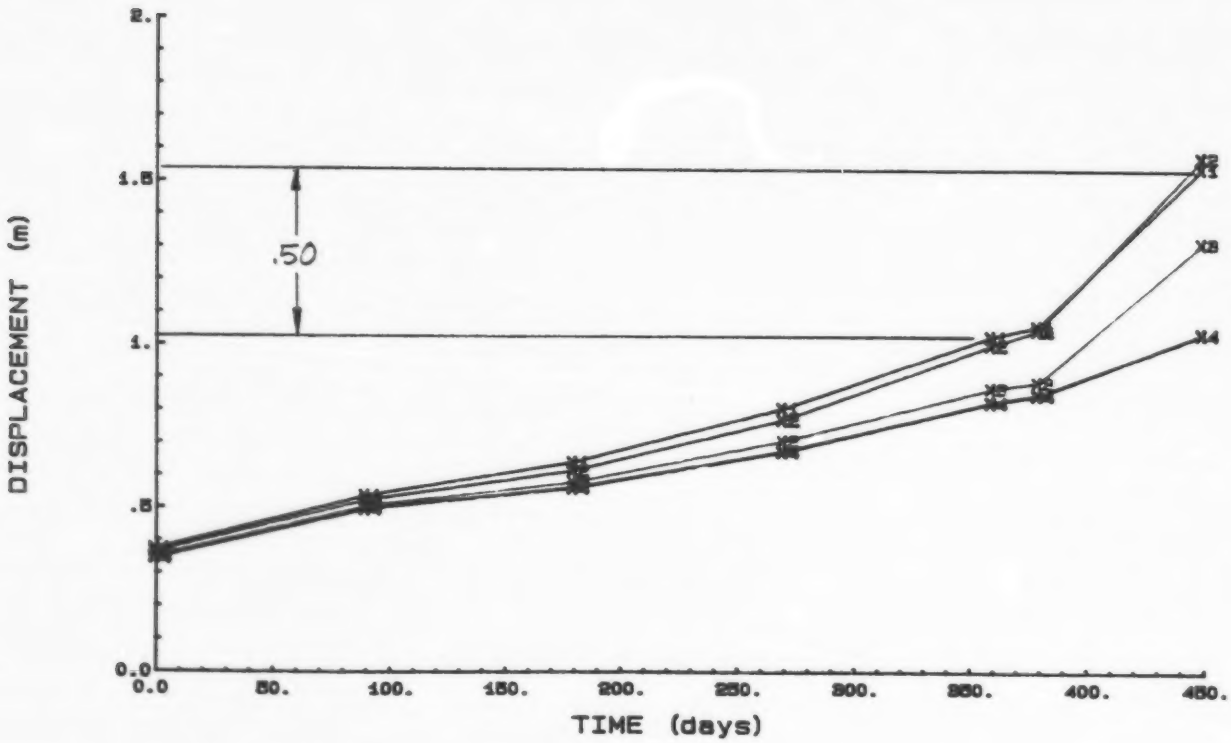

FIG. A.15.6 Displacement of Critical Nodes in the Final Slope as a Function of Time.

RUN DESIGNATION	-	TESD04/TESS04
MATERIAL PROPERTY	-	"Strong"
SLOPE GEOMETRY	-	$\alpha = 45°$, $\beta = 57°$
EXCAVATION TIMING	-	3 months
EXCAVATION SEQUENCE	-	Delayed Coal Removal
INITIAL STRESS STATE	-	Hydrostatic

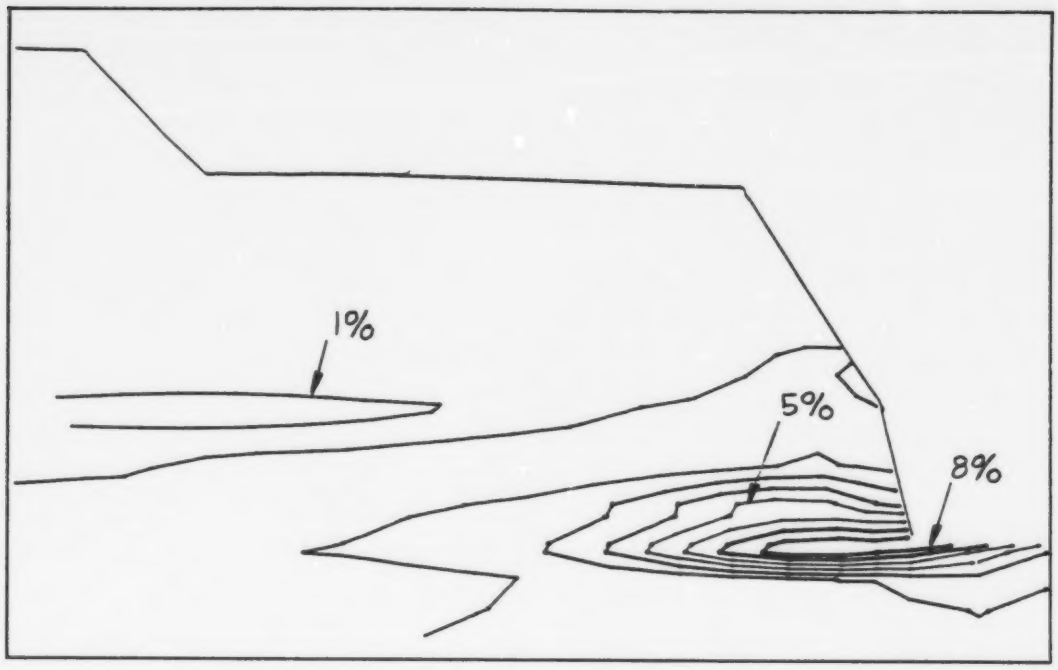

FIG. A.16.1 Octahedral Shear Strain Contour Plot for the Final Slope.

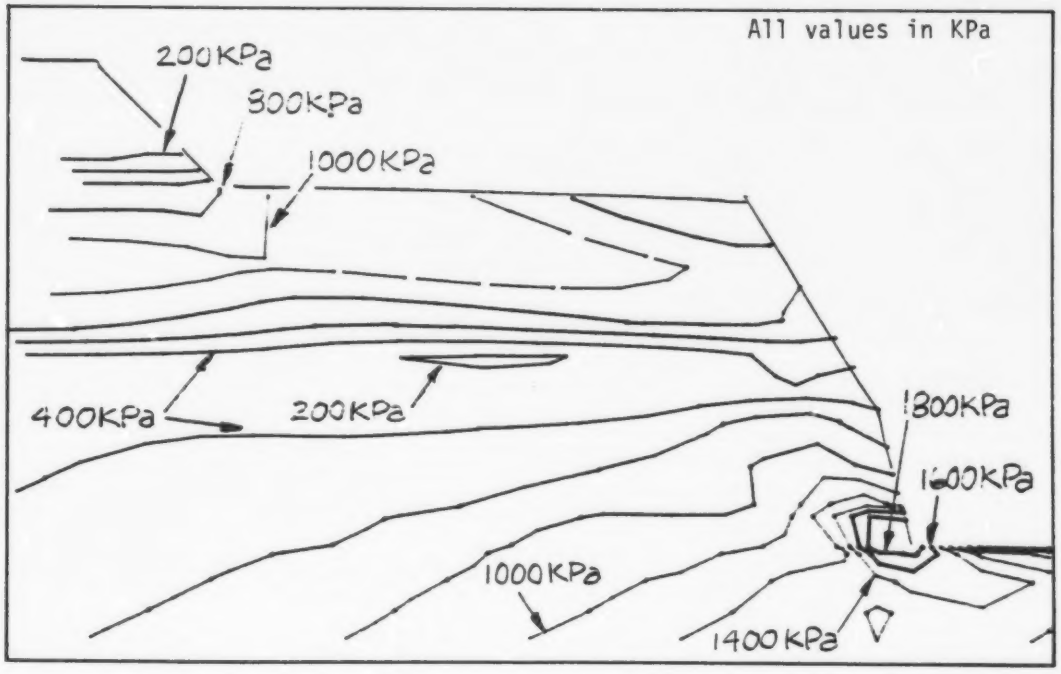

FIG. A.16.2 Octahedral Shear Stress Contour Plot for the Final Slope.

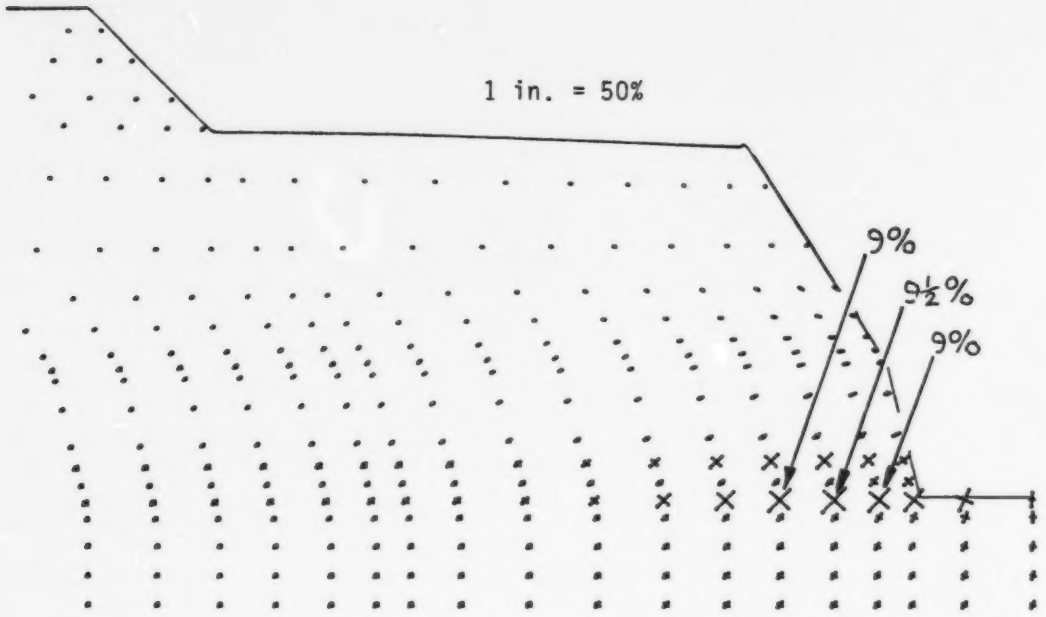

FIG. A.16.3 Principal Strain Distribution Around Final Slope.

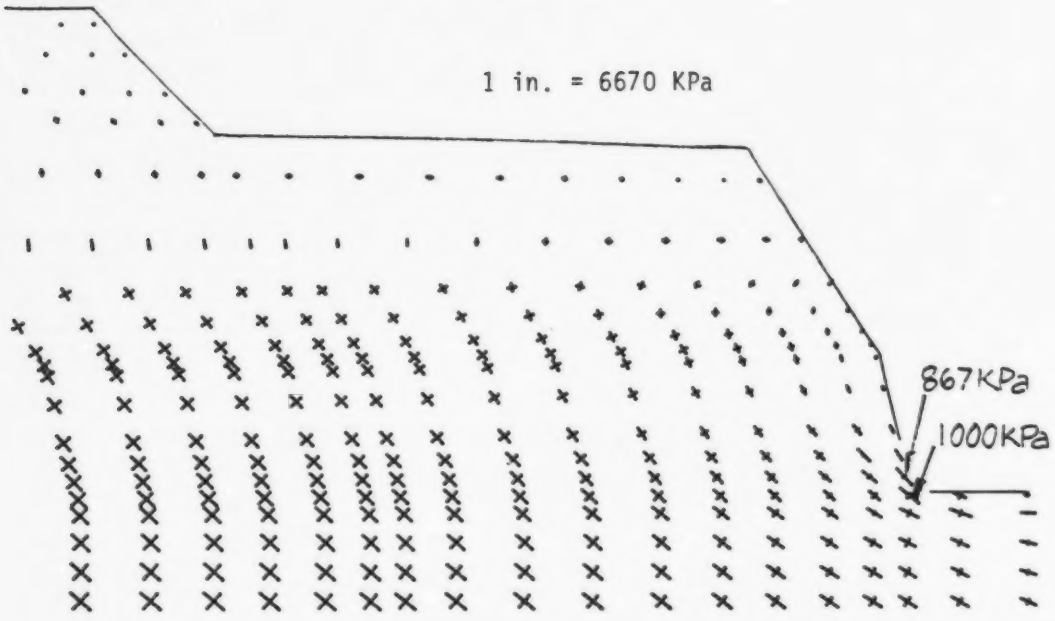

FIG. A.16.4 Principal Stress Distribution Around Final Slope.

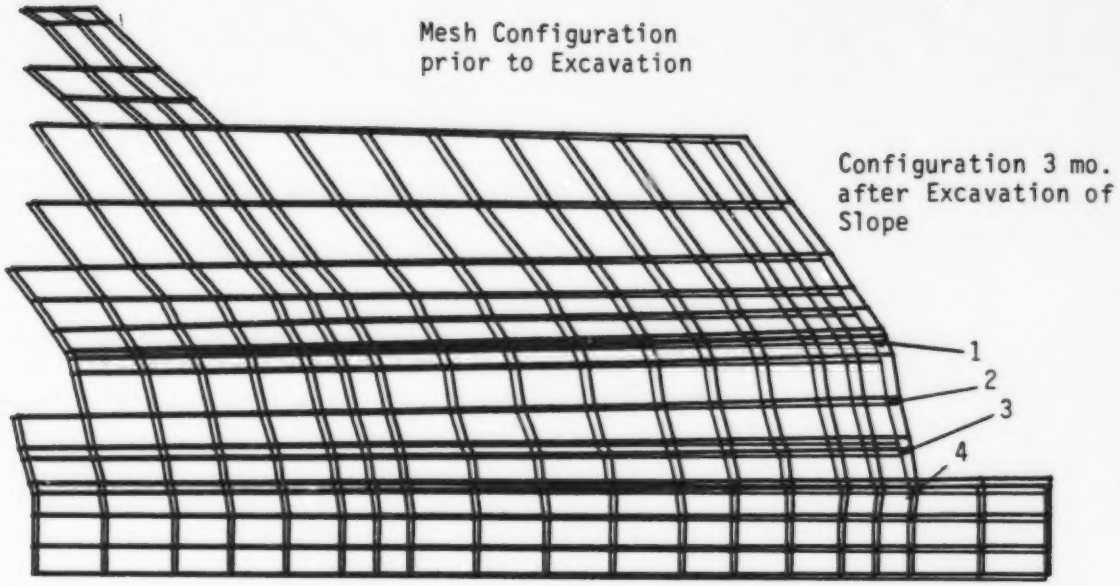

FIG. A.16.5 Deformation of Mesh Corresponding to Final Slope.

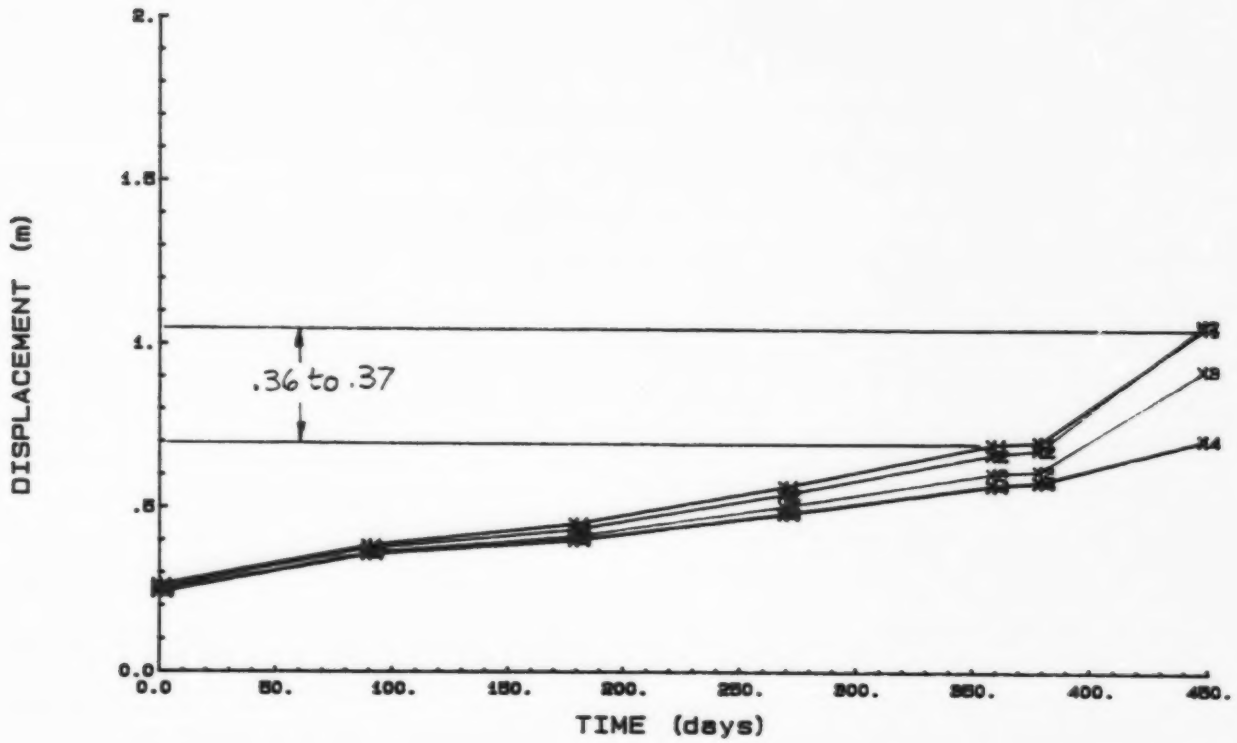

FIG. A.16.6 Displacement of Critical Nodes in the Final Slope as a Function of Time.

RUN DESIGNATION	-	TESD03/TESS03
MATERIAL PROPERTY	-	"Norm"
SLOPE GEOMETRY	-	$\alpha = 55°$, $\beta = 72°$
EXCAVATION TIMING	-	3 months
EXCAVATION SEQUENCE	-	Delayed Coal Removal
INITIAL STRESS STATE	-	Hydrostatic

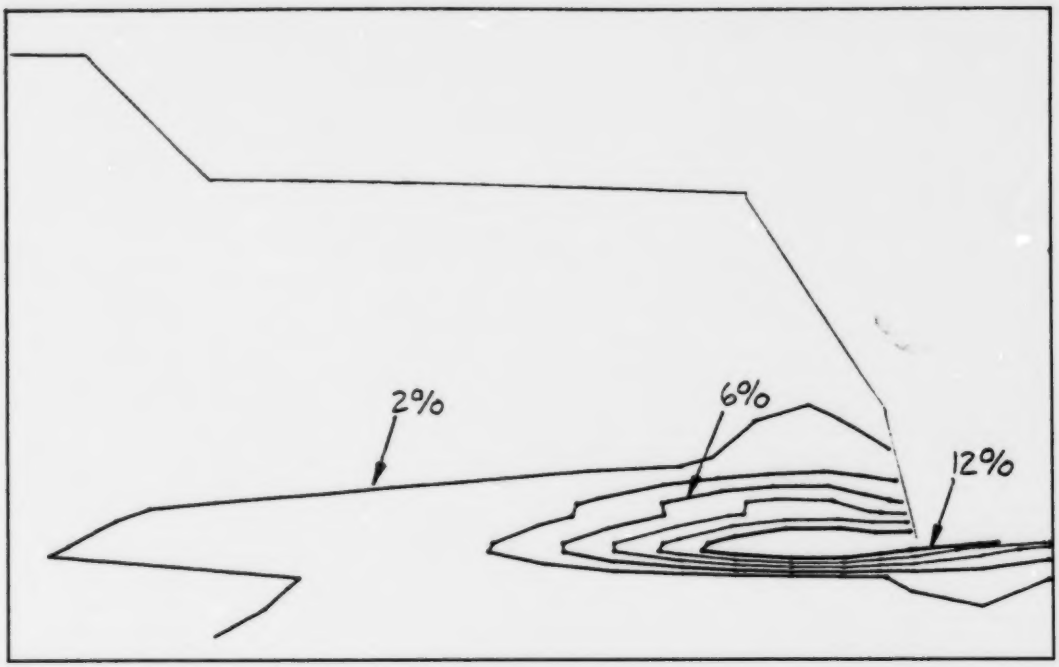

FIG. A.17.1 Octahedral Shear Strain Contour Plot for the Final Slope.

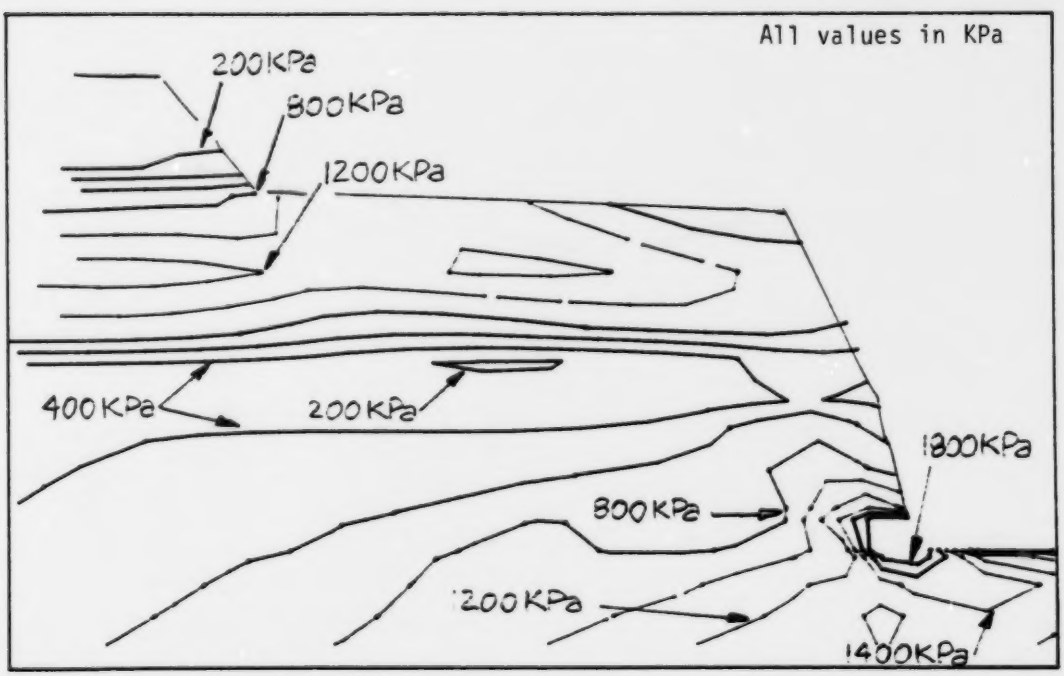

FIG A.17.2 Octahedral Shear Stress Contour Plot for the Final Slope.

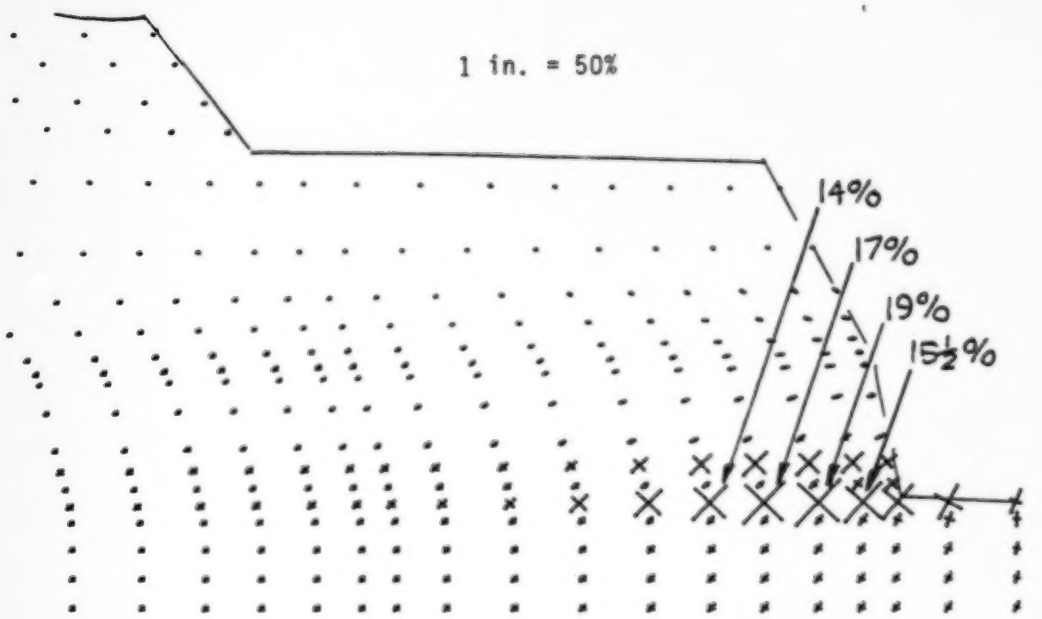

FIG. A.17.3 Principal Strain Distribution Around Final Slope.

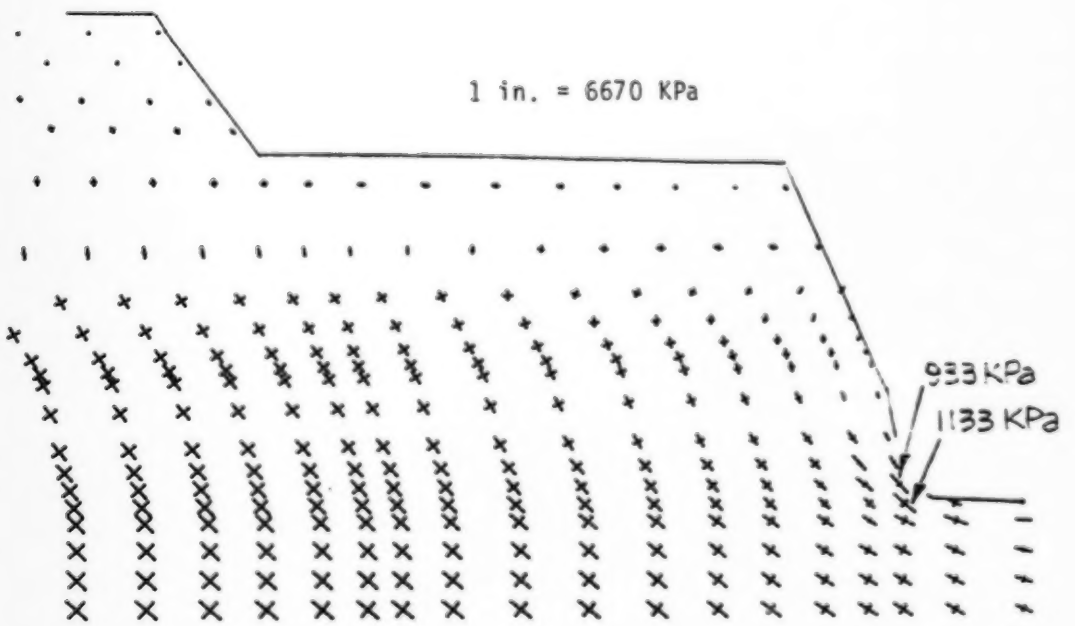

FIG. A.17.4 Principal Stress Distribution Around Final Slope.

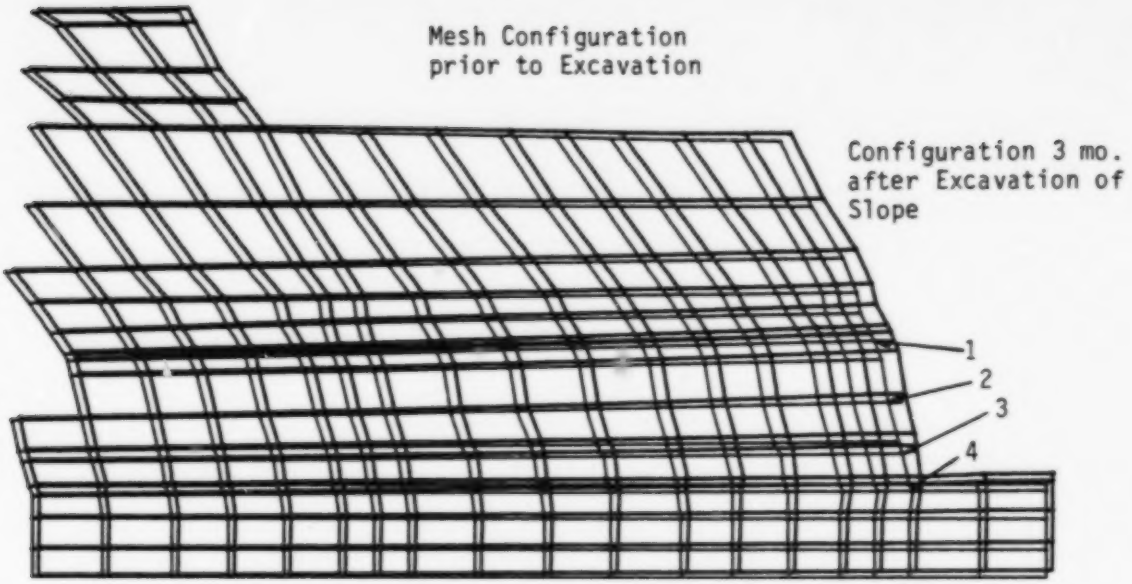

FIG. A.17.5 Deformation of Mesh Corresponding to Final Slope.

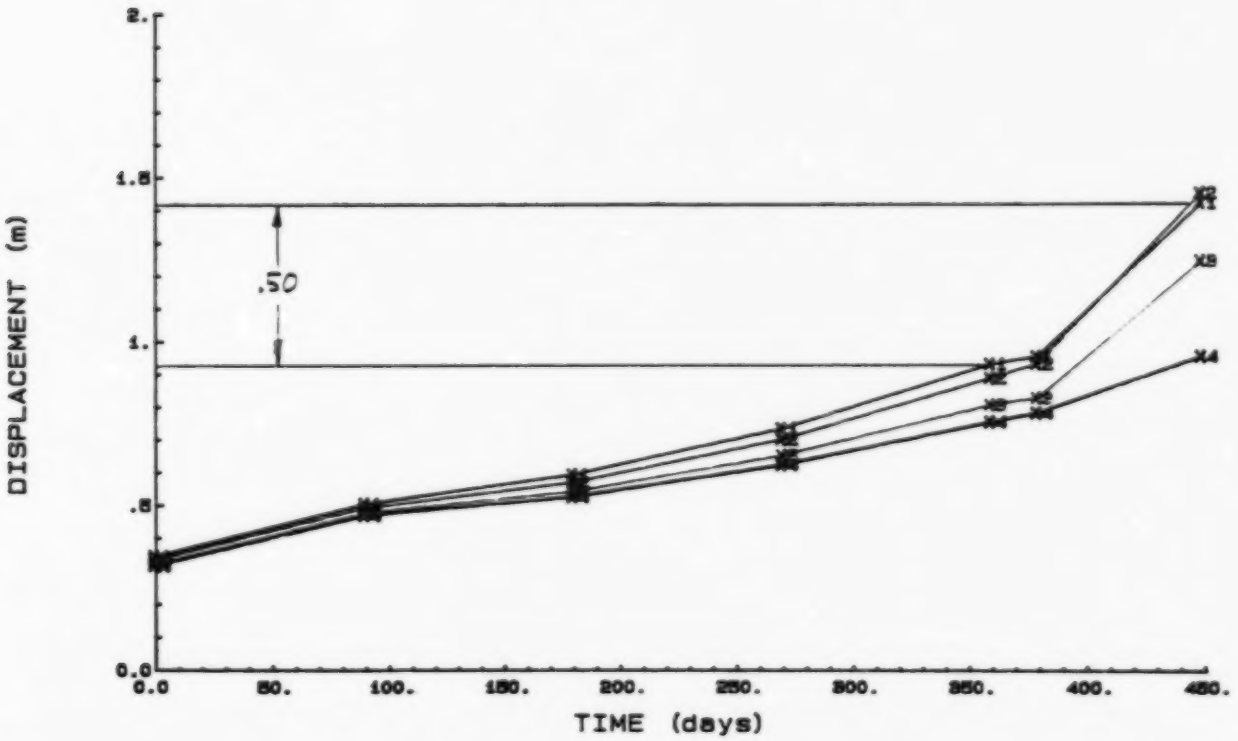

FIG. A.17.6 Displacement of Critical Nodes in the Final Slope as a Function of Time.

RUN DESIGNATION	-	TESD10/TESS10
MATERIAL PROPERTY	-	"Norm"
SLOPE GEOMETRY	-	$\alpha = 45°$, $\beta = 57°$
EXCAVATION TIMING	-	3 months
EXCAVATION SEQUENCE	-	Simultaneous Coal/Overburden Removal
INITIAL STRESS STATE	-	20% Excess Lateral Stresses

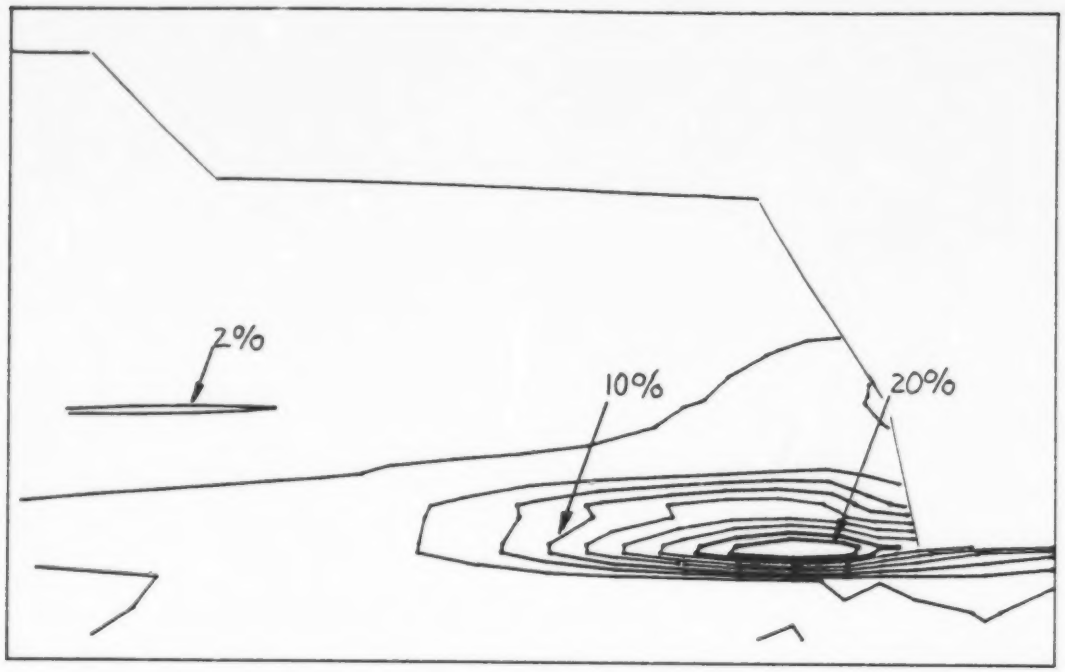

FIG. A.18.1 Octahedral Shear Strain Contour Plot for the Final Slope.

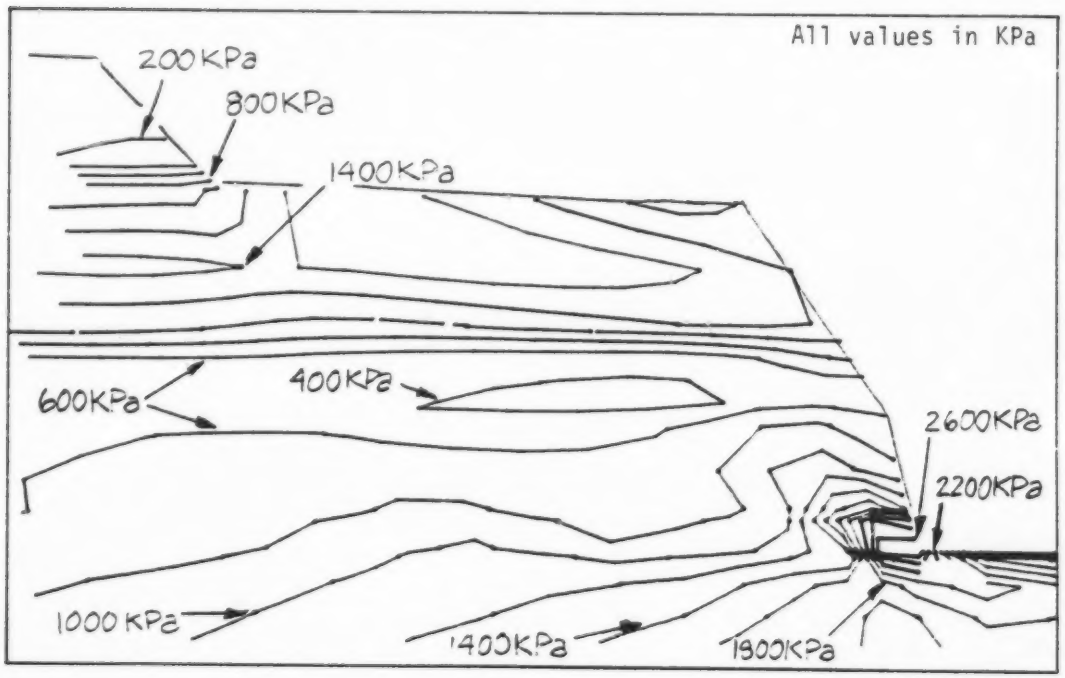

FIG. A.18.2 Octahedral Shear Stress Contour Plot for the Final Slope.

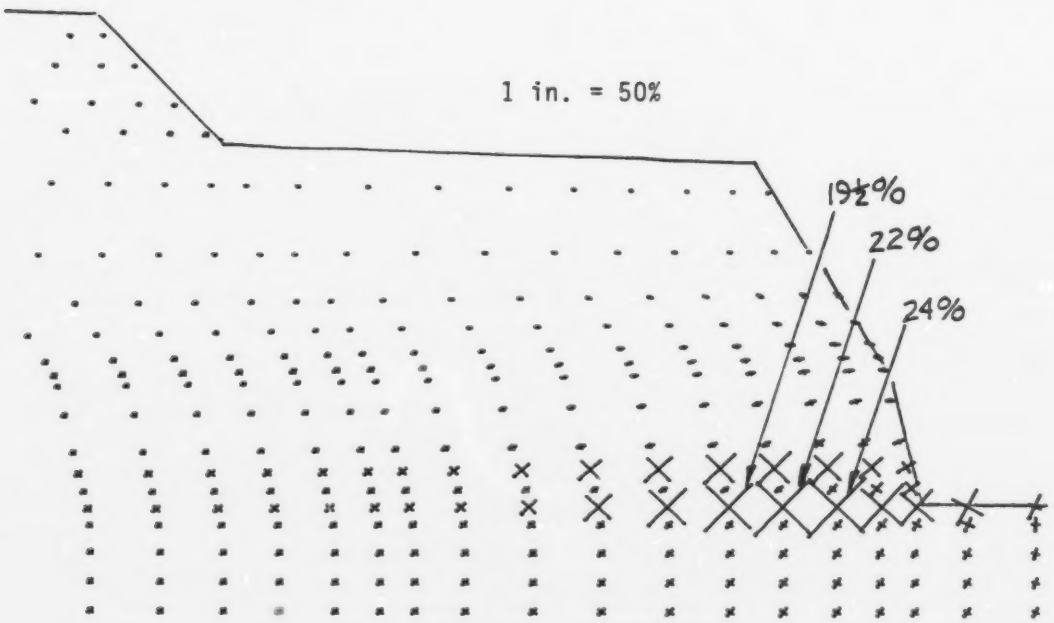

FIG. A.18.3 Principal Strain Distribution Around Final Slope.

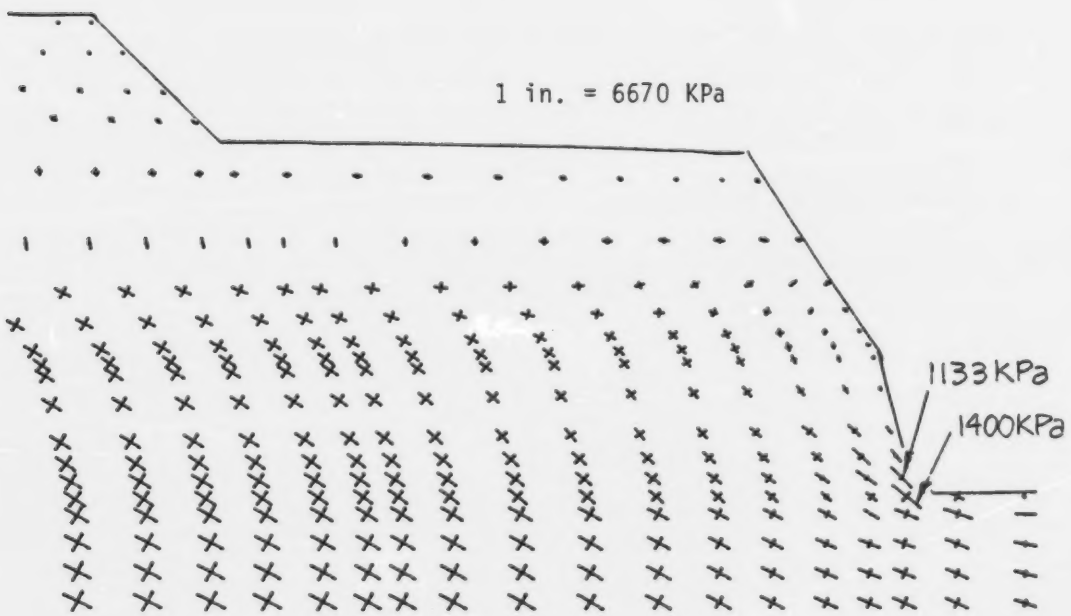

FIG. A.18.4 Principal Stress Distribution Around Final Slope.

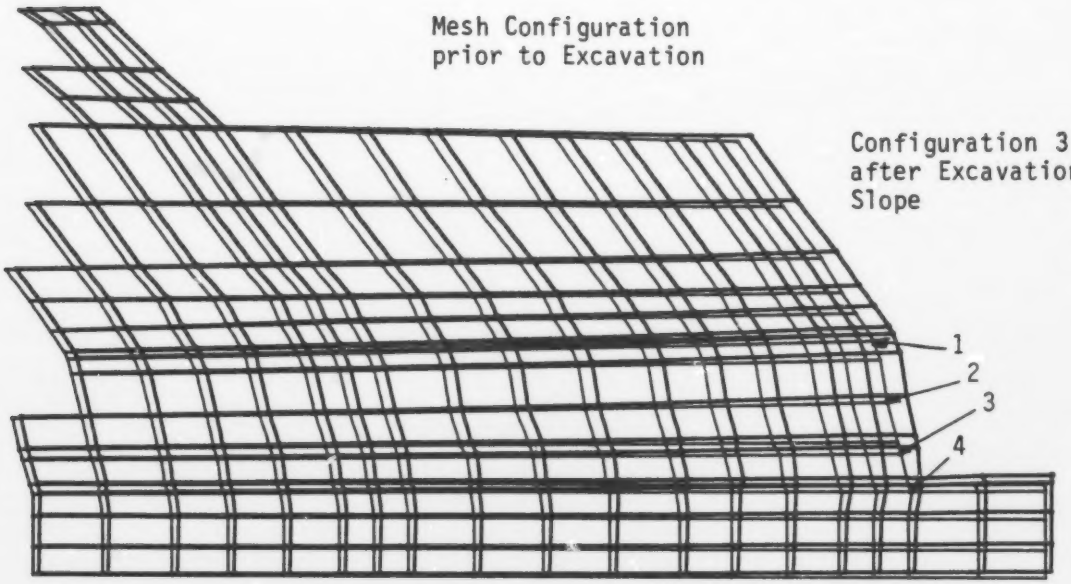

FIG. A.18.5 Deformation of Mesh Corresponding to Final Slope.

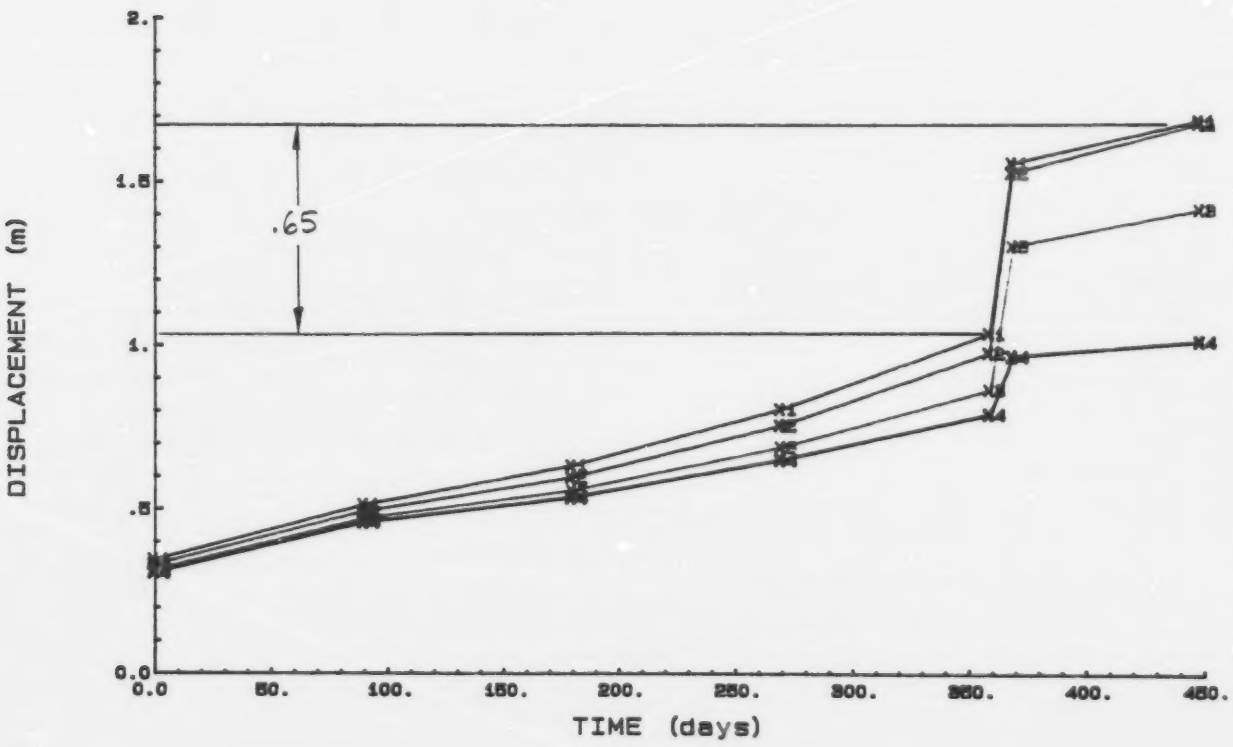

FIG. A.18.6 Displacement of Critical Nodes in the Final Slope as a Function of Time.

RUN DESIGNATION	-	TESD11/TESS11
MATERIAL PROPERTY	-	"Norm"
SLOPE GEOMETRY	-	$\alpha = 55°$, $\beta = 72°$
EXCAVATION TIMING	-	3 months
EXCAVATION SEQUENCE	-	Simultaneous Coal/Overburden Removal
INITIAL STRESS STATE	-	20% Excess Lateral Stresses

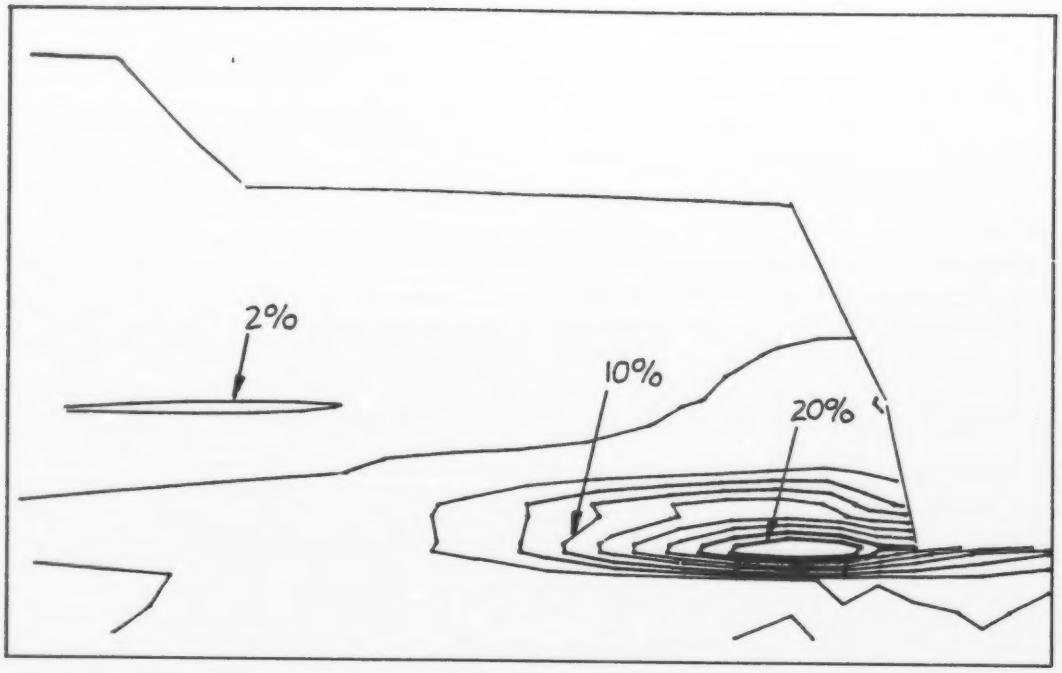

FIG. A.19.1 Octahedral Shear Strain Contour Plot for the Final Slope.

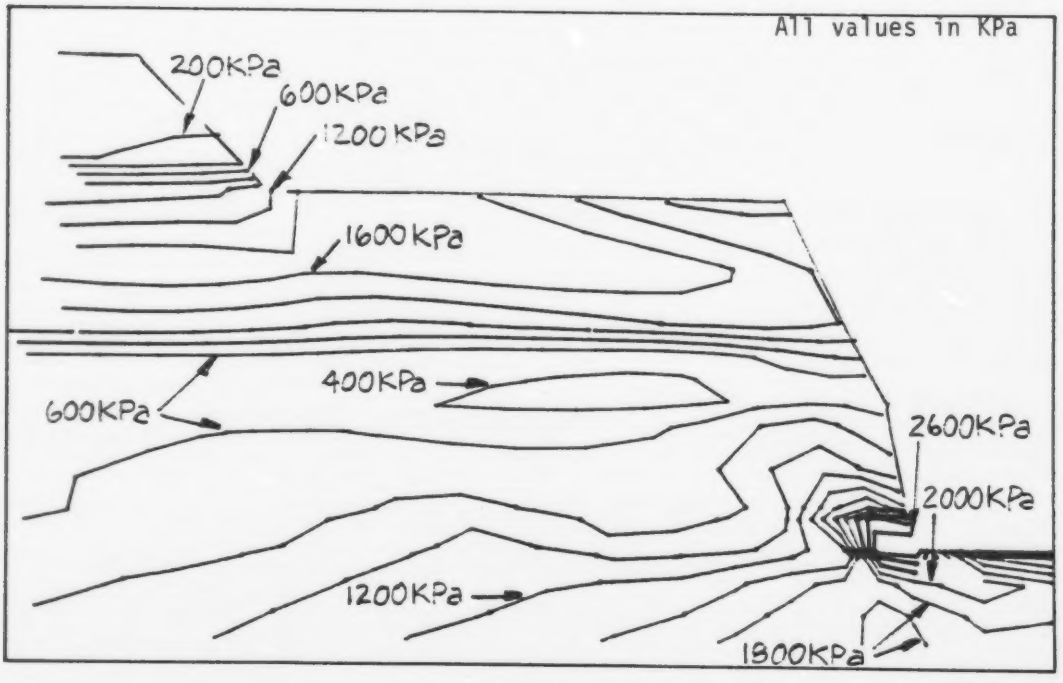

FIG. A.19.2 Octahedral Shear Stress Contour Plot for the Final Slope.

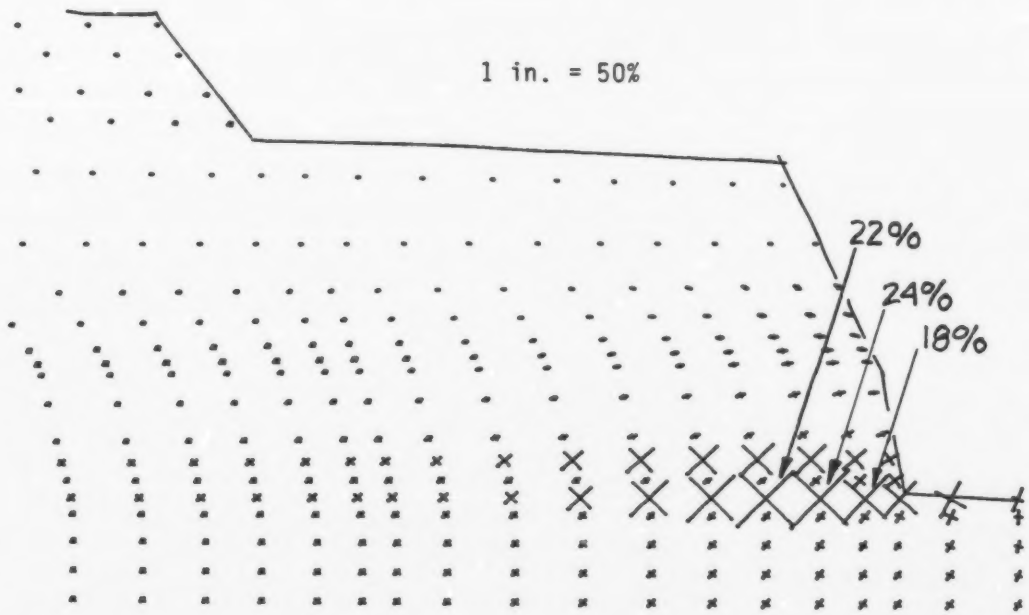

FIG. A.19.3 Principal Strain Distribution Around Final Slope.

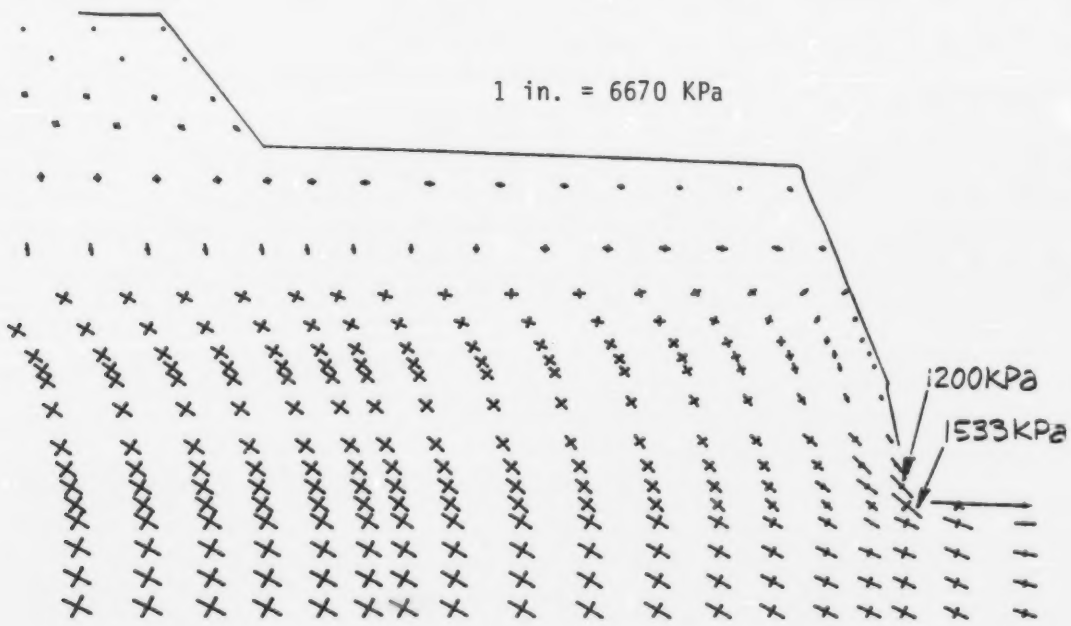

FIG. A.19.4 Principal Stress Distribution Around Final Slope.

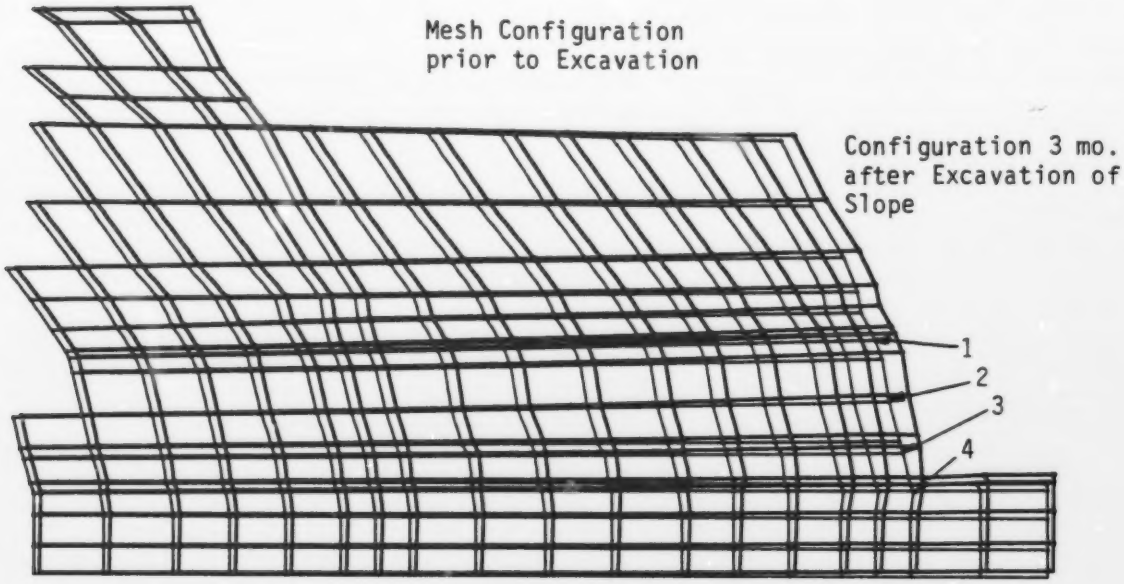

FIG. A.19.5 Deformation of Mesh Corresponding to Final Slope.

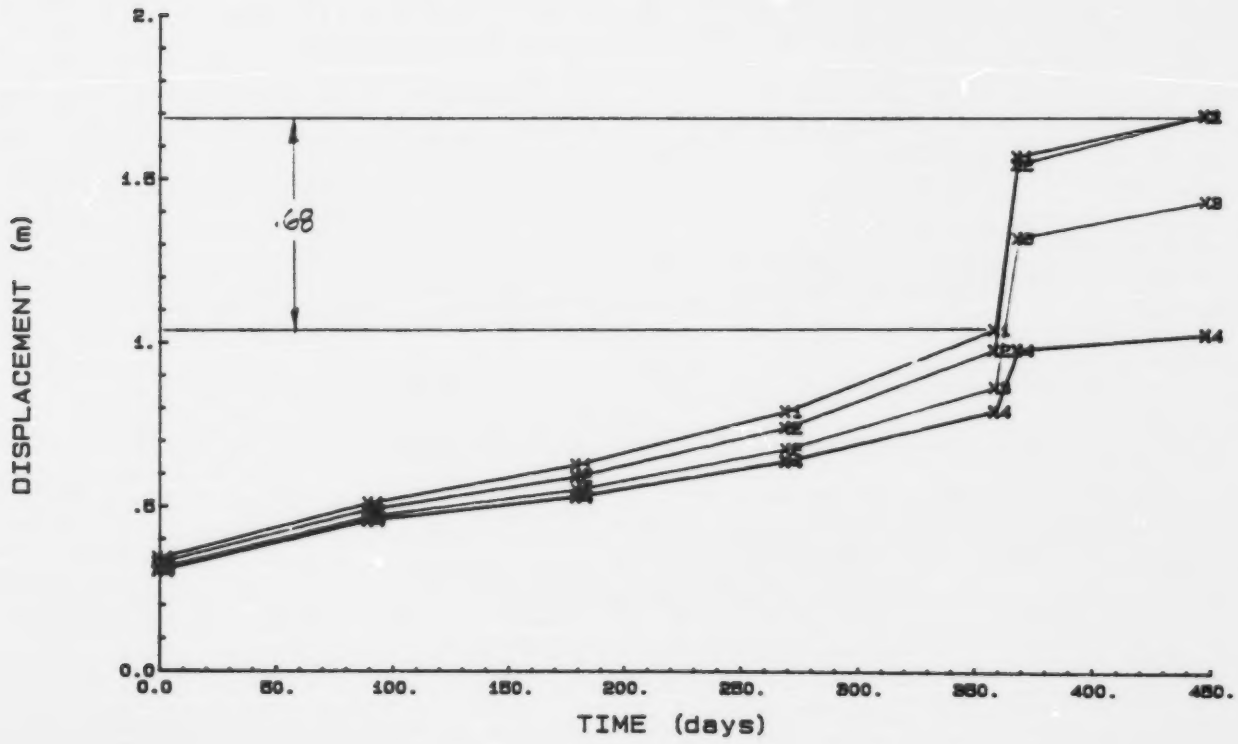

FIG. A.19.6 Displacement of Critical Nodes in the Final Slope as a Function of Time.